From the Institute for Experimental and Clinical

Pharmacology and Toxicology

Of the University of Lübeck

Director: Prof. Dr. Markus Schwaninger

Characterization of brain endothelial cell death and assessment of stem cell-drug interactions for the treatment of intracerebral hemorrhage

Dissertation

for Fulfillment of

Requirements

for the Doctoral Degree

of the University of Lübeck

from the Department of Natural Sciences

Submitted by

Maulana Ikhsan

aus Binjai, Indonesia

Lübeck 2020

First referee: Prof. Dr. Markus Schwaninger

Second referee: Prof. Dr. Kristina Kusche-Vihrog

Date of oral examination:19.05.2021

Approved for printing. Lübeck, 19.05.2021

Acknowledgements

Throughout my dissertation, I have received a great deal of support and assistance.

I would like to express my gratitude to my supervisor Dr. Marietta Zille. Her invaluable support, guidance, encouragement, and overall insights in this field have made this an inspiring experience for me. Her patience, motivation, and immense knowledge has guided me to choose the right direction and to successfully complete my dissertation.

I would like to say a special thanks and appreciation to Prof. Dr. Markus Schwaninger, who agreed to take over my supervision in his lab and who gave me access to the equipment of the institute. His fruitful feedback pushed me to sharpen my thinking and brought my work to a higher level.

My sincere thanks to Prof. Dr. Dr. Johannes Boltze, who introduced me to this field and accepted me in his lab. He helped me to settle in Lübeck at the very beginning and who has supported me since the first time I contacted him and has continued to support me until now. The opportunity that he gave me in the beginning of my PhD has opened many doors in my academic career.

I would like to acknowledge my "brainies" colleagues Alex Palumbo, Svenja Kim Landt, Sören Pietsch, and Dorothee Rose for their wonderful collaboration and support for my research. It was a wonderful four years with a lot of fun and new things. My special thanks to Fraucke Spiecker who helped me adapt in the lab and gave technical guidance in the cell culture. I thank all PhD students and technicians in the Institute for Experimental and Clinical Pharmacology and Toxicology who were always kind and helpful.

In addition, I would like to thank my parents, wife and kids for their patience and for supporting me and listening to me during my PhD journey. I could not have done this whole process without their support and prayers.

Finally, I would not have been able to complete this dissertation without the financial support from the Indonesian endowment fund of the Indonesian ministry of finance (LPDP).

Table of content

List of abbreviations

AIF	Apoptosis-inducing factor
BAK	BCL-2 antagonist/killer-1
BAX	BCL-2-associated X protein
BBB	Blood-brain barrier
BCL-2	B-cell lymphoma 2
BID	BH3 interacting domain death agonist
DAPI	4′,6-diamidino-2-phenylindole
DNA	Deoxyribonucleic acid
DPQ	4-dihydro-5-[4-(1-piperidinyl) butoxy]-1(2h)-isoquinolinone
EPC	Endothelial progenitor cell
FADD	Fas-associated protein with death domain
FCS	Fetal calf serum
GPX4	Gluthathione peroxidase 4
GSH	Gluthathione
ICH	Intracerebral hemorrhage
JNK	c-Jun N-terminal kinases
LC3-II	Microtubule-associated protein 1a/1b-light chain 3-II
MAPK	Mitogen-activated protein kinase
MDA	Malondialdehyde
MLKL	Mixed lineage kinase domain-like protein
mPTP	Mitochondrial permeability transition pore
mTOR	Mechanistic target of rapamycin
NGS	Normal goat serum
NSC	Neuronal stem cell
pBCEC	Primary porcine brain cortical endothelial cells
PARP	Poly-(ADP-ribose) polymerase
PI	Propidium iodide
PRISMA	Preferred reporting items for systematic reviews and meta-analyses
RIPK	Receptor interacting protein kinase

SD	Standard deviation
SMD	Standardized mean difference
TfR1	Transferrin receptor 1
TNFR1	Tumor necrosis factor receptor 1
TRADD	Tumor necrosis factor receptor type 1-associated death domain

List of figures

List of tables

Abstract

Intracerebral hemorrhage is a type of stroke leading to a high mortality and disability rate. Despite of its alarming incidence, studies about this disease are scarce compared to ischemic stroke. Conventional surgical intervention has limited effects on patient outcomes. Therefore, alternative therapies are urgently needed. In this thesis, I suggest two therapeutic options for the treatment of intracerebral hemorrhage: 1) cytoprotection and 2) stem cell therapy. First, I investigated the mechanisms of cell death in brain endothelial cells that are relevant for cerebrovascular diseases including intracerebral hemorrhage. While neuronal cell death has already been characterized in detail, our understanding of brain endothelial cell death is limited. My experiments indicate that endothelial cell death induced by the hemolysis product hemin is mediated by ferroptosis, necroptosis, and autophagy. I detected the presence of the ferroptosis markers transferrin receptor 1 and malondialdehyde and the autophagy marker microtubule-associated protein 1a/1b-light chain 3 (LC3) in the absence of the apoptosis marker cleaved caspase-3. Furthermore, cell death was abrogated partially by the administration of N-acetylcysteine and Trolox (both antioxidants/ferroptosis inhibitors), deferoxamine (iron scavenger/ferroptosis inhibitor), GSK872 (necroptosis inhibitor), and bafilomycin A1 (autophagy inhibitor). These findings will enable targeting cell death in both neurons and brain endothelial cells in future therapeutic approaches. In the second part of my thesis, I investigated the interactions of drugs used in the elderly on stem cells as the elderly usually suffer from multiple comorbidities and hence are subject to polypharmacy. I performed a systematic screening of the literature to understand the potential interactions of neuronal stem cells and endothelial progenitor cells with drugs commonly used in elderly. My meta-analysis revealed that antidepressants significantly increase the proliferation of neuronal stem cells. Furthermore, I identified a number of interactions and underlying pathways that may affect the efficacy of stem cell therapy. However, further research is needed to validate these pathways and to reveal further interactions. Taken together, cell protection and stem cell therapy can be supportive treatments of intracererbral hemorrhage. They can be combined with the primary intervention of evacuating the hematoma and help fill the cavity. Other approaches besides stem cell therapy and cytoproctive drugs should also be considered in the future such as biomaterials and immunomodulatory agents.

Abstrakt

Intrazerebrale Blutungen sind eine Art des Schlaganfalls mit einer hohen Sterblichkeits- und Invaliditätsrate. Trotz seiner gefährlichen Inzidenz sind Studien dieser Krankheit im Vergleich zu ischämischem Schlaganfall rar. Herkömmliche chirurgische Eingriffe haben nur begrenzte Auswirkungen auf ein verbessertes Outcome der Patienten. Daher sind alternative Therapien dringend erforderlich. In dieser Arbeit schlage ich zwei therapeutische Optionen für die Behandlung von intrazerebralen Blutungen vor: 1) Zytoprotektion und 2) Stammzelltherapie. Zunächst untersuchte ich die Mechanismen des Zelltods in Endothelzellen des Gehirns, die für zerebrovaskuläre Erkrankungen einschließlich intrazerebraler Blutungen relevant sind. Während der neuronale Zelltod bereits detailliert charakterisiert wurde, ist unser Verständnis des Endothelzelltods im Gehirn begrenzt. Meine Experimente zeigen, dass Endothelzelltod, welcher durch das Blutabbauprodukt Hämin induziert wurde, durch Ferroptose, Nekroptose und Autophagie vermittelt wird. Ich stellte das Vorhandensein der Ferroptosemarker Transferrin-Rezeptor 1 und Malondialdehyd und des Autophagiemarkers Mikrotubuli-assoziiertes Proteins 1a / 1b-leichte Kette 3 (LC3) in Abwesenheit des Apoptosemarkers Cleaved Caspase-3 fest. Der Zelltod wurde teilweise durch die Verabreichung von N-Acetylcystein und Trolox (beides Antioxidantien/Ferroptosehemmer), Deferoxamin (Eisenchelator/Ferroptosehemmer), GSK872 (Nekroptosehemmer) und Bafilomycin A1 (Autophagiehemmer) aufgehoben. Diese Ergebnisse werden es ermöglichen, den Zelltod sowohl in Neuronen als auch in Hirnendothelzellen in zukünftigen therapeutischen Ansätzen gezielt zu addressieren. Im zweiten Teil meiner Arbeit untersuchte ich mittels systematischer Literaturrecherche die Wechselwirkungen von neuronalen Stammzellen und endothelialen Vorläuferzellen mit Arzneimitteln, die durch älteren Patienten verwendet werden, da diese üblicherweise an mehreren Komorbiditäten leiden und daher einer Polypharmazie unterliegen. Meine Literaturrecherche und Metaanalyse ergaben unter anderem, dass Antidepressiva die Proliferation neuronaler Stammzellen signifikant erhöhen. Darüber hinaus identifizierte ich eine Reihe von Wechselwirkungen und zugrundeliegenden Signalwegen, die die Wirksamkeit der Stammzelltherapie beeinflussen können. Es sind jedoch weitere Untersuchungen erforderlich, um diese Wege zu validieren und weitere Wechselwirkungen aufzudecken. Zusammengenommen können Zellschutz und Stammzelltherapie unterstützende Behandlungen bei intrazerebralen Blutungen sein. Sie können mit chirurgischen Eingriffen wie der Evakuierung des Hämatoms kombiniert werden und helfen, den dadurch entstehenden Hohlraum zu füllen. Neben der Stammzelltherapie und zytoprotektiven Medikamenten sollten

in Zukunft auch andere Ansätze wie Biomaterialien und immunmodulatorische Wirkstoffe in Betracht gezogen werden.

1. Introduction

1.1. Intracerebral hemorrhage

Intracerebral hemorrhage (ICH) is a type of stroke caused by the rupture of a blood vessel in the brain. ICH accounts for around 19 % of all strokes (Dang et al., 2017; Feigin et al., 2009), with higher rates in low- to middle-income countries compared to developed countries (Feigin et al., 2009) and Asian countries being most strongly affected (An et al., 2017). Although the incidence is lower compared to ischemic stroke, the fatality rate can reach over 50 % (An et al., 2017). This high mortality rate did not significantly decrease over the past 20 years, while there was a decline in the incidence of ischemic stroke (Fang et al., 2014).

1.2. Current ICH treatment options target primary injury

Upon the rupture of a blood vessel in the brain, a hydrostatic jet of blood causes immediate primary injury to the surrounding tissue (Askenase & Sansing, 2016). The hematoma further expands within the first 24 hours in around a third of all ICH patients (Brott et al., 1997), leading to the worsening of patient outcomes (Dowlatshahi et al., 2011). Current medical treatment of ICH focuses on intensive care and comprehensive monitoring assessment (Cordonnier et al.,2018). In addition, hematoma removal by surgery, alongside blood pressure control and coagulopathy correction have been proposed as immediate strategies to prevent hematoma expansion. Yet, the effectiveness of surgical intervention is limited (Cordonnier et al., 2018; Wilkinson et al., 2018; Zhao et al., 2020). Early treatment by craniectomy and hematoma removal does not significantly reduce the mortality rate (Mendelow et al., 2013). Minimally invasive surgery to evacuate the hematoma led to a slight improvement in functional outcome, but the mortality rate remained high (Hanley et al., 2019). Since current treatment options targeting hematoma removal in ICH are not sufficient, alternative interventions need to be further explored.

1.3. Secondary injury in ICH is induced by hemolysis products

The presence of the hematoma has been shown to generate secondary injury to the brain. The infusion of red blood cells into the brain parenchyma leads to neurological deficits in rodent models of ICH (Krafft et al., 2012; Lei et al., 2014; Willmore & Triggs, 1991). Hemolysis products such as hemoglobin and hemin have been widely demonstrated as neuronal cell death inducers (Chu et al., 2018; Su et al., 2018; Zille et al., 2017). Furthermore, their injection into the rodent brain causes brain edema (Huang et al., 2002; Krafft et al., 2012) and blood-brain barrier (BBB) disruption (Ding et al., 2014; Imai et al., 2019).

Under physiological conditions, red blood cells are protected by the presence of cellular glutathione (GSH), which serves as a reductant and reactive electrophiles scavenger (Park et al., 1996), and methemoglobin reductase, which inhibits the ongoing oxidation of hemoglobin in the circulating blood (Jaffe, 1981). The brain parenchyma is, however, not a beneficial environment for erythrocyte survival. While microglia can clear erythrocytes in the brain, their capacity is exceeded in ICH (Wilkinson et al., 2018). The remaining erythrocytes lyse as a result of complement activation and heme-mediated oxidative stress (Hua et al., 2000). After ICH, erythrocytes have been demonstrated to change their morphology within several hours and erythrolysis occurs within one to three days after ICH in many species (Cao et al., 2016; Dang et al., 2017; Wang et al., 2019) and within one day (Liu et al., 2019) or later (Venkatasubramanian et al., 2011) after ICH in human.

The lysis of erythrocytes leads to the release of hemoglobin and its breakdown products, such as globin and iron, into the surrounding area (Babu et al., 2012; Koeppen et al., 1995; Wilkinson et al., 2018; Xi et al., 2006). The released hemoglobin is no longer protected by GSH and methemoglobin reductase. This leads to the autooxidation of the heme structure inside the hemoglobin from the ferrous (Fe^{2+}) to the ferric (Fe^{3+}) state, which weakens the heme-globin bond. Subsequently, hemoglobin is broken down to iron protoporphyrin IX and globin in the extracellular space (Chen-Roetling et al., 2014) (**Figure 1**).

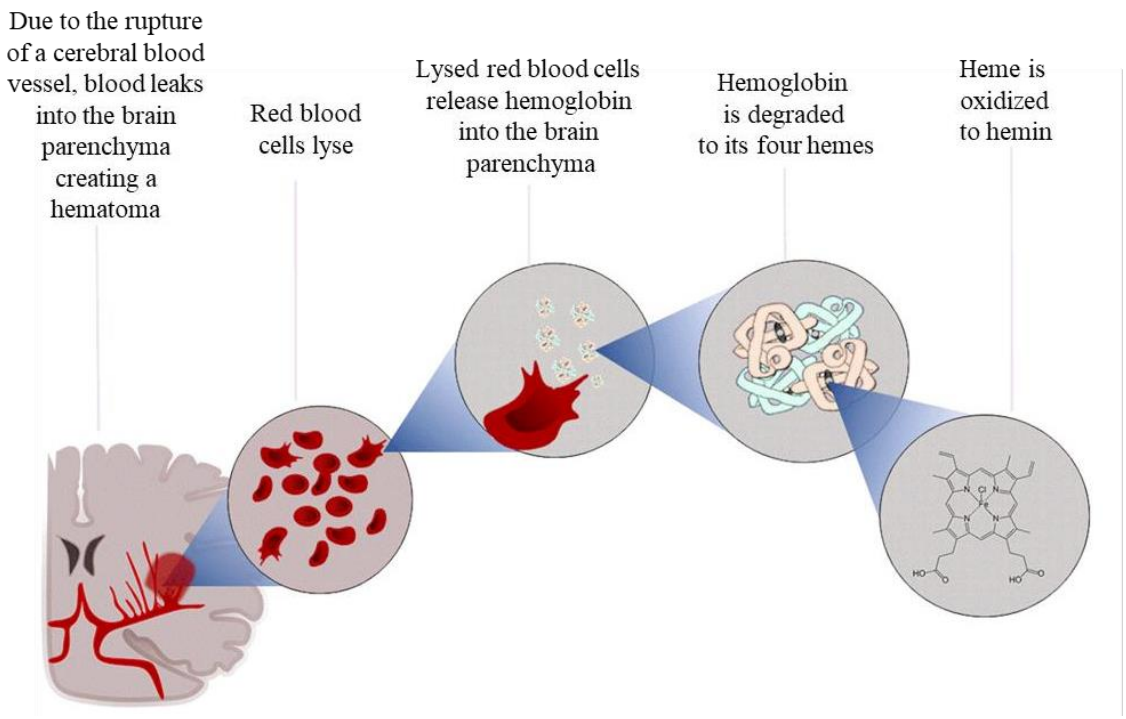

Figure 1. The degradation of red blood cells in ICH.

Hemoglobin has been demonstrated to accumulate in the hematoma within one week after hemorrhagic stroke in piglets (Cao et al., 2016). The primary mechanism of hemoglobin removal is the hemoglobin-binding protein haptoglobin, while hemopexin, that is able to bind heme, acts as a backup when haptoglobin is depleted (Bamm et al.,2004; Wang et al., 2018). In the brain, haptoglobin is synthesized by oligodendrocytes and hemopexin is expressed by neurons and microglia (Wang et al., 2018; Zhao et al., 2011). Haptoglobin and hemopexin play an important role in minimizing hemolysis-induced toxicity. Haptoglobin released from oligodendrocytes is cytoprotective in neurons exposed to lysed erythrocytes and hypoxia (Zhao et al., 2011). The deletion of haptoglobin or hemopexin worsens neurological outcome in mouse ICH, while the overexpression of human haptoglobin 2 ameliorates deficits (Wang et al., 2018; Zhao et al., 2011).

While there is approximately 2.5 mM hemoglobin in the blood, which can theoretically yield 10 mM hemin (Robinson et al., 2009), estimates of hemin concentrations in the hematoma and perihematomal area are scarce. In a model of autologous blood infusion into the subarachnoid space of dogs, 390 ± 247 µM hemin were detected in the hematoma after 7 days (Letarte et al., 1993).

Albumin can inhibit hemin uptake into the cells (Robinson et al., 2009). In addition, the residual hemin in the brain parenchyma is cleared by phagocytes and resident microglia upon recognition by the CD163 receptor within weeks up to months (Madangarli et al.,2019). Neurons and astrocytes also help in clearing hemin in the penumbra area via numerous scavengers (Chen-Roetling et al., 2014; Robinson et al., 2009; Wang et al., 2018).

It has been suggested that hemin is transported into the cells by heme carrier protein-1 or the hemin-hemopexin complex (Dang et al., 2011; Robinson et al., 2009) (**Figure 2**). Intracellularly, hemin is degraded to biliverdin, Fe^{2+}, and carbon monoxide by heme oxygenase-1 (HO-1) and NADPH-cytochrome P450 reductase (Robinson et al., 2009). Whereas HO-1 levels are low under physiological conditions, they have been demonstrated to increase within hours and days in rodent models of ICH (Wang et al., 2017b; Zhang et al., 2017). The presence of HO-1 in the acute phase of ICH has been suggested to induce neurotoxicity, while in the chronic phase, HO-1 is considered to be neuroprotective (for review see (Li et al., 2018b)) .

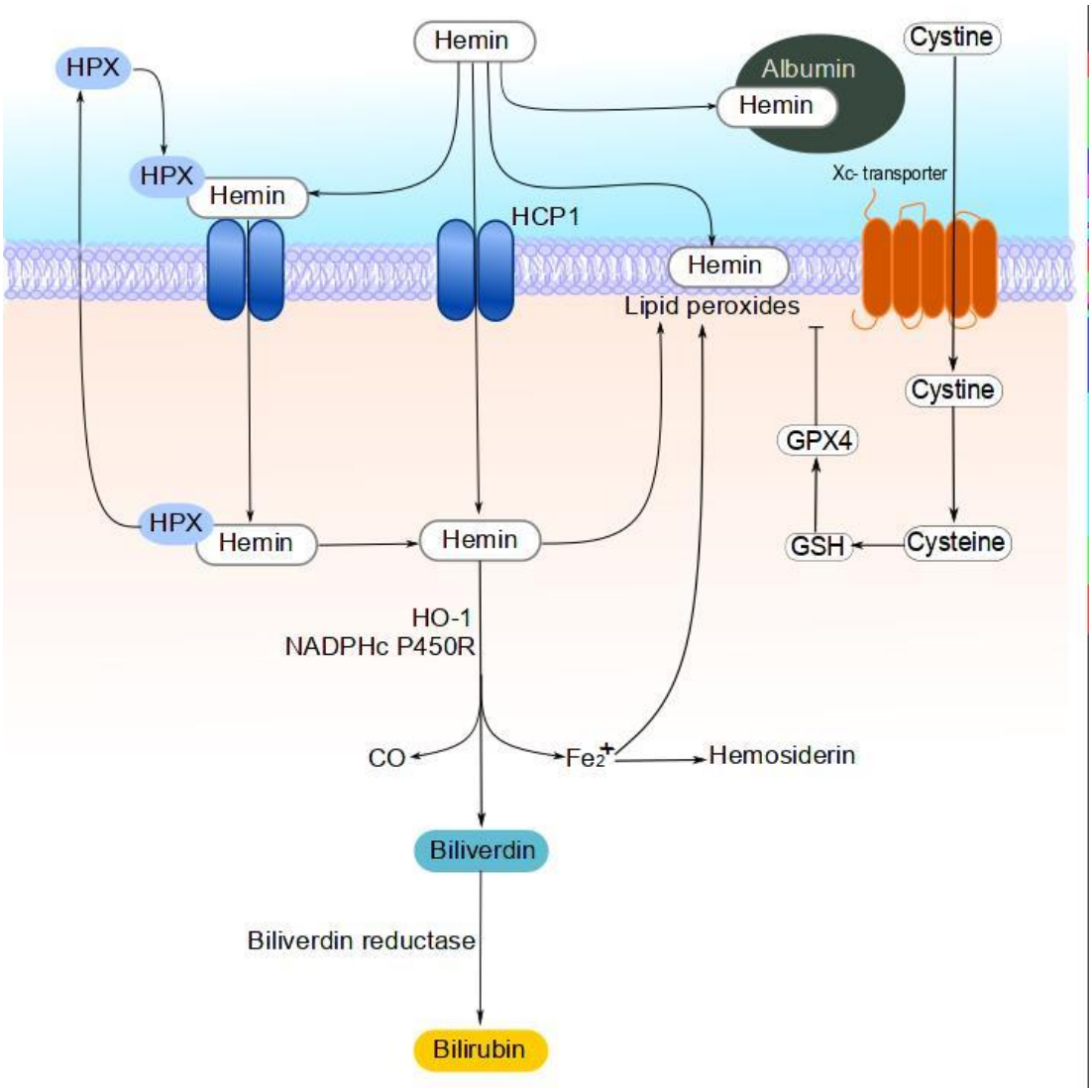

Figure 2. The possible pathways of cellular hemin uptake and toxicity. CO: carbon monoxide; HPX: hemopexin; HCP1: heme carrier protein-1; HO-1: heme oxygenase-1; GPX4: gluthathione peroxidase 4: GSH: glutathione; NADPHc P450R: NADPH cytochrome P450 reductase (adapted from Robinson et al 2009).

Hemin can cause plasma membrane oxidation since it carries a positive charge, is hydrophobic, and has a low molecular weight that allows bind into the plasma membrane of cells (Madangarli et al., 2019; Ryter & Tyrrell, 2000). The ferric iron in hemin can also theoretically generate hydroxide anions and highly reactive hydroxyl radicals able to remove the hydrogen ion from polyunsaturated fatty acids in the cell membrane and to create lipid peroxides and additional reactive carbons. This triggers a chain reaction at other hydrogen molecules in the membrane (Fenton reaction). The generated lipid peroxides are relatively persistent in the lipid bilayer of the cell membrane. Although there is insufficient experimental evidence that the Fenton reaction is responsible for the oxidative stress caused by hemin, the presence of lipid peroxides

in the cell membrane, that can be independent from the Fenton reaction, has been clearly demonstrated (Gaschler & Stockwell, 2017; Ratan, 2020).

Another pathway that can trigger cellular damage is GSH depletion. The depletion of GSH storages, for example due to the lack of cysteine inside the cells, can lead to the inactivity of gluthatione peroxidase 4 (GPX4) that uses GSH as a substrate (Ratan, 2020; Robinson et al., 2009). Since GPX4 reduces lipid peroxides into non-toxic lipid alcohols, this inactivity results in the accumulation of lipid peroxides, which lead to cellular damage (Gaschler & Stockwell, 2017).

In summary, hemolysis products such as hemoglobin and hemin induce cell death in the brain. Understanding the cell death mechanisms as well as targeting hematoma lysis are current priorities in ICH research (Hemorrhagic Stroke Academia Industry Roundtable, 2018).

1.4. Cell death mechanisms

According to the definition of the Nomenclature Committee on Cell Death, a cell is considered dead when at least one of three criteria is met: 1) plasma membrane disintegration, 2) nucleus and cell organelle dissolution, and/or 3) the *in vivo* engulfment of the residuals of the dead cells by neighbouring cells (Kroemer et al., 2009).

Historically, cell death was subdivided into apoptosis and necrosis based on their morphological features identified using electron microscopy. Apoptosis was defined as a state in which cells show cell shrinkage, nuclear fragmentation, chromatin condensation, and chromosomal DNA fragmentation (Kerr et al., 1972). In contrast, necrosis was characterized by organelle swelling and the disruption of the plasma membrane leading to the release of intracellular content (Clarke, 1990). However, during the last decades, advanced molecular analysis has revealed that the picture is much more complex. There are indeed a number of modes of regulated cell death besides apoptosis such as necroptosis, autophagy-dependent cell death, ferroptosis, and parthanatos (for an extensive review, see (Galluzzi et al., 2018)). These cell death mechanisms will be explained in the next paragraphs of this thesis.

1.4.1. Apoptosis

Apoptosis can be activated either via an extrinsic pathway or an intrinsic pathway. Both pathways eventually lead to the activation of caspases (**Figure 3**).

The extrinsic pathway is induced by the stimulation of death receptors through the binding of a death ligand. The receptors recruit adapter proteins such as fas-activated death domain (FADD),

resulting in the formation of the ligand-receptor-adapter complex, which activates procaspase-8. In its active form, caspase-8 is an initiater caspase that cleaves other executioner caspases to initiate apoptosis (Wong, 2011).

The intrinsic pathway is activated by stimuli within the cell such as hypoxia, oxidative stress, exacerbated Ca^{2+} levels or irreparable genetic damage. It is characterized by an increased permeability of the mitochondria that is regulated by members of the B-cell lymphoma 2 (BCL-2) family (Wong, 2011). Under cellular stress, the pro-apoptotic protein BCL-2 homology 3 interacting domain death agonist (BID) displaces the pro-apoptotic BCL-2 antagonist killer-1 (BAK) and BCL-2 associated X protein (BAX) from anti-apoptotic members of the BCL-2 family such as BCL-2 and BCL-xL. BAX is then able to assemble a complex of proteins, the mitochondrial permeability transition pore (mPTP). This complex forms an opening in both mitochondrial membranes through which cytochrome c is released into the cytoplasm, where it activates pro-caspase-9. Cleaved caspase-9 activates the executioner caspases, caspase-3 and caspase-7 that lead to apoptotic cell death (Ashkenazi et al., 2017).

Besides BID, c-Jun N-terminal kinases (JNK) is also able to induce BAK and BAX leading to the release of cytochrome c via mitochondrial membrane activation (Aoki et al., 2002; Wei et al., 2008). P38, a stress-induced protein kinase similar to JNK, can likewise induce apoptosis by inhibiting the active subunit p20 in caspase-8 and caspase-3 (Alvarado-Kristensson et al., 2004; Cuenda & Rousseau, 2007; Gomey-Crisostomo et al., 2013).

There are a number of chemical inhibitors that can be used to block apoptosis (**Figure 3**). For instance, benzyloxycarbonyl-Val-Ala-Asp-fluoromethyl ketone (Z-VAD-FMK) inhibits active caspase-3 (Pero et al., 2018). SP600125 is an inhibitor of JNK that subsequently inhibits c-jun phosphorylation (Bennett et al., 2001). The p38 pathway can be blocked by SB203580 (Cuenda et al., 1995). MPTP pore opening can be inhibited and stabilized by the administration of cyclosporine A (McGuinness et al., 1990).

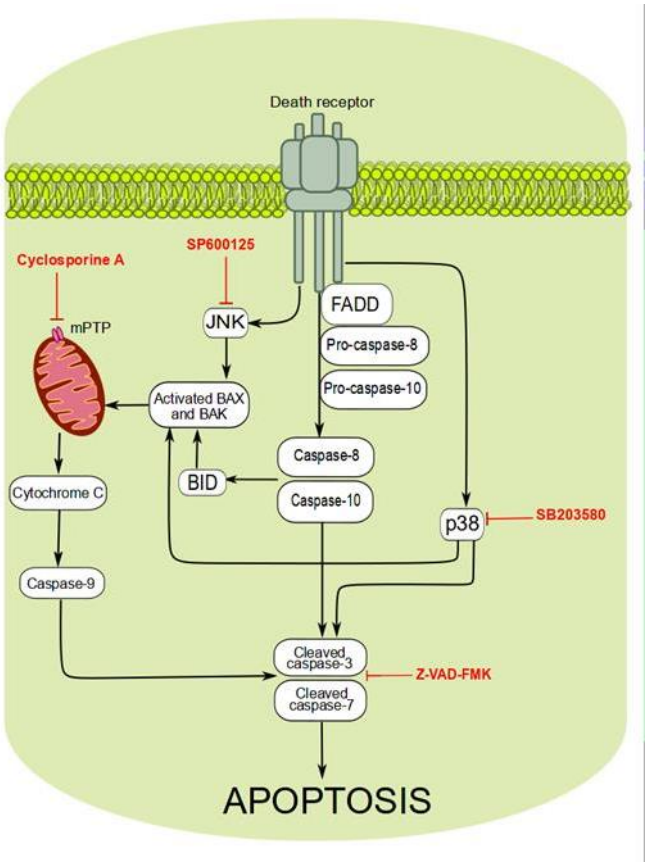

Figure 3. Apoptosis pathway and its inhibitors. BID: B-cell lymphoma 2 (BCL-2) homology 3 (BH3) interacting domain death agonist; BAK: BCL-2 antagonist killer-1; BAX: BCL-2 associated X protein; FADD: fas-associated protein with death domain; mPTP: mitochondrial permeability transition pore; JNK: c-Jun N-terminal kinases; Z-VAD-FMK: benzyloxycarbonyl-Val-Ala-Asp-fluoromethyl ketone.

However, the blockade of caspases does not necessarily lead to an inhibition of overall cell death. The cells can undergo alternative cell death pathways such as necroptosis (Degterev et al., 2005).

1.4.2. Necroptosis

Necroptosis is a type of cell death with morphological features of necrosis including an increase of the cell volume, swollen organelles, and the plasma membrane rupture leading to the release of the intracellular content outside the cells. In contrast to accidental, abrupt necrosis, necroptosis is a regulated form of cell death (Degterev et al., 2005).

Necroptosis is driven by the sequential activation of receptor interacting protein kinase (RIPK) 3 and mixed lineage kinase domain-like (MLKL) (Galluzzi et al., 2018; Oliveira et al.,2018) (**Figure 4**). Death receptors such as tumor necrosis factor receptor 1 (TNFR1), Fas cell surface death receptor or pathogen recognition receptors sense perturbations of the extracellular or

intracellular microenvironment. Upon necroptosis initiation by TNFR1, the adapter protein TNFR1-associated DEATH domain (TRADD) is recruited which associates with FADD and binds to and activates pro-caspase-8. Caspase-8 forms a complex with FLIP, which prevents caspase-8-mediated apoptosis. Upon interference with the activation of caspase-8 or the loss of FLIP or caspase-8, RIPK1 binds to RIPK3 and forms the necrosome. This necrosome induces the downstream pseudokinase MLKL (Linkermann & Green, 2014). MLKL oligomers translocate to the plasma membrane where they bind specific phosphatidylinositol phosphate species triggering plasma membrane permeabilization (Delehouze et al., 2017; Dondelinger et al., 2014; Galluzzi et al., 2018).

Alternatively, RIPK3 can also be activated independent of RIPK1: 1) via toll-like receptor (TLR) adaptor molecule 1 upon the activation of TLR3 by double-stranded RNA within endosomes or TLR4 induction by lipopolysaccharide or damage-associated molecular patterns; or 2) via Z-DNA binding protein 1 that senses cytosolic DNA-promoting type I interferon synhesis and Nuclear Factor kappa B activation (Galluzzi et al., 2018).

Necroptosis inhibitors such as necrostatin-1 (inhibitor of RIPK1), GSK872 (inhibitor of RIPK3), and necrosulfonamide (inhibitor of MLKL) can be used to identify necroptosis (King et al., 2014; Zille et al., 2019a) (**Figure 4**). Importantly, RIPK1 has also been implicated in tumor necrosis factor-induced complex IIb apoptosis. Furthermore, the ubiquitination of RIPK1 also enhances cell survival (Delehouze et al., 2017). Hence, RIPK1 activity or the blockage of RIPK1 alone is not sufficient to define necroptosis and needs to be complemented by RIPK3 or MLKL activation/blockage.

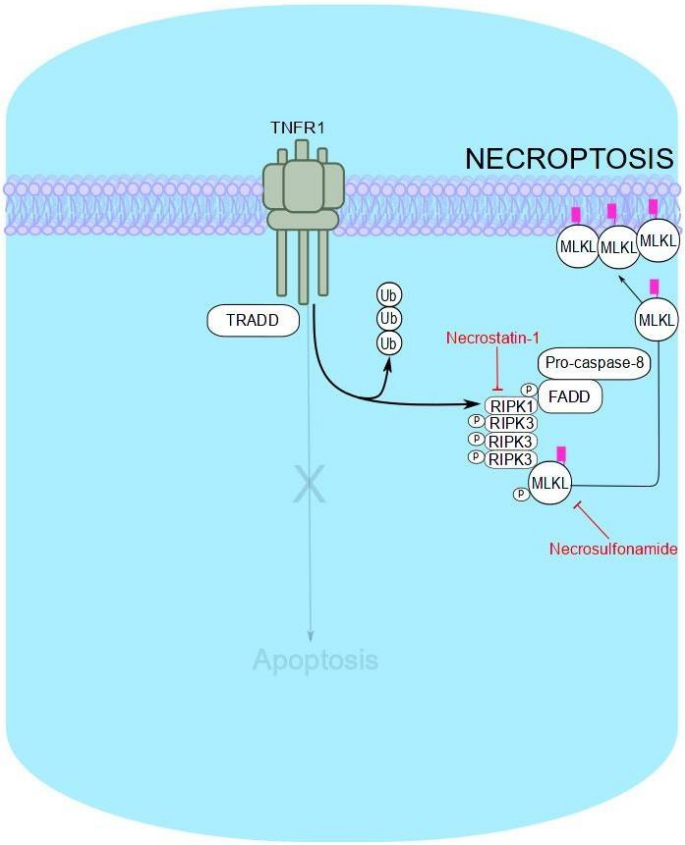

Figure 4. Necroptosis pathway upon tumor necrosis factor receptor 1 activation and its inhibitors. FADD: fas-associated protein with death domain; MLKL: mixed lineage kinase domain-like protein. RIPK: receptor interacting protein kinase; TNFR1: tumor necrosis factor receptor 1; TRADD: TNFR-1 associated DEATH domain protein.

1.4.3. Autophagy

Autophagy describes a process in which cellular materials are transported into the lysosome for degradation. It consists of three different types, i.e. macroautophagy, micro-autophagy and chaperone-mediated autophagy (Glick et al., 2010). In the thesis, I will discuss macroautophagy, which I will from now on refer to as autophagy.

The purpose of autophagy is to enhance cell survival under stress conditions such as starvation, hypoxia, DNA damage, and intracellular pathogens (Baehrecke, 2005; Kroemer et al., 2010). Autophagy often appears as an additional event besides apoptosis. However, under certain conditions, autophagy can induce cell death (Denton & Kumar, 2019; Denton et al., 2012). Although the difference between the stimuli that trigger survival-related autophagy and autophagy-dependent cell death is not clear yet, the existence of autophagy-dependent cell

death can be detected indirectly, assessing the survival of the cells after the administration of autophagy inhibitors (Denton et al., 2012). Morphologically, autophagy-dependent cell death can be recognized by the presence of extensive autophagic vacuoles and autophagolysosomes in the cytoplasm without condensed chromatin and independent of phagocytes (Baehrecke, 2005; Clarke, 1990).

On the molecular level, cell stress stimuli such as starvation induce the inhibition of the mechanistic target of rapamycin (mTOR) that otherwise phosphorylates and inactivates the Unc-51-like activating kinase complex (**Figure 5**). The activation of this complex induces the class III phosphatidyl inositol triphosphate kinase (PtdIns3K) complex that interacts with Beclin-1 to form a phagophore. Upon binding to other phosphatidyl inositol triphosphate proteins, the phagophore elongates and forms a closed double membrane structure called the autophagosome that is filled with materials that are to be degraded. With the help of microtubule-associated protein 1A/1B-light chain 3 (LC3), the autophagosome fuses with a lysosome to form an autophagolysosome, inside which the insulated materials are degraded and released into the cytoplasm for recycling (He & Klionsky, 2009).

Autophagy inducers such as rapamycin and autophagy inhibitors such as 3-methyladenine (targeting PtdIns3K, autophagosome formation), bafilomycin A1 (inhibiting endosomal acidification), chloroquine (inhibiting lysosomal function), and mdivi-1 (mitochondrial division inhibitor 1 that targets dynamin-related protein-1) are useful in assessing autophagy (Onorati et al.,2018; Sotthibundhu et al., 2016; Wu et al., 2018) (**Figure 5**). Of note, autophagy is also often used by cells to cope with stress such as starvation, and hence, the administration of particular inhibitors can stimulate cell death instead of delaying it (Lee & Gao, 2009).

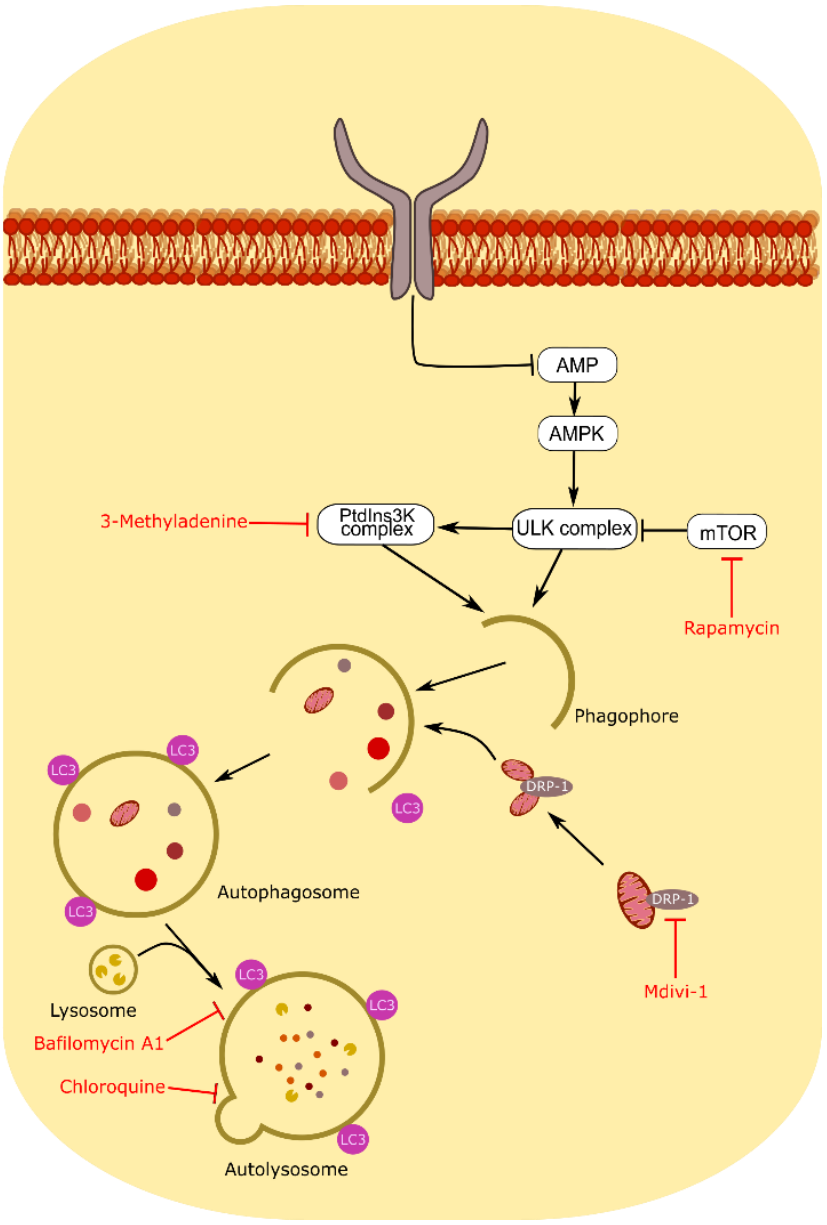

Figure 5. Autophagy pathway and its inhibitors. DRP-1: dynamin-related protein -1; LC3: microtubule-associated protein 1A/1B-light chain 3; mdivi-1: mitochondrial division inhibitor-1; mTOR: mechanistic target of rapamycin; PtdIns3K: phosphatidyl inositol triphosphate kinase; ULK: Unc-51-like activating kinase.

1.4.4. Ferroptosis

Ferroptosis is an iron-dependent, caspase-independent form of regulated cell death. It was identified by Stockwell and colleagues when they observed that erastin, an antitumor drug, can inhibit the cystine/glutamate antiporter, Xc- transporter, thereby causing the death of tumor cells (Dixon et al., 2012). In the cell, cystine is reduced to cysteine, the availability of which is rate-limiting for GSH synthesis. As described above, GSH is an antioxidant and a substrate of

GPX4 that reduces lipid peroxides to lipid alcohols (Xu et al., 2019b). Hence, cystine deprivation leads to the inactivity of GPX4 and the subsequent accumulation of lipid peroxides that are both hallmarks of ferroptosis (**Figure 6**).

The presence of lipid peroxides can be indirectly measured by malondialdehyde (MDA), an aldehyde form that is generated after multiple oxidation steps (Gaschler & Stockwell, 2017). Transferrin receptor 1 (TfR1), a transporter, that mediates the iron transfer into the cells, has also been proposed as a marker for ferroptosis (Feng et al., 2020).

Ferroptosis can also be triggered by signal transducer and activator of transcription 3, which, among others, is stimulated by the mitogen-activated protein kinase (MAPK) pathway. It has been reported that MAPK inhibitor is able to abrogate erastin-induced ferroptotic cell death (Gao et al., 2018a).

Some chemical inhibitors have been suggested to modulate ferroptosis (**Figure 6**). N-acetylcysteine supplies the rate-limiting amino acid cysteine for GSH synthesis and neutralizes lipids generated by arachidonate-dependent 5-lipoxygenase (Karuppagounder et al., 2018). Ferrostatin-1 inhibits the peroxidation of polyunsaturated fatty acids by blocking 15-lipoxygenase (Anthonymuthu et al., 2020). The water-soluble vitamin E analog Trolox prevents the propagation of lipid peroxidation and potentially blocks lipoxygenases (Stockwell et al., 2017). Deferoxamine, an iron scavenger, is proposed to decrease the iron overload in the cells and to exert cytoprotection by targeting a family of iron-dependent dioxygenases, the hypoxia-inducible factor (HIF) prolyl hydroxylases (Ratan, 2020). U0126 is a MAPK kinase inhibitor with an antioxidant activity (Stockwell et al., 2017).

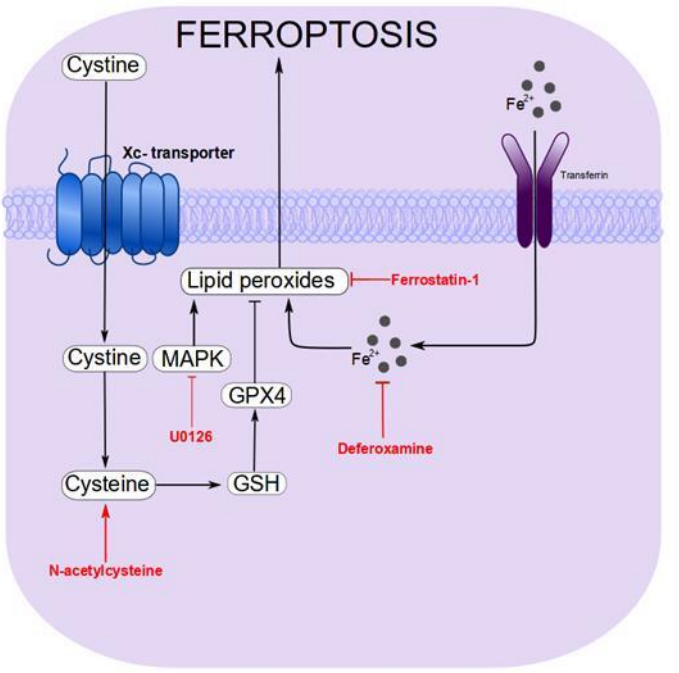

Figure 6. Ferroptosis pathway and its inhibitors. GSH: gluthathione; GPX4: gluthathione peroxidase 4; MAPK: mitogen-activated protein kinase

1.4.5. Parthanatos

Parthanatos is a cell death mechanism that is mediated by the accumulation of poly-(ADP-ribose) (PAR) polymers synthesized by PAR polymerase (PARP) upon DNA damage. Under physiologic conditions, the PARylation of proteins including PARP1 itself, occuring near the DNA damage site, facilitates the recruitment of DNA repair proteins (Fatokun et al., 2014). But once hyperactivated after excessive DNA damage, PARP-1 causes high PARylation that leads to the release of apoptosis-inducing factor (AIF) from mitochondria. AIF then binds macrophage migration inhibitory factor and translocates to the nucleus, where it causes DNA fragmentation and chromatin condensation. Moreover, activated PARP-1 consumes NAD+ and depletes ATP resulting in cellular energy collapse. Accummulation of these events leads to a cell death that resembles necrosis (Robinson et al., 2019) (**Figure 7**).

To block parthanatos, PARP inhibitors can be used. Olaparib mimics nicotinamide and competes with the catalytic end of PARP-1. However, Olaparib is not specific to PARP-1, but also targets PARP-2. In contrast, 3,4-dihydro-5-[4-(1-piperidinyl) butoxy]-1(2H)-isoquinolinone (DPQ) is a PARP inhibitor that more effectively intervenes with single stand breaks in DNA repair process (Ma et al., 2012).

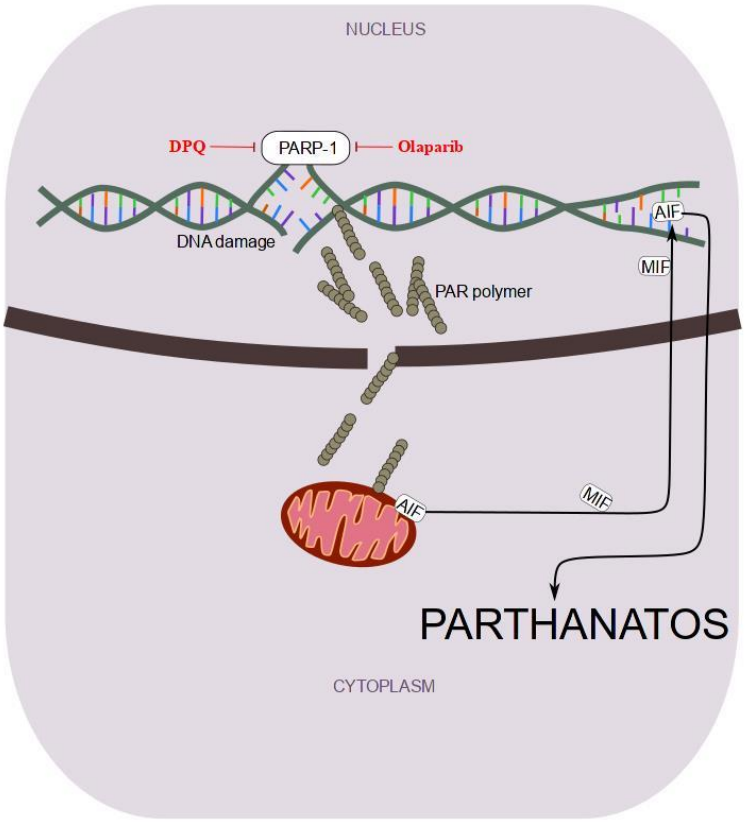

Figure 7. Parthanatos pathway and its inhibitors. AIF: apoptosis-inducing factor; DNA: deoxyribonucleic acid: MIF: macrophage migration inhibitory factor.

1.4.6. Hemin-induced cell death in ICH

Several studies have been conducted to understand how hemolysis products from ICH affect the survival of brain cells. Hemin-induced neuronal death has been extensively characterized and has been demonstrated to be mediated by ferroptosis and necroptosis (Zille et al., 2017). Astrocytes have been demonstrated to die after exposure to hemin (Chen & Regan, 2004; Dang et al., 2011; Laird et al., 2008; Owen et al., 2016; Regan et al., 2001). A study by Laird and colleagues suggested that this process is mediated by necroptosis (Laird et al., 2008).

Regarding brain endothelial cells, it has been reported that b.End3 cells, a brain endothelial cell line, were positive for Annexin V, a marker for apoptosis, when exposed to hemin (Sukumari-Ramesh et al., 2010; Xu et al., 2019a) and that cell death was prevented by Trolox and deferoxamine (Sukumari-Ramesh et al., 2010), which are currently regarded as inhibitors of ferroptosis. Furthermore, Liu and colleagues observed TUNEL-positive cells, a sign of apoptosis, in human brain microvascular cells under heme treatment (Liu et al., 2013). Furthermore, Imai and colleagues demonstrated that brain endothelial cell death was triggered by iron accumulation inside the cells (Imai et al., 2019). Besides these few studies, little is known about endothelial cell death in ICH. Our recent systematic review revealed only 29 records on endothelial cell death in hemorrhagic stroke between January 1, 2010 and August 7, 2019 (Zille et al., 2019a). This is surprising, considering that ICH is a common neurovascular disease.

Understanding the pathways leading to endothelial cell death is important to develop novel therapeutic interventions that target not only neurons but also endothelial cells.

1.5. Stem cell therapy in ICH

Besides protecting brain cells, stem cell therapy is an emerging therapy in ICH (Huang et al., 2020). Stem cells are thought to be able to replace and repair the damaged tissue, promote the generation of new brain cells, inhibit cell death, and to act as immunomodulators (for review see (Gao et al., 2018b; Ma et al., 2015)).

1.5.1. The potential of stem cell therapy in ICH

There are many studies that investigated the potential of stem cell therapy in ICH, including studies dealing with the most beneficial type of stem cells, how to produce them, how to administer them into the body, how many cells are needed, and what the best time window for therapy is (for review see (Gao et al., 2018b; Ma et al., 2015)). In rodent models, stem cell therapy has been demonstrated to reduce brain injury and improve behavioral outcome after ICH. Most of the studies used bone marrow-derived stem cells, induced pluripotent stem cells or human neuronal stem cells (for review, see (Cordeiro & Horn, 2015)).

Bone marrow-derived stem cells are multipotent somatic stem cells that promote angiogenesis and tissue remodeling, exert anti-inflammatory effects and stimulate the release of growth factors in rodent ICH (Bedini et al., 2018). Although bone marrow-derived stem cells can penetrate the BBB, only few cells have been detected in the brain. This indicates that their effect may occur rather due to the secretion of beneficial factors from the cells (Bedini et al., 2018). In line with this notion, the administration of conditioned medium from bone marrow-derived stem cells was equally effective in improving neurological outcome and tissue changes as transplantation of the stem cells (Cui et al., 2017).

Other stem cells such as embryonic stem cells have been reported to differentiate into neurons and glia near the hematoma cavity, but there is no evidence that they can migrate into the hematoma when injected intraventricularly in a rat model of ICH (Nonaka et al., 2004). More recently, induced pluripotent stem cells, that express similar properties as embryonic stem cells, have been demonstrated to improve functional outcome in rat ICH due to neuronal supplementation, neurotropic stimulation, and anti-inflammatory effects (Gao et al., 2018b; Qin et al., 2013). Hematopoetic stem cells are another potential candidate for stem cell therapy in ICH. They can be delivered via the blood circulation using granulocyte colony stimulating factor and exert neurorestorative functions in the brain (England et al., 2012).

Another alternative are neural stem cells that are derived from the nervous system and that have the ability to proliferate and differentiate. This type of stem cells can be obtained from the fetus (exogenous) or from endogenous sources such as the subgranular zone of the hippocampus and the subventricular zone (Kuhn, Dickinson-Anson, & Gage, 1996). Several studies have reported beneficial effects of neural stem cells for the treatment of ICH in rodents due to the advantage that these cells are endogenous to the brain and may therefore incorporate better into the host tissue (Jeong et al., 2003; Lee et al., 2007; Lee et al., 2009; Wakai et al., 2014). However, neural stem cell therapy is still far from clinical application due to the difficult collection procedure.

Although the safety of stem cell therapy for human brain injury has been confirmed, only a dozen clinical trials have been performed in ICH patients (Huang et al., 2020). Mesenchymal stem cells from umbilical cord or bone marrow were the two most commonly investigated types of stem cells in human clinical trials of ICH. Overall, the results of these few clinical studies indicate that stem cell transplantation may be beneficial for the treatment of ICH. A critical limitation of the performed trials is that the time of administration of the stem cells ranged from several weeks until more than one year after ICH, and studies of acute ICH need to be performed.

1.5.2. Aging as a challenge in stem cell therapy

Age is one of the challenges in stem cell therapy in the clinic (Goodell & Rando, 2015; Schulman et al., 2018). It is important to note that ICH mainly affects the elderly (Sharrief & Grotta, 2019) and that the management of geriatric patients requires special attention, since they often suffer from several chronic diseases, including hypertension, diabetes, chronic pain, or depression (Diederichs et al., 2011). Therefore, many of these patients are exposed to polypharmacy (Lauretani et al., 2014).

The inevitable combination of stem cells and drugs in clinical practice should be considered in therapeutic intervention to yield beneficial, potentially synergistic effects while avoiding detrimental ones (Napoli & Borlongan, 2016). Hence, a deeper understanding of the functional mechanisms of each drug and their interactions with stem cells is an important prerequisite for successful combination therapies (Sommer & Schaebitz, 2017).

2. Aims and experimental strategy

Both cytoprotective drugs and stem cell transplantation are promising candidates for secondary intervention after ICH. In my thesis, I systematically characterized the mechanisms underlying brain endothelial cell death in a model of ICH *in vitro* and performed a systematic literature search and meta-analysis on the interactions of drugs used in the elderly on stem cells.

In the first part of my PhD thesis, I hypothesized that the mechanisms underlying brain endothelial cell death are different from neuronal cell death, requiring different therapeutic strategies. Therefore, I systematically assessed chemical inhibitors of regulated cell death, including apoptosis, ferroptosis, necroptosis, autophagy, and parthanatos, for their ability to protect against hemin-induced toxicity in brain endothelial cells *in vitro*. These studies were complemented by investigations to detect cell death-specific biomarkers.

In the second part of my PhD thesis, I systematically searched the available literature about the interaction of drugs commonly used in elderly with neuronal stem cells (NSCs) and endothelial progenitor cells (EPCs). I identified (i) the effects of drugs on stem cell proliferation and differentiation, (ii) potential differences in exerting those effects according to drug classes, subclasses or particular drugs, and (iii) the mechanisms underlying drug-stem cell interactions.

3. Material and methods

3.1. Characterization of brain endothelial cell death in an *in vitro* model of hemorrhagic stroke

3.1.1. Materials

Table 1. Cells

Cell type	**Source**
b.End3 cells, mouse brain, endothelialpolyoma middle T antigen transformed	ATCC, CRL-2299
Primary porcine brain cortical endothelial cells (pBCEC)	donation from local slaughterer

Table 2. Chemicals

Item	**Company, catalogue number**
3-(4,5-dimethylthiazol-2-yl)-2,5-diphenyltetrazolium bromide (MTT)	Carl Roth, M5655-1G
3-Methyladenine	Enzo Life Sciences, BML-AP502-0025
Acetic acid	Sigma-Aldrich, D135801
Actinomycin D	Sigma-Aldrich, A1410
Amphotericin	Biochrom, A2612
Bafilomycin A1	LC Laboratories, B1080
Bovine serum albumin (BSA), albumin fraction V, M-66000 g/mol	Carl Roth, 80764
Chloroquine	Sigma-Aldrich, C6628
Collagen IV placenta	Sigma-Aldrich, C5533
Collagenase II	Biochrom, C228
Cycloheximide	Sigma-Aldrich, 018100
Cyclosporine A	LC Laboratories, C-6000
4′,6-diamidino-2-phenylindole (DAPI)	PanReac AppliChem, A1001

Item	Company, catalogue number
Deferoxamine	Sigma-Aldrich, D9533
Dimethylsulfoxide (DMSO)	Carl Roth, 47201
Dispase (neutral protease grade II)	Sigma-Aldrich, 04942078001
Dispase II	Roche, 04942078001
DNAse	Roche, 11284932001
3,4-dihydro-5-[4-(1-piperidinyl)butoxy]-1(2H)-isoquinolinone (DPQ)	Cayman Chemical, 14450
Dulbecco's Modified Eagle's Medium-Nutrient Mixture Ham's F-12 (DMEM/F-12) with L-glutamine	Thermo Fisher, 21041025
Dulbecco's Phosphate Buffered Saline without calcium without magnesium	Biowest, L0651500
Dulbecco's Modified Eagle's Medium (DMEM) with 4,5 g/l glucose, stable glutamine, 0,11 g/ml sodium pyruvate; 3.7 g/l $NaHCO_3$	Pan Biotech, P0404510
Erastin	Selleck Chemicals, S7242
Ferrostatin-1	Sigma-Aldrich, SML0583
Fetal calf serum (FCS)	Merck, S0115
Formaldehyde	Carl Roth, 73981
Gentamicin (50 mg/ml)	Thermo Fisher, 15750045
Glutamax (100 mM)	Thermo Fisher, 35050061
GSK872	Merck, 530389
Hemin (bovine)	Sigma-Aldrich, H9039
HEPES buffer solution (1 M)	Thermo Fisher, H4034500G
Hoechst 33342	Sigma-Aldrich, 14533
M199 medium with Earle's Salts, L-glutamine	Thermo Fisher, 31150022
Mdivi-1	Enzo Life Sciences, BML-CM127-0010
Methanol	Chemsolute, 1437.2511
Normal goat serum (NGS)	Jackson Immunoresearch, 005.000.001
N-acetylcysteine	Sigma-Aldrich, A7250

Item	Company, catalogue number
Necrostatin-1	Enzo Life Sciences, BML-AP309-0020
Necrostatin-1 inactive control	Merck, 480066
Necrosulfonamide	Millipore, 480073
Olaparib	LC Laboratories, O-9201
Penicillin/streptomycin (100X)	Merck, A2213
Percoll	GE healthcare, 17089101
Phosphate Buffer Saline (PBS) pH 7.2 without calcium, without magnesium	Thermo Fisher, 20012068
Propidium iodide	Carl Roth, CN74.1
Puromycin	Sigma-Aldrich, P883325MG
Rapamycin	Sigma-Aldrich, R87811
SB203580	LC Laboratories, S-3400
SP600125	LC Laboratories, S-7979
Triton X-100	Promega, H514a
Trolox	Enzo Life Sciences, ALX-270-267-M100
Trypsin	Sigma-Aldrich, L2143
U0124	Merck, 662006
U0126	LC Laboratories, U-6770
Z-VAD-FMK	Enzo Life Sciences, ALX-260-020-M001

Table 3. Primary antibodies

Antibody	**Company, catalogue number, RRID**	**Dilution**
Claudin-5, rabbit polyclonal antibody	Thermo Fisher, 34-1600, RRID:AB_2533157	1:500
Cleaved caspase-3 (Asp175) (5A1E), rabbit monoclonal antibody	Cell Signaling, 9664, RRID:AB_2070042	1:500
CD71 (3B8 2A1)/transferrin receptor 1, mouse monoclonal antibody	Santa Cruz, #sc-32272 RRID: AB_627167	1:50
Desmin, rabbit polyclonal antibody	Sigma-Aldrich, #D8281, RRID: AB_476910	1:500
α-smooth muscle actin (αSMA), mouse monoclonal antibody	Dako, #M0851, RRID:AB_2313736	1:500
Malondialdehyde (MDA), clone 1F83, mouse monoclonal antibody	JaiCA, #JAI-MMD-030N	1:100
LC3A, rabbit monoclonal antibody	Cell signaling, #4599 RRID: AB_10548192	1:2000

Table 4. Secondary antibodies

Antibody	**Company, catalogue number, RRID**	**Dilution**
Goat anti-rabbit IgG (H+L) cross-adsorbed secondary antibody, Alexa Fluor 546	Thermo Fisher, A-11010, RRID:AB_2534077	1:1000
Goat anti-rabbit IgG (H+L) highly cross-adsorbed secondary antibody, Alexa Fluor 488	Thermo Fisher, A-11034, RRID:AB_2576217	1:1000
Goat anti-mouse IgG (H+L) highly cross-adsorbed secondary antibody, Alexa Fluor 488	Thermofisher, A-11001 AB_2534069	1:1000

Table 5. Equipment

Equipment	**Company, model number**
Flow cytometer	BD Biosciences Accuri C6
Fluorescence microscopes	Leica DMI6000 B Zeiss Axio Observer
Incubator	Binder
Neubauer hemocytometer	Optik Labor
Plate reader	Clariostar, 521. R2
Shaker with heater function	Infors HT Ecotron
Time-lapse microscope	Olympus IX81

Table 6. Software

Software	**Version, RRID**
EndNote	Version X7, RRID:SCR_014001
GraphPad Prism	Version 5.0, RRID:SCR_002798
IBM SPSS	Version 23, RRID:SCR_002865
ImageJ/Fiji	Version 1.51S, RRID:SCR_003070
Cochrane's Review Manager	Version 5.3, RRID:SCR_003581

3.1.2. Cell culture

The use of immortalized brain endothelial cells has the advantage that it is cost-effective and that the cells are easy to handle due to their stable phenotype and the high availability of the cells (Helms et al., 2016). BEnd.3 cells express some of the transporters such as glucose transporter 1, monocarboxylate transporter 1 and organic anion transporter 1 (Omidi et al., 2003). In contrast, primary porcine brain endothelial cells (pBCEC) reach higher transepithelial electrical resistance values than immortalized endothelial cells, a measure of BBB tightness

(Cohen-Kashi Malina et al., 2009; Patabendige et al., 2013). However, pBCEC isolation requires more time and is more cost intensive, and the variability between cell isolations is high (Helms et al., 2016). Therefore, we decided to perform the initial systematic screening of cell death inhibitors in bEnd.3 cells and validated the protective chemical inhibitors in pBCECs.

3.1.2.1. bEnd.3 cell culture

I cultivated the mouse brain endothelial bEnd.3 cell line in DMEM medium (containing 10 % FCS and 1 % penicillin/streptomycin) in culture flasks in a humidified incubator at 37 °C with 5 % CO_2. Cells were passaged by trypsination and used at passages 7-20. Twenty-four hours after trypsination, the medium was exchanged to reduce the debris. For experiments, I seeded the cells, after counting with a Neubauer hemocytometer, at 1 000-8 000 cells/well in 96-well plates.

To assess whether the bEnd.3 cell cultures were indeed pure endothelial cells cultures, I fixed the cells when they were grown confluent and stained them with smooth muscle actin and desmin as markers for mural cells (smooth muscle cells and pericytes) (see section **3.1.7. Immunofluorescence**).

3.1.2.2. pBCEC cell culture

I performed pBCEC culture based on a protocol from Tontsch & Bauer with modifications (Tontsch & Bauer, 1989).

3.1.2.3. Coating of the well plates

I coated the 96-well plates with 0.1 mg/ml collagen IV (in 0.05 % acetic acid in PBS) the day before the cell isolation to ensure proper attachment of the cells. The plates were kept at 4 °C in the refrigerator overnight. Before cell seeding, I washed the plates once with PBS to remove the acetic acid.

3.1.2.4. Isolation of pBCECs

The pig brains were donated from a local slaughterer and transferred into PBS solution containing 1 % penicillin/streptomycin on ice immediately. During the dissection of the tissue, I removed the meninges and collected the grey matter carefully and minced it as small as possible with a scalpel. I transferred the minced grey matter into 10 mg/ml dispase solution (3 half brains per reaction tube in 30 ml). Dispase is a neutral protease that hydrolyzes the N-terminal peptide bonds on non-polar amino acids. It can be used to separate the tissue without damaging the cell membrane and also prevents clumping. I dissociated the grey matter tissue using a 25-ml serological pipette followed by a 10-ml pipette. I transferred the dissociated tissue

into cell culture flasks (1 reaction tube per 175 cm²-flask) and incubated it on a heated shaker (37 °C, 150 rpm) for 70 minutes.

Then, I added 20 ml of the tissue solution to a gradient solution (containing 12 ml Percoll and 18 ml DMEM) and mixed it by inverting. Percoll is a colloidal silica with a lower viscosity compared to other substances, which helps to separate tissues by isopycnic centrifugation. I centrifuged the solution at 4 °C and 2890xg for 30 minutes without break. I discarded the fatty layer and carefully collected the cloud (capillary fragments) above the red pellet (erythrocytes), which I then added into a reaction tube containing 30 ml of DMEM. The suspension was centrifuged at 4 °C and 240xg for 20 minutes with break. I discarded the supernatant and resuspended the pellet in collagenase II (1.5 ml/two pellets; 3 ml for three or more pellets) and then reunited all the pellets. Collagenase digests nearly all collagen fibers including those in the extracellular matrix. I transferred the suspension into a 50 ml reaction tube that was fixed it on a shaker at 150 rpm at 37 °C. I resuspended the cell suspension after 7 and 14 minutes. After 20 minutes, I added 3.3 µL DNase (10 µg/ml) to the suspension and incubated it for another 5 minutes at 37 °C. Then, I resuspended the suspension again and added 30 ml DMEM. The suspension was centrifuged at 4°C and 240xg with break for 10 minutes. I discarded the supernatant and resuspended the pellet in 5 ml plating medium (M199 medium including 10 % FCS, 1 % P/S, 1 % gentamicin and 1 mM glutamax).

3.1.2.5. Flow cytometric cell counting

The dissection method of the pBCECs from primary brain tissue results in a cell suspension containing erythrocytes, pBCECs as well as other cells with nuclei (such as pericytes and smooth muscle cells). Since the number of erythrocytes varies between different dissections, counting with a Neubauer hemocytometer will result in imprecise cell counts because it is not straightforward to distinguish erythrocytes from other cells. Therefore, I established a flow cytometric cell counting method.

Flow cytometry works by aligning the cells into single flow using the hydrodynamic properties of the sheath fluid. Erythrocytes and other cell types can be distinguished based on the forward and sideward scatter. The forward scatter is related to the cell size and sideward scatter is related to granularity of the cells. The difference in size and granularity of erythrocytes, due to the absence of a nucleus, yields a cluster of cells distinct from cells that contain a nucleus (**Figure 8).**

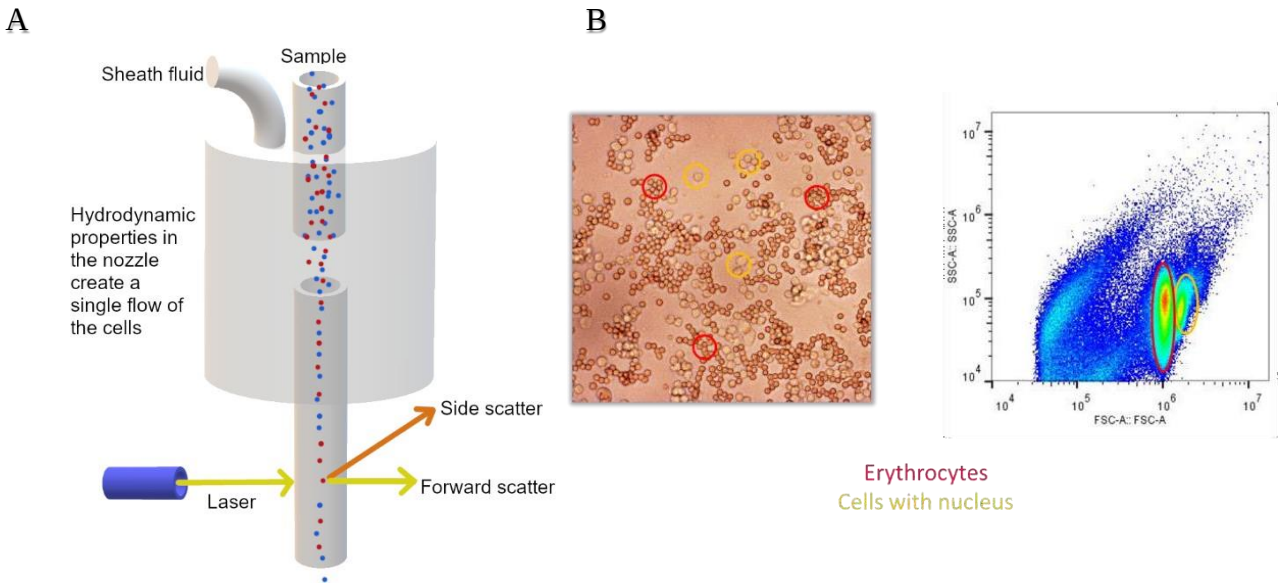

Figure 8. Cell sorting mechanism of flow cytometry. A. The working mechanism of flow cytometry for cell counting. **B.** The microscopic picture of the pBCEC cell culture after plating (left) and cell analysis using FACS (right) to distinguish erythrocytes (red) and cells with nucleus (yellow).

For cell counting by flow cytometry on a BD Accuri C6, I diluted 10 µl of the cell suspension 1:100 in culture medium and measured the number of events in 100 µl cell suspension. The number of cells containing nuclei per ml was calculated with the following formula:

Number of events x 10 x 100 = n cells per ml

3.1.2.6. Selection of pBCECs in culture

I plated the cells based on the number of cells with nucleus as counted using flow cytometry. 120 000 to 240 000 cells/well in 96-well plates were plated in M199 medium containing 10 % FCS, 1 % P/S, 1 % gentamicin, 1 mM Glutamax and 0 to 4 µg/ml puromycin. Puromycin is an antibiotic that causes premature chain termination during translation. It is used to select for endothelial cells because puromycin is a substrate for ABC transporters in endothelial cells and is therefore exported out of these cells (Demeuse et al., 2004; Theile et al.,2010). In contrast, cells lacking ABC transporters cannot export puromycin and die upon incubation with this antibiotic at certain concentrations.

Here, I incubated the isolated cells with puromycin for 48 hours with a media change at 24 hours in culture to remove dead cells and debris. At 48 hours, I exchanged the media to culture medium

without puromycin. Subsequently, I exchanged the medium every 3 days. During the whole time of cultivation, the cells were incubated in a humidified incubator at 37 °C with 5 % CO_2.

To assess the purity of the pBCECs in culture, I fixed the cells when grown confluent, and stained them with smooth muscle actin and desmin as markers for mural cells (smooth muscle cells and pericytes) (see section **3.1.7. Immunofluorescence**).

3.1.3. Cell culture experiments

3.1.3.1. Pharmacological characterization of brain endothelial cell death

When the cells reached 80 % confluence (day 3 after seeding in bEnd.3 or day 9 after seeding in pBCEC), I performed the cell treatments. I used hemin to mimic the secondary damage that is caused by hemolysis products in ICH.

First, I wanted to determine the concentration of hemin at which 50 % of the cells die at 24 hours of treatment. I dissolved hemin in sodium hydroxide and further diluted in distilled water to a 10 mM stock solution. I applied increasing concentrations of hemin between 0 and 1000 µM in culture medium (pH 7.2). I assessed cell death using the MTT assay (see section **2.5. MTT assay**) and Hoechst/PI staining (see section **2.6. Hoechst/PI staining**).

To determine the cell death mechanisms underlying hemin toxicity in endothelial cell, I performed co-treatment of hemin with different pharmacological inhibitors of cell death pathways at five different concentrations (**Table 7**). The pharmacological inhibitors were first dissolved in DMSO, except deferoxamine and N-acetylcysteine that were dissolved in water and Trolox that was solved in ethanol. The inhibitors were further diluted in cultured medium at the day of the experiment. The experiments were performed in a blinded manner.

Table 7. The concentrations of cell death inhibitors used in this study.

Cell death inhibitor		Target	Concentration [µM]				
Ferroptosis	Actinomycin D	mRNA synthesis	0.001	0.01	0.1	0.5	1
	Cycloheximide	Protein synthesis	0.01	0.1	1	10	50
	N-acetylcysteine	Reactive oxygen species (ROS), reactive lipid species (RLS)	125	250	500	1000	2000
	Deferoxamine	Iron, hypoxia-inducible factor prolyl hydroxylase domain-containing inhibition	12.5	25	50	100	200
	Ferrostatin-1	Canonical ferroptosis inhibitor, RLS	0.01	0.1	1	5	10
	Trolox	RLS	0.01	0.1	1	10	100
	U0126	Mitogen activated protein kinase kinase 1/2	0.1	1	5	10	20
	U0124	U0126 inactive control	0.1	1	5	10	20
Apoptosis	Z-VAD-FMK	Caspases	0.1	1	10	50	100
	SB203580	P38 mitogen-activated protein kinase	0.1	1	5	10	30
	SP600125	c-JUN-N-terminal kinase	0.01	0.1	0.5	1	5
	Cycloheximide	Protein synthesis	0.01	0.1	1	10	50
Necroptosis	Necrostatin-1	Receptor-integrating protein kinase (RIPK) 1	1	10	50	100	250
	Necrostatin-1 inactive control	Inactive necrostatin-1 analog	1	10	50	100	250
	GSK872	RIPK3	1	3	10	20	30
	Necrosulfonamide	Mixed lineage kinase domain-like	0.1	1	5	10	20
Parthanatos	Olaparib	Poly (ADP ribose) polymerase 1 and 2 (PARP1 and 2)	0.1	1	10	25	50
	DPQ	PARP1 and 2	0.1	1	5	10	20
Autophagy	3-Methyladenine	Phosphatidyl inositol triphosphate kinase, autophagosome formation	1	10	100	500	1000

Cell death inhibitor		Target	Concentration [µM]				
	Bafilomycin A1	Endosomal acidification	0.0001	0.001	0.01	0.05	0.1
	Chloroquine	Lysosomal function	0.01	0.1	1	5	10
	Mdivi-1	GTPase activity in dynamin-related protein 1, abnormal mitophagy	0.1	1	10	50	100

Each concentration was added to four different wells (technical replicates, **Figure 9**) per biological replicate/experiment. I determined the sample size for the bEnd.3 cells *a priori* based on power calculations with the significance level at 0.05 and test power at 0.8 using G*power.

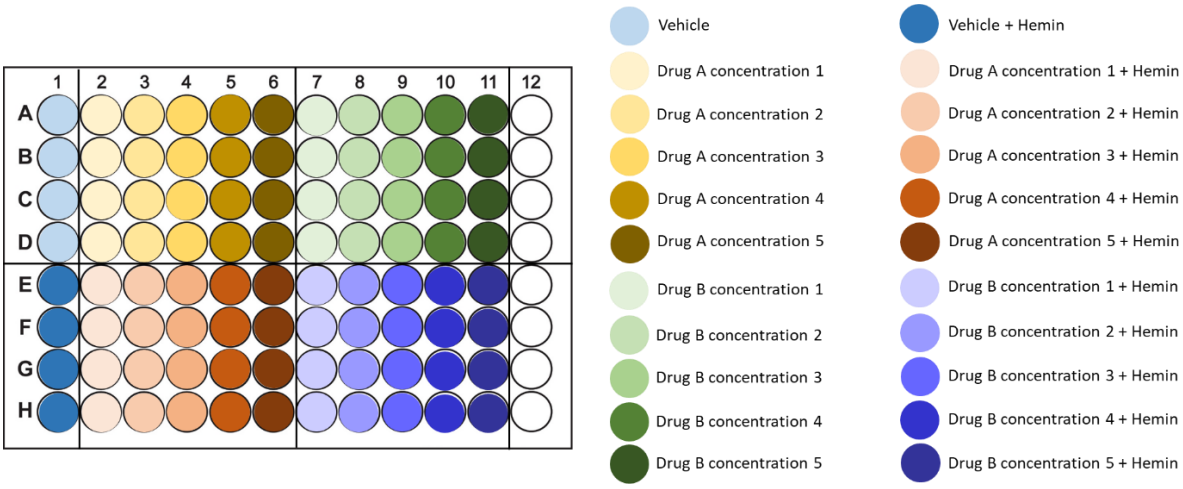

Figure 9. Pipetting scheme of the cell death inhibitors in a 96-well plate.

3.1.4. Positive controls of the cell death mechanisms

3.1.4.1. Staurosporine-induced apoptosis

I used staurosporine as a positive control for apoptosis. Staurosporine is a well-known inducer of apoptosis in a number of cell types where it leads to the cleavage of caspase-3 (Jacobsen et al.,1996).

I assessed whether staurosporine can induce cell death in bEnd.3 cells. Staurosporine was dissolved in DMSO and further diluted in culture medium on the day of the experiment. I used a concentration of 500 nM staurosporine, shown to induce apoptosis (Malsy et al., 2019; Thuret et al., 2003), in the absence or presence of 100 µM of the pan-caspase inhibitor Z-VAD-FMK. After 9 hours of treatment, I fixed the wells and stained them for cleaved caspase-3 (see section **3.1.7. Immunofluorescence**).

3.1.4.2. Erastin-induced ferroptosis

I used HT22 cells, a mouse hippocampal neuronal cell line, treated with erastin as a positive control for the induction of ferroptosis (Zille et al., 2019b). I did not use bEnd.3 cells treated with erastin as a positive control here since there is no record about erastin-induced ferroptosis in bEnd.3 cells. Cells were treated with 0.5 µM erastin in the absence or presence of 5 µM ferrostatin-1, a ferroptosis inhibitor.

3.1.4.3. Rapamycin-induced autophagy

Rapamycin was used to induce autophagy in bEnd.3 cells (Chan et al., 2018). I treated the cells with 0.5 µM rapamycin, shown to induce autophagy (Lei et al., 2012; Subirada et al., 2019), in the absence or presence of 0.01 µM bafilomycin-A1, an autophagy inhibitor.

3.1.5. MTT assay

To assess the overall cell viability, I used the 3-(4,5-dimethylthiazol-2-yl)-2,5-diphenyltetrazolium bromide (MTT) assay. The MTT assay is a well-known colorimetric assay that has many advantages, such as time- and cost-efficiency. It converts the yellowish MTT into purple-colored formazan. While mitochondrial involvement in MTT reduction has been suggested, most MTT reduction occurs through NADH and NADPH that transfer electrons to MTT (**Figure 10**) (Berridge & Tan, 1993). The optical density of the MTT signal in the cell culture is inversely correlated to the cell death. However, if a treatment interferes with the levels of NADH or NADPH without triggering cell death, a false signal occurs. The MTT assay only measures the metabolic activity of a cell population. Therefore, additional confirmation using microscopy or another cell death measurement is needed. Although the metabolic activity is not always identical with the number of cells, the MTT assay provides a fast and reliable approach to assess cell viability.

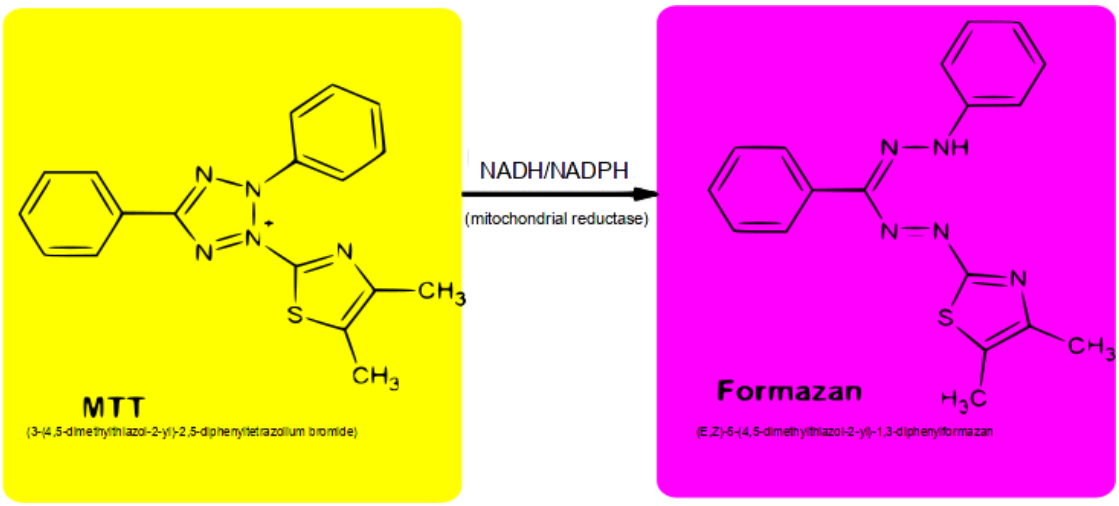

Figure 10. Reaction of the MTT assay.

For the assay, I removed the culture medium and incubated the cells with the MTT solution (10 % of a half-saturated solution prepared in PBS was added to the culture medium) for two hours at 37 ºC. Then, I removed the MTT and washed the plates once with PBS because at high concentrations, hemin increases the absorbance by itself due to its inherent color, which would interfere with the MTT measurements. Then, I replaced the PBS by DMSO (50 µl/well) to dissolve the formazan crystals and measured the plates with a Clariostar plate reader. Measurements were performed with the absorbance spectra detection mode using discrete wavelengths. Changes in absorbance were measured at 550 nm. However, as DMSO has an inheritent absorbance of approximately 0.03 OD, I also measured the wells at the reference wavelength of 655 nm and subsequently subtracted the OD value from that at 550 nm. The values were normalized to the vehicle-treated cells.

3.1.6. Hoechst/PI staining

Propidium iodide (PI) is a non-cell-permeable red-fluorescent dye. It is excited at wavelengths between 400 and 600 nm and emits light between 600 and 700 nm, when bound to DNA. It only enters dead cells with compromised cell membranes (Crowley et al., 2016b). Hoechst 33342 is a cell-permeable blue-fluorescent dye (excitation/emission maxima ~350/461 nm, when bound to DNA) that stains the chromatin in living cells (Crowley et al., 2016a). Condensed chromatin in dying cells (mostly apoptotic) will appear more brightly than the

chromatin in normal cells. Therefore, PI can be used to measure cell death, while Hoechst can be used as an indicator for living cells (except when chromatin is condensed in apoptotic cells).

I added 1 µg/ml of Hoechst and 3.3 µg/ml PI solution per well to the cells without changing the medium. The plates were incubated for 15 minutes at 37 ºC and photomicrographs were taken immediately with a Leica DMI6000 B fluorescence microscope. I acquired three images per concentration and quantified the number of Hoechst- and PI-positive cells using ImageJ in a blinded manner. I applied manual thresholding were possible and additionally analyzed the cells using manual counting to adjust for cell aggregations that cannot be separated by manual thresholding. The ratio of PI- to Hoechst-positive cells was used as a measure of cell death.

3.1.7. Immunofluorescence

Immunofluorescence is a method to detect the presence of an antigen in the tissue by tagging it with a specific antibody (Madangarli et al., 2019). Fixation maintains the cell structure and its antigenicity while the primary antibody binds to the antigen. The secondary antibody that is fluorescently labeled then enhances the signal by binding to the heavy chain of the primary antibody. The use of a nonionic detergent such as Triton X-100 helps to limit the background signal by reducing the hydrophobic binding of immunoglobulin and tissue proteins (Bamm et al., 2004).

I fixed the cells with 4 % paraformaldehyde in PBS for 10 minutes at room temperature, except for MDA, TfR1, and LC3 staining, where I fixed the cells with 100 % cold methanol for 15 minutes at -20°C. Then, I washed the cells twice with PBS and incubated them with blocking solution (2 % BSA in 0.5 % Triton X-100 in PBS or 5 % NGS in 0.5 % Triton X-100 in PBS, for MDA, TfR1, and LC3) for 30 minutes at room temperature. The cells were incubated with the primary antibodies at 4°C overnight. The next day, I washed the cells three times with PBS and then incubated them with the secondary antibodies in the respective blocking solution at room temperature for one hour in the dark. After washing the cells with PBS, I performed nuclear counterstaining using the fluorescent dye DAPI (4′,6-diamidino-2-phenylindole, 2 mg/ml) for 10 minutes at room temperature. Then, I washed the cells three times with PBS. The cells were protected from light until fluorescence microscopy was performed using a Leica DMI6000 B microscope. I quantified the number of positive cells relative to the total number of cells in a blinded manner on three fields of view per experimental condition and biological replicate.

3.1.8. Statistical analysis

I evaluated normality by Kolmogorov-Smirnov test and variance homogeneity using Levené test. For normally distributed data with homogeneous variance, one-way analysis of variance followed by post hoc Bonferroni test was performed. When one of the criteria was not met, Kruskal-Wallis test was performed followed by post hoc Mann-Whitney *U* test with α-correction according to Bonferroni to adjust for the inflation of type I error because of multiple testing. Data are represented as mean ± standard deviation (SD) except for nonparametric data, in which case medians and interquartile ranges are given. A value of $P < 0.05$ was considered statistically significant. For Kruskal-Wallis test followed by Mann-Whitney *U* test, $P = 0.05/k$ was used, with *k* as number of single hypotheses. To analyze contingency tables, Fisher's exact test was used. I performed all statistical analyses with IBM SPSS version 21.

3.2. Systematic review

I conducted a systematic review according to the guidelines for Preferred Reporting Items for Systematic Reviews and Meta-Analyses (PRISMA) (Moher et al., 2009).

3.2.1. Search strategy and selection criteria

I searched for publications listed in PUBMED describing the effect of drugs frequently used in geriatric patients on NSCs and EPCs. The detailed search queries are provided in the **Supplemental Data**. Publications between January 1, 1991 and June 7, 2018 for NSCs and between January 1, 1991 and September 18, 2020 for EPCs were included. Data from pathological cells (e.g., tumor cell lines) and non-mammalian species were excluded. I included *in vitro* and *in vivo* studies as well as clinical trials of the central nervous system. For EPCs, I included only studies that analyzed the effect of EPCs in the brain under drug treatment. Only publications in peer-reviewed journals containing primary data were used for analysis. Review articles, articles without full-text accessibility, and non-English articles were excluded.

3.2.2. Selection of publications and data extraction

I screened the abstracts and subsequently reviewed the full-text versions of the potentially eligible publications. In case of doubt, publications were discussed in consensus meetings with two other investigators (Dr. Marietta Zille and Prof. Dr. Dr. Johannes Boltze). After screening,

I performed a quality synthesis that included all aspects that shape the quality of the papers, such as the addressing outliers, the use of technical or biological replicates, and the statement of blinded assessment. I then assessed the distribution of the use of drugs and drug classes, the sample numbers and effect sizes and determined the outcome parameters related to proliferation and differentiation. Where data were stated in the text, numerical values were extracted. When a study reported several experiments, each experiment was considered as an independent experiment. I used only the largest concentration that had an effect on the stem cells.

In NSCs, I discriminated three distinct conditions under which the data were gathered: 1) "physiologic", in which the physiological state of the NSCs was investigated, without any modification of the cells or animals during the experiment, 2) "injury" (including mental disorders), where the sample a) mimicked a phenotype of disease (as disease models) or b) received a psychological challenge such as depression or a harmful or negative physical stimulus (e.g., pain), and 3) "modified", in which the animals were either genetically modified (transgenic), were housed in an enriched environment, or exposed to a combination of drugs. I identified proliferation by bromodeoxyuridine, Ki67, 3H-thymidine, 5-iodo-2-deoxyuridine staining and differentiation by detection of doublecortin, neuronal nuclei, neuron-specific class III beta-tubulin, ionized calcium-binding adaptor molecule 1, nestin, glial fibrillary acidic protein, microtubule-associated protein 2, or beta-III tubulin. In EPCs, I divided the papers based on the drugs and the disease model that was used.

For meta-analysis, two persons independently extracted the relevant data from the included publications (Alex Palumbo and myself) as recommended by the PRISMA guidelines. We collected data on sample size, mean, standard deviation, *P*-value, statistical analysis, and the reported mechanism underlying the action of the drugs on NSCs. I contacted the authors of the publications that did not provide the complete dataset to collect the missing information. In case the data were only available as graphs, I performed graphical measurement using ImageJ to calculate the mean and standard deviation.

3.2.3. Statistical analysis

To compare the data from the different publications, I used the standardized mean difference (SMD) since the measurement units of proliferation and differentiation were very diverse among the publications. Hedge's g SMD with correction factor was chosen due to the small sample size (below 20 samples for each study). I applied partitioning of heterogeneity to

determine the significance of the reported study quality explaining the differences in observed efficacy. I calculated an estimate of effect size based on the visual assessment of the forest plot and I^2 value by the DerSimonian and Laird random effect model meta-analysis. A confidence interval of 95 % was applied. I generated the analyses using Cochrane's Review Manager Software for meta-analysis. A probability value of $p < 0.05$ was considered statistically significant.

4. Results

4.1. Characterization of brain endothelial cell death in an *in vitro* model of hemorrhagic stroke

4.1.1. Establishment of brain endothelial cell culture

To investigate endothelial cell death after hemorrhagic stroke, I first needed to establish the optimal culture conditions for bEnd.3 cells and pBCECs.

4.1.1.1. Determination of the optimal plating densities and the time of treatment
I first determined the optimal cell density for plating to ensure sufficient confluence at the time of treatment. As pBCECs were freshly isolated from pig cortices, the isolated cell suspension still contained other cells including erythrocytes, neurons, astrocytes, and mural cells that needed to be excluded by puromycin treatment (see section **3.1.2.6. Selection of pBCECs in culture**). Cell counting based on the forward/sideward scatter allowed to estimate the number of all cells with nucleus. I plated 120 000, 180 000 and 240 000 isolated cells with nucleus per well in 96-well plates. At day 7 after plating, 180 000 cells per well reached a confluency of 70-80 % that was chosen for the following experiments **(Figure 11).**

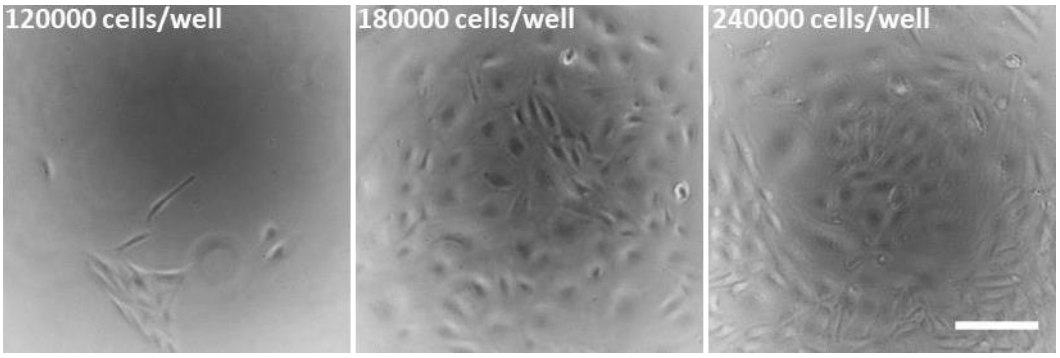

Figure 11. Different densities of pBCEC in culture. The cells were observed at day 7 after seeding in 96-well plates. Scale bar = 50 µm.

In contrast to pBCECs, bEnd.3 cells are a pure cell line; hence, the plating numbers are comparably lower. I plated bEnd.3 cells at a density of 1 000, 2 000, 4 000, 5 000, 6 000, and 8 000 cells/well in 96-well plate. At two days after plating, 4000 cells/well reached a confluency of 70-80 % (**Figure 12**).

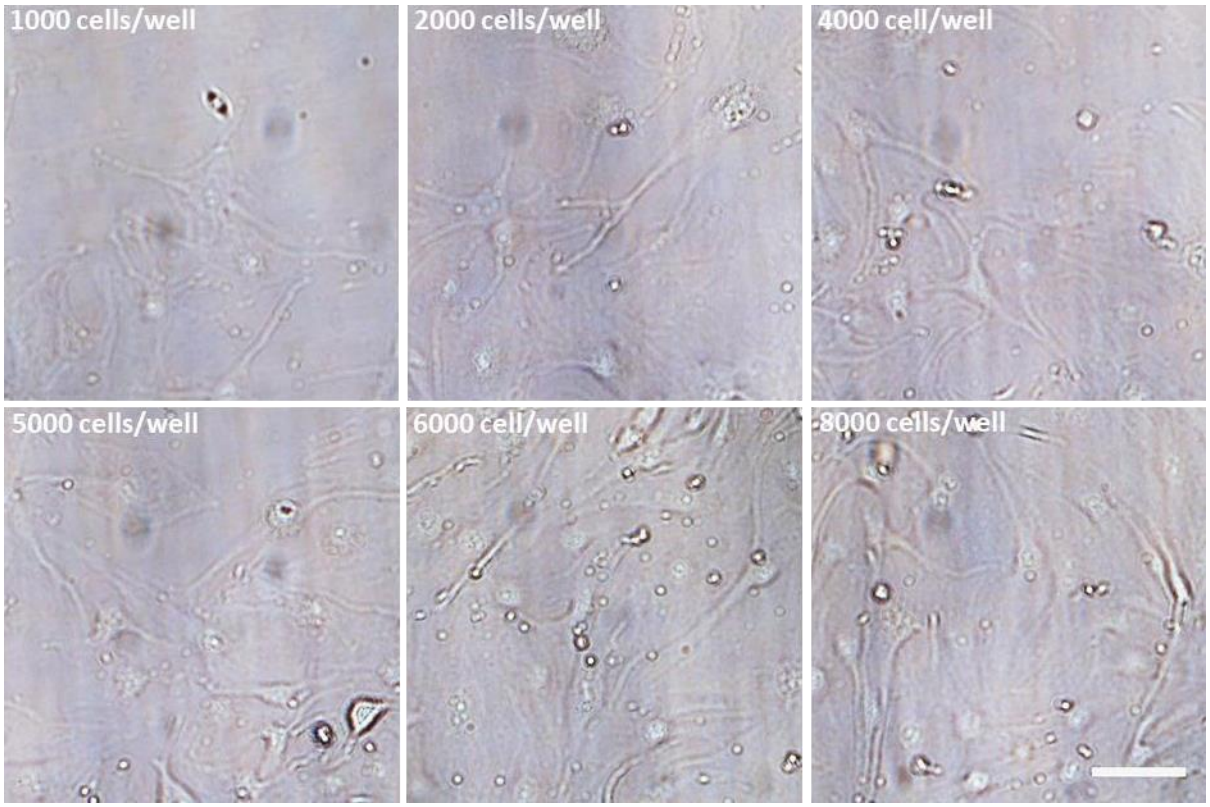

Figure 12. Different densities of bEnd.3 cells. The cells were observed at day 3 after seeding in 96-well plates. Scale bar = 50 µm.

4.1.1.2. Determination of optimal medium and serum conditions

As the cells continue to proliferate in culture, the increase in cell numbers due to the proliferation may mask some of the effects of the different treatments I wanted to study. Therefore, I investigated whether a reduction of the serum concentration in the medium or the use of a different medium affected the proliferation of the cells in culture.

I plated bEnd.3 cells with 0, 1, 2.5, 5 or 10 % FCS in DMEM or DMEM F12 and quantified the metabolic activity as a surrogate of cell density for 72 hours. Under all different culture conditions, bEnd.3 cells continued to proliferate **(Figure 13)**. I therefore decided to continue with the plating medium for all following treatments.

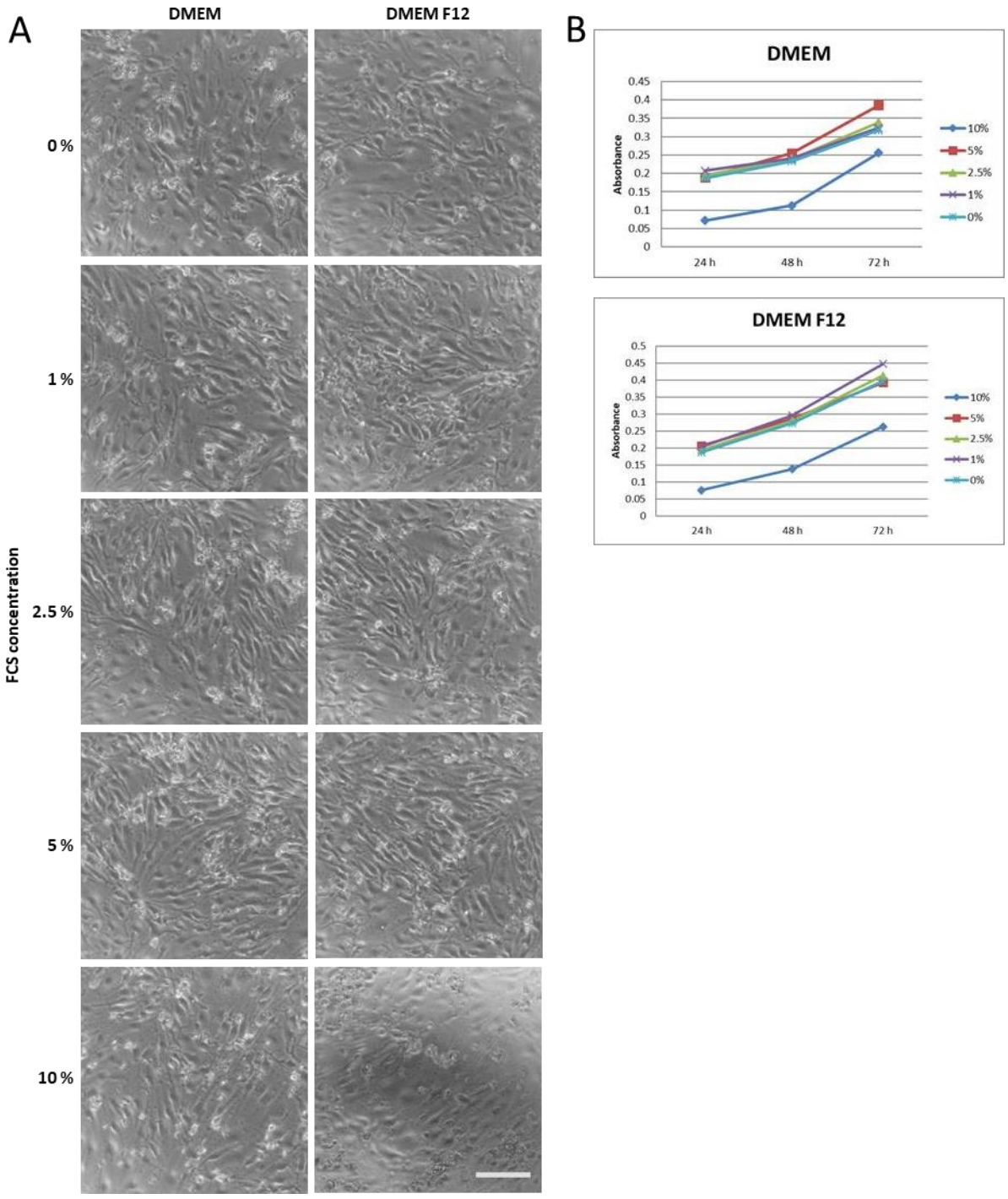

Figure 13. Different serum concentrations did not affect the metabolic activity of bEnd.3. bEnd.3 cells were cultured in 96-well plates using a density of 4000 cells/well. **A**) Phase-contrast images of different FCS concentrations in DMEM and DMEM F12 medium after 24 hours. **B**) MTT values of the different FCS concentrations (0, 1, 2.5, 5, and 10 %) at 24, 48, and 72 hours in culture. Scale bar = 50 µm.

4.1.1.3. Purity of brain endothelial cell cultures

For the pBCEC culture, I used puromycin to select for endothelial cells in the culture. Puromycin is a protein synthesis inhibitor that is toxic to cells except for brain endothelial cells as they express P-glycoprotein that exports puromycin outside the cells. This property was therefore used to purify the culture from non-endothelial cells. To verify the purity of the pBCEC culture, I tested different concentrations of puromycin and performed immunostaining for mural cells (pericytes and smooth muscle cells) with desmin and αSMA. Desmin is a contractile protein that is commonly found in pericytes and smooth muscle cells and αSMA is a smooth muscle actin marker. I observed that puromycin effectively reduced the presence of cells positive for desmin and αSMA (**Figure 14A**). As expected, bEnd.3 cells were negative for desmin and αSMA (**Figure 14B**).

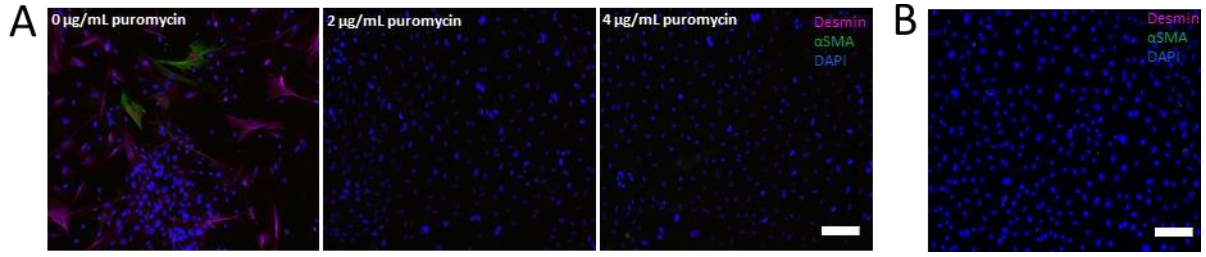

Figure 14. Purity of brain endothelial cell cultures. Cells were immunostained with desmin (magenta, pericytes and smooth muscle cells), αSMA (green, smooth muscle cells), and DAPI (blue, nuclei). **A**) pBCEC culture at day *in vitro* 7 under different puromycin concentrations and **B**) bEnd.3 culture. Scale bars = 200 µm.

4.1.2. Hemin concentration-response in bEnd.3 cells

Since hemin has been demonstrated to induce cell death in different cell types at different concentrations, I sought to determine the half-maximal effective concentration (EC_{50}) of hemin at which to investigate the cell death mechanisms. BEnd.3 cells were treated with different concentrations of hemin for 24 hours and the cell death was qualitatively observed using phase-contrast microscopy and quantified using Hoechst/PI cell counting and MTT assay.

Phase-contrast imaging demonstrated that the bEnd.3 cells died in a concentration-dependent manner. Starting at 300 µM hemin, the cells changed their morphology to a round one, indicating cell death and detachment (**Figure 15A**). Similarly, the percentage of PI-positive of all Hoechst-positive cells started to increase from 300 µM hemin (**Figure 15B**) and was statistically significant from control (vehicle) at 400 µM hemin and above with an EC_{50} of 348.3 µM (**Figure 15C**). In contrast, the MTT assay revealed a decrease in metabolic activity

that was statistically significant from 100 µM onwards with an EC_{50} of 161.3 µM (**Figure 15D**).

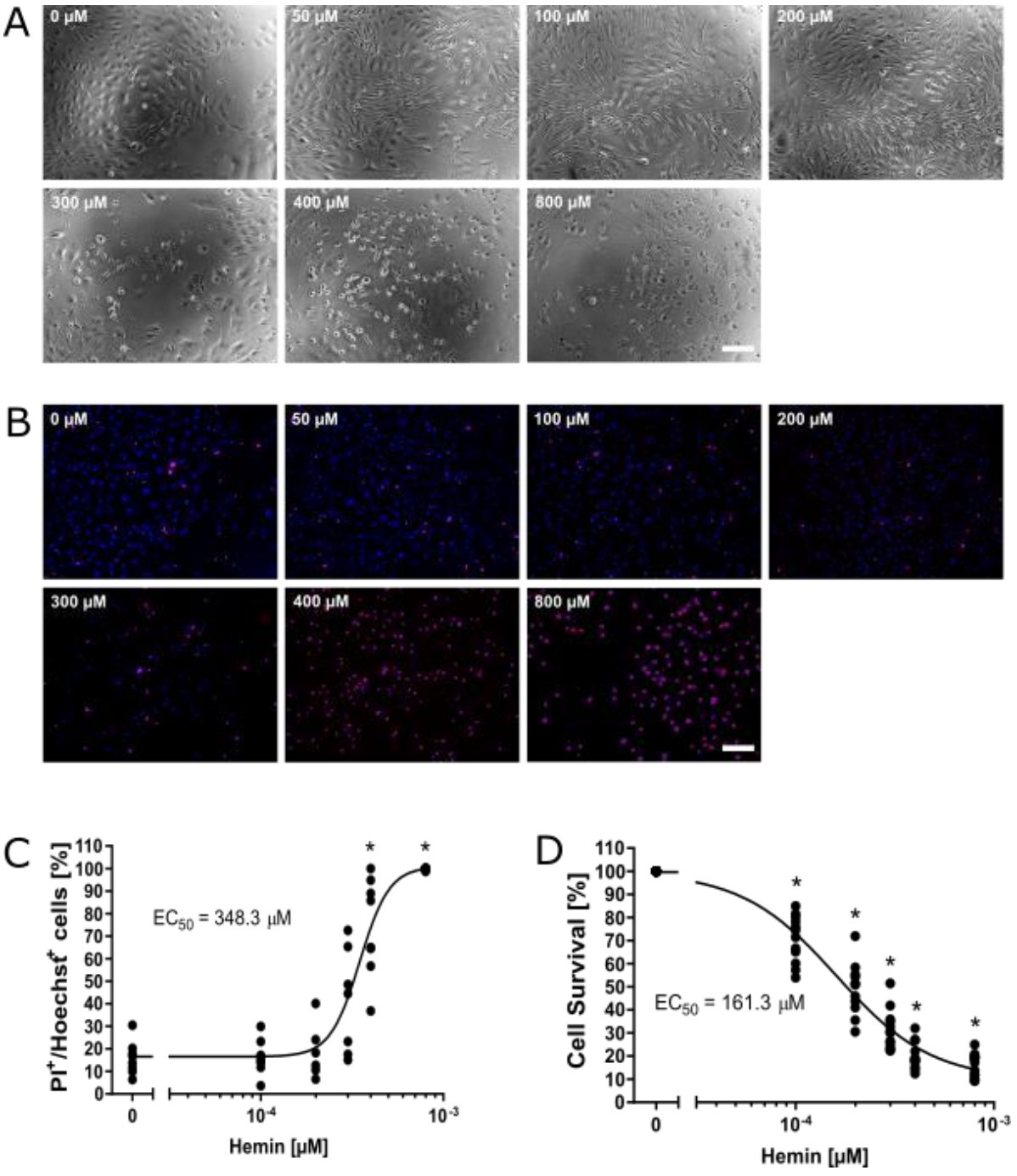

Figure 15. Hemin induced endothelial cell death in a concentration-dependent manner. Hemin concentration response in bEnd.3 cell induces cell death in a concentration-dependent manner that can be seen in **A**) phase contrast and **B**) Hoechst 33342 and propidium iodide (PI) staining. This is confirmed by the quantification of the **C**) Hoechst 33342/PI staining and **D**) MTT assay. N = 8 biological replicates for Hoechst/PI and N = 14 for MTT assay (means of four technical replicates per biological replicate). * *P* = 0.001 for 400-800 µM vs. vehicle (C)

and * $P < 0.001$ for 100-800 µM vs. vehicle (D). For detailed statistics, refer to **Table 8**. Scale bars = 200 µm.

Table 8. Statistical analysis of the hemin concentration-response in MTT assay and Hoechst 33342/PI staining in bEnd.3 cells.

	Kolmogorov-Smirnov test	Levené test	Omnibus test	Posthoc Mann-Whitney U with Bonferroni correction at $\alpha = 0.01$
Hoechst 33342/PI	Z = 0.205, $P < 0.001$	F(5,42) = 8.272, $P < 0.001$	Kruskal-Wallis test, [chi]2(4,N = 40) = 22.516, $P < 0.001$, $\eta^2 = 0.577$	$P = 0.001$ for 400-800 µM hemin vs. vehicle
MTT	Z = 0.156, $P < 0.001$	F(5,78) = 6.172, $P < 0.001$	Kruskal-Wallis test, [chi]2(4,N = 70) = 63.320, $P < 0.001$, $\eta^2 = 0.918$	$P < 0.001$ for 100-800 µM hemin vs. vehicle

To observe the time-course of hemin-induced endothelial cell death, I recorded the cells using time-lapse imaging every 30 minutes for 48 hours. At higher concentrations (800 µM), hemin led to abrupt cell death, while at the EC_{50}, the cells gradually died over time by rounding up and finally detaching (**Figure 16)**.

I chose to continue the characterization of the underlying cell death mechanisms using 350 µM hemin based on the morphological changes observed and the results of the Hoechst/PI staining because, together, they convincingly demonstrated that the cells died at this concentration. While the MTT assay indicated a lower EC_{50} value, this may be attributed to a decrease in metabolic activity that may precede cell death.

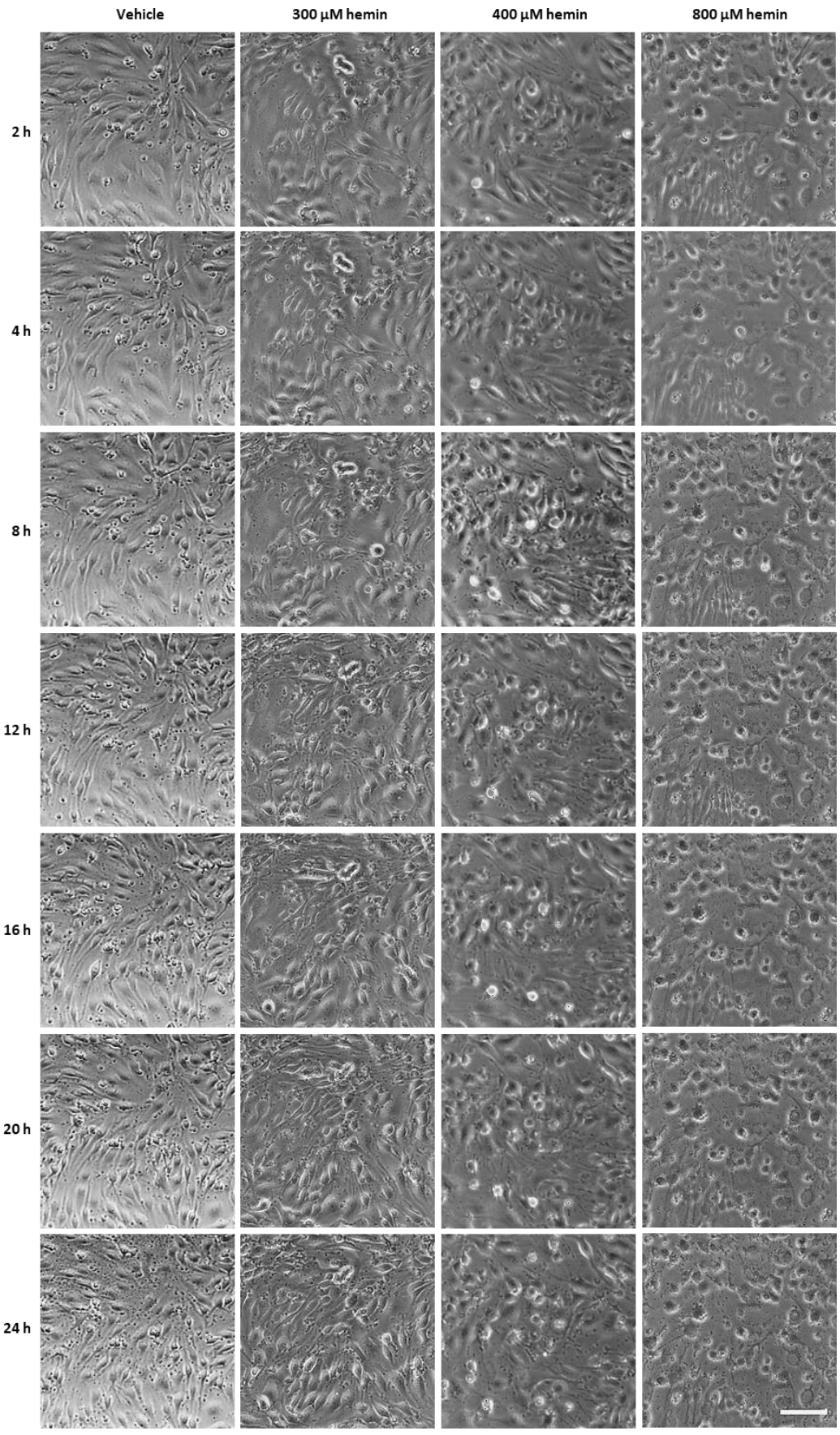

Figure 16. Time-lapse recording of bEnd.3 cells exposed to hemin over 24 hours. Scale bar = 50 µm.

4.1.3. Identification of brain endothelial cell death subroutines

I assessed different cell death subroutines in bEnd.3 cells exposed to hemin to identify the mechanisms underlying endothelial cell death after hemorrhagic stroke: a) apoptosis, b) necroptosis, c) autophagy, d) ferroptosis, and e) parthanatos. I used chemical cell death inhibitors in co-treatment with 350 µM hemin for 24 hours as well as biochemical markers examined by immunofluorescence to assess each cell death subroutine.

4.1.3.1. Apoptosis

The activation of the executer caspase-3 is a main hallmark of apoptosis. Therefore, I used Z-VAD-FMK as a pan-caspase inhibitor that blocks caspase-3 as well as caspase-7. Z-VAD-FMK partially abrogated hemin-induced cell death in bEnd.3 cells (**Figure 17**). In addition, I also investigated whether inhibiting the MAP kinases JNK (SP600125) and p38 (SB20350) as well as inhibiting the opening of the mPTP (cyclosporine A), all involved in apoptosis, were effective in ameliorating hemin-induced endothelial cell death. However, none of these inhibitors significantly reduced hemin-induced toxicity, but cycloheximide treatment concentration-dependently reduced the cellular metabolic activity in vehicle- and hemin-treated cells (**Figure 17**).

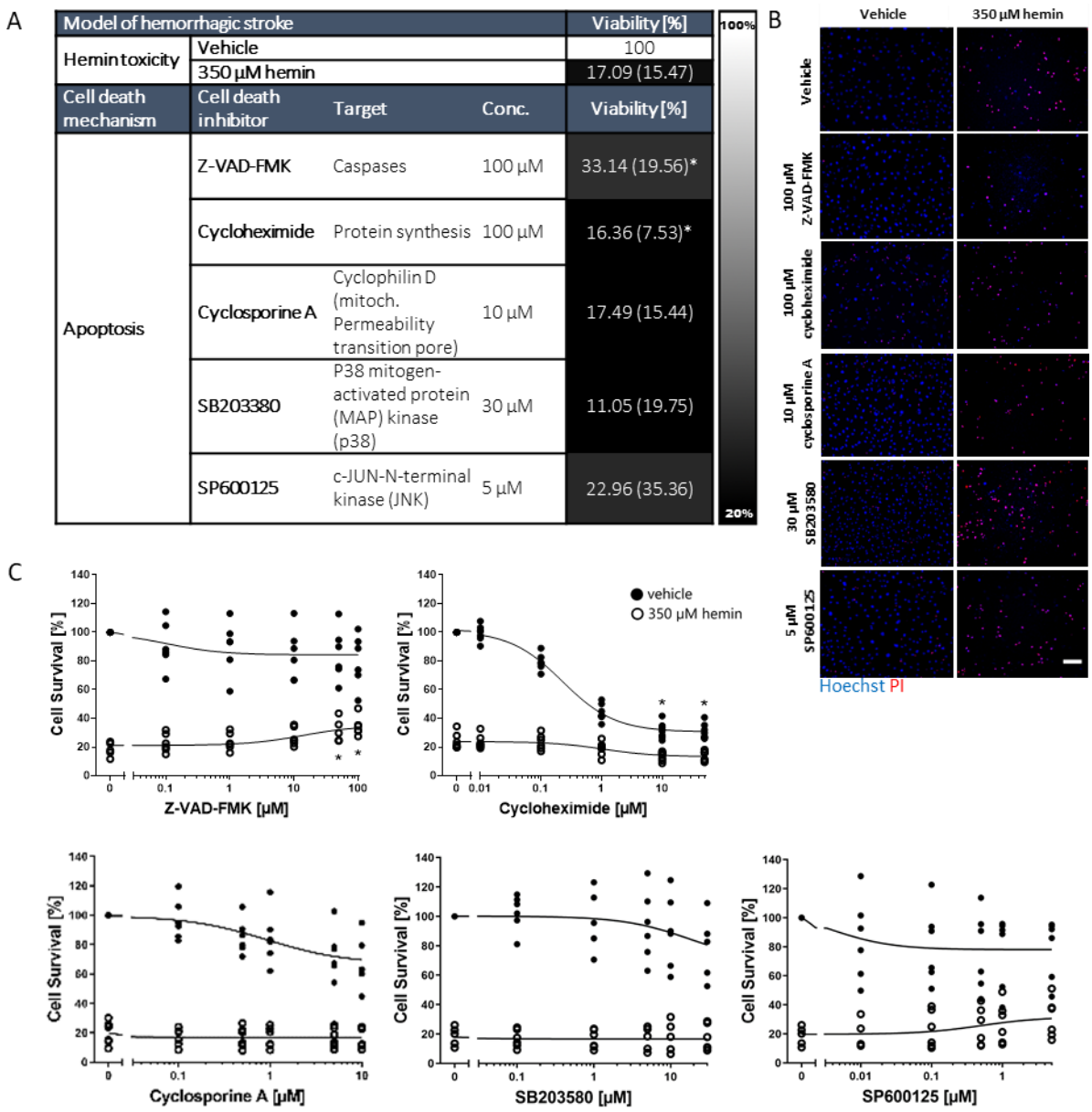

Figure 17. Apoptosis inhibitors partially abrogated hemin-induced cell death in bEnd.3 cells. A) bEnd.3 cells were treated with 350 µM hemin (EC_{50}) and chemical inhibitors of apoptosis. Values show medians (interquartile range) at representative concentrations. Grayscale coding indicates the degree from no protection (black) to maximal cell viability (white) in the presence of hemin. **B**) Representative Hoechst/PI staining are shown. Scale bar = 200 µm. **C**) Concentration-responses of inhibitors in hemin-induced death assessed by MTT assay. Lines indicate non-linear regressions. N = 6-7 biological replicates (means of four technical replicates per biological replicate). * $P < 0.05$ versus hemin + vehicle. For detailed statistics, refer to **Table 9.**

Table 9. Statistical analysis of apoptosis inhibitors in hemin-induced toxicity in bEnd.3 cells.

Cell death inhibitor	Kolmogorov-Smirnov test	Levené test	Omnibus test	Posthoc Mann-Whitney U with Bonferroni correction at α = 0.0083
Z-VAD-FMK	Z = 0.210, *P* < 0.001	F(11,60) = 3.569, *P* = 0.001	Kruskal-Wallis test, [chi]2(11,N = 72) = 59.184, *P* < 0.001, η^2 = 0.833	*P* = 0.002 for hemin vs. vehicle, *P* = 0.004 for hemin + 50-100 µM Z-VAD-FMK vs. hemin + vehicle
Cycloheximide	Z = 0.230, *P* < 0.001	F(11,72) = 1.465, *P* = 0.164	Kruskal-Wallis test, [chi]2(11,N = 84) = 75.791, *P* < 0.001, η^2 = 0.913	*P* = 0.001 for hemin vs. vehicle, *P* = 0.01 for hemin + 10-50 µM cycloheximide vs. hemin + vehicle
Cyclospo-rine A	Z = 0.236, *P* < 0.001	F(11,60) = 2,104, *P* = 0.034	Kruskal-Wallis test, [chi]2(11,N = 72) = 57.558, *P* < 0.001, η^2 = 0.811	*P* = 0.002 for hemin vs. vehicle
SB203380	Z = 0.227, *P* < 0.001	F(11,60) = 3.529, *P* = 0.001	Kruskal-Wallis test, [chi]2(11,N = 72) = 54.828, *P* < 0.001, η^2 = 0.772	*P* = 0.002 for hemin vs. vehicle
SP600125	Z = 0.149, *P* < 0.001	F(11,60) = 5.176, *P* = 0.001	Kruskal-Wallis test, [chi]2(11,N = 72) = 55.224, *P* < 0.001, η^2 = 0.778	*P* = 0.002 for hemin vs. vehicle

To assess the absence or presence of apoptosis in hemin-induced endothelial cell death, I performed immunostaining of cleaved caspase-3. I first confirmed the specificity of the antibody using the apoptosis inducer staurosporine in bEnd.3 cells as a positive control (Malsy et al., 2019; Thuret et al., 2003). Staurosporine (500 nM) induced a significant increase in the number of cleaved caspase-3-positive cells, which was abrogated by the pan-caspase inhibitor Z-VAD-FMK (**Figure 18**).

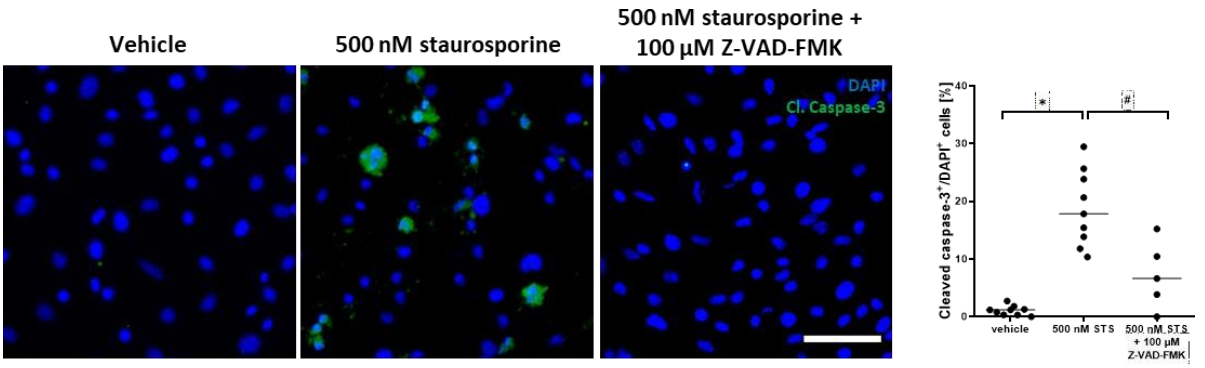

Figure 18. Validation of the apoptosis marker cleaved caspase-3 in staurosporine-treated bEnd.3 cells. Staurosporine (STS, 500 nM) induced cleaved caspase-3 (cl. caspase-3) after 9 hours incubation. Scale bar = 50 µm. N = 5-9 biological replicates. Kolmogorov-smirnov test, Z = 0.199, *P* = 0.018; Levene test, F(2,20) = 9.571, *P* = 0.001; Kruskal-Wallis test, [chi]2(2,N = 23) = 15.679, *P* < 0.001, $\eta^2 = 0.713$; posthoc Mann-Whitney U with Bonferroni correction at $\alpha = 0.025$: * *P* < 0.001 for 500 nM STS vs. vehicle, # *P* = 0.014 for 500 nM STS vs. 500 nM STS + 100 µM Z-VAD-FMK.

Then, I assessed the cleavage of caspase-3 under hemin treatment in bEnd.3 cells (**Figure 19**). At none of the concentrations assessed, there was a significant increase in the cleavage of caspase-3 at 24 hours after hemin application (**Figure19A**). Since it is possible that caspase-3 is activated earlier after hemin treatment, I also assessed the cleavage of caspase-3 after 2, 4, and 8 hours of 300 µM hemin, which also did not show any incrase (**Figure 19B**).

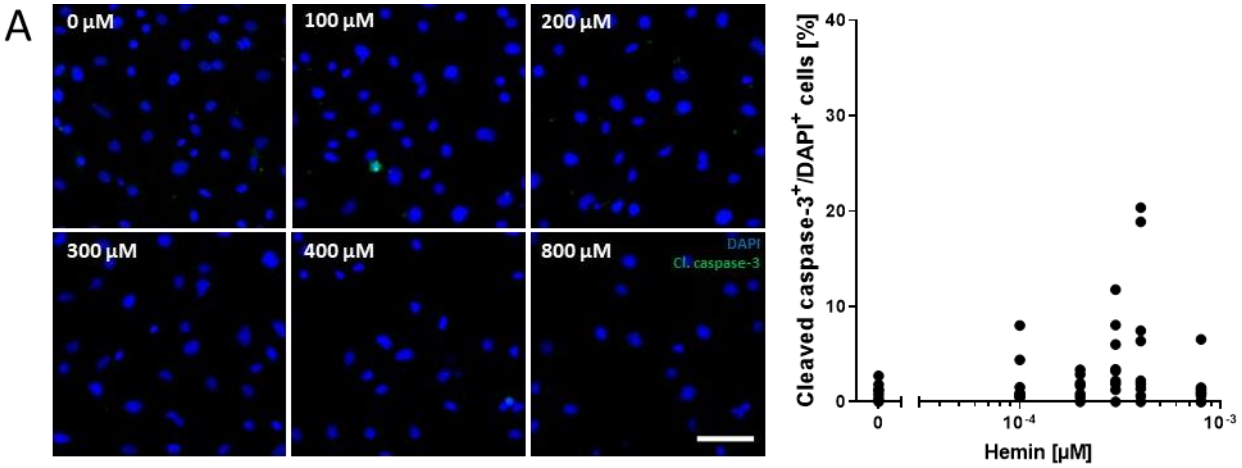

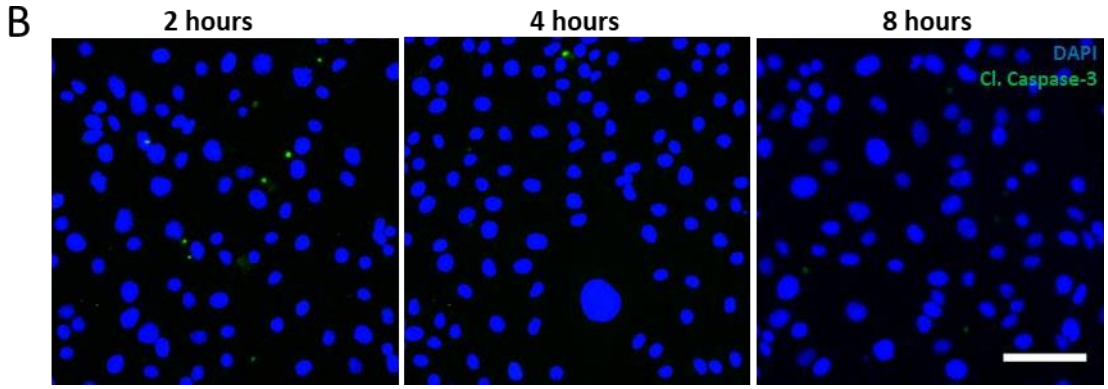

Figure 19. Expression of cleaved caspase-3 in hemin-treated bEnd.3 cells. A) Cleaved caspase-3 (cl. caspase-3) was not significantly increased in hemin-treated bEnd.3 cells at 24 hours after the addition of hemin to the cells. N = 9 biological replicates (means of three technical replicates per biological replicate). Kolmogorov-smirnov test, Z = 0.274, $P < 0.001$; Levene test, F(5,48) = 7.004, $P < 0.001$; Kruskal-Wallis test, [chi]2(5,N = 54) = 10.153, $P = 0.071$, $\eta^2 = 0.192$. **B**) The staining of bEnd.3 cells treated with 300 µM hemin at 2, 4, and 8 hours after hemin application also confirmed the absence of cleaved caspase-3. Scale bars = 50 µm.

Taken together, these data cannot completely rule out that apoptosis is involved in hemin-induced endothelial cell death as Z-VAD-FMK was protective. I therefore assessed the ability of Z-VAD-FMK to protect against hemin-induced toxicity in pBCECs (see **4.1.4. The effect of cell death inhibitors on hemin-induced cell death in pBCECs**).

4.1.3.2. Necroptosis

I investigated the role of necroptosis in hemin-induced brain endothelial cell death by applying the RIPK1 inhibitor necrostatin-1, the RIPK3 inhibitor GSK872, and the MLKL inhibitor necrosulfonamide. To exclude off-target effects of the inhibitors, one strategy is to use an inactive analog that is structurally similar to the active compound. I therefore used necrostatin-1 inactive control for necrostatin-1. Among those inhibitors, GSK872 showed a partial

protective effect on hemin-treated bEnd.3 cells, while necrosulfonamide starting from 10 µM reduced the cellular metabolic activity of the vehicle-treated cells (**Figure 20**).

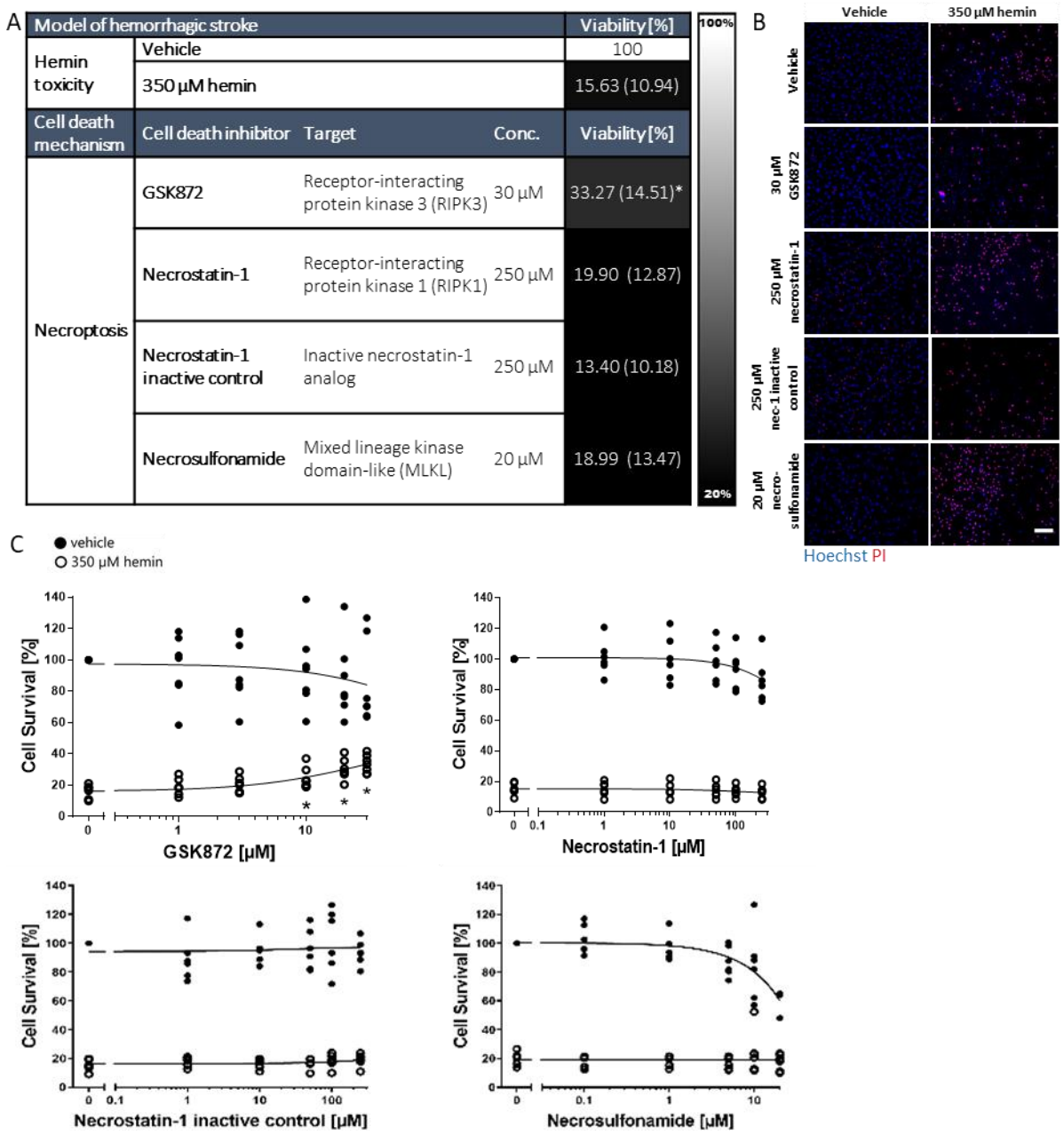

Figure 20. Necroptosis inhibitors in hemin-induced cell death in bEnd.3 cells. **A**) bEnd.3 cells were treated with 350 µM hemin (EC_{50}) and chemical inhibitors of necroptosis. Values show medians (interquartile range) at representative concentrations. Grayscale coding indicates the degree from no protection (black) to maximal cell viability (white) in the presence of hemin. **B**) Representative Hoechst/PI staining are shown. Scale bar = 200 µm. **C**) Concentration-responses of inhibitors in hemin-induced death assessed by MTT assay. Lines indicate non-linear regressions. N = 6-7 biological replicates (means of four technical replicates per biological replicate). * P<0.05 versus hemin + vehicle. For detailed statistics, refer to **Table 10**.

Table 10. Statistical analysis of necroptosis inhibitors in hemin-induced toxicity in bEnd.3 cells.

Cell death inhibitor	Kolmogorov-Smirnov test	Levené test	Omnibus test	Posthoc Mann-Whitney U
GSK872	Z = 0.171, $P < 0.001$	F(11,60) = 3.168, $P = 0.002$	Kruskal-Wallis test, [chi]2(11,N = 72) = 60.344, $P < 0.001$, $\eta^2 = 0.850$	with Bonferroni correction at α = 0.0083: $P = 0.001$ for hemin vs. vehicle, $P = 0.015$ for hemin + 10 µM GSK872; $P = 0.002$ for hemin + 50-100 µM GSK872
Necrostatin-1 + Necrostatin-1 inactive control	Z = 0.280, $P < 0.001$	F(21,110) = 3.856, $P < 0.001$	Kruskal-Wallis test, [chi]2(21,N = 132) = 104.474, $P < 0.001$, $\eta^2 = 0.791$	with Bonferroni correction at α = 0.0031: $P = 0.002$ for hemin vs. vehicle
Necrosulfona-mide	Z = 0.260, $P < 0.001$	F(11,60) = 3.062, $P = 0.003$	Kruskal-Wallis test, [chi]2(11,N = 72) = 58.804, $P < 0.001$, $\eta^2 = 0.828$	with Bonferroni correction at α = 0.0083: $P = 0.002$ for hemin vs. vehicle
Actinomycin D	Z = 0.197, $P < 0.001$	F(11,72) = 2.344, $P = 0.016$	Kruskal-Wallis test, [chi]2(11,N = 84) = 73.134, $P < 0.001$, $\eta^2 = 0.881$	with Bonferroni correction at α = 0.0083: $P = 0.001$ for hemin vs. vehicle

4.1.3.3. Autophagy

To investigate the role of autophagy in hemin-induced endothelial cell death, I investigated whether the following chemical modulators of autophagy increase cell viability: a) 3-methyladenine that inhibits the PI3K complex; b) bafilomycin A1 that prevents endosomal and lysosomal acidification; c) chloroquine that blocks the fusion of lysosomes with autophagosomes; and d) rapamycin, an autophagy inducer that targets the mTOR protein kinase.

Among the investigated autophagy modulators, only bafilomycin A1 significantly reduced hemin-induced cell death in brain endothelial cells, while mdivi-1 further exacerbated cell

death. Rapamycin, 3-methyladenine, and mdivi-1 reduced the overall metabolic activity in vehicle-treated cells (**Figure 21**).

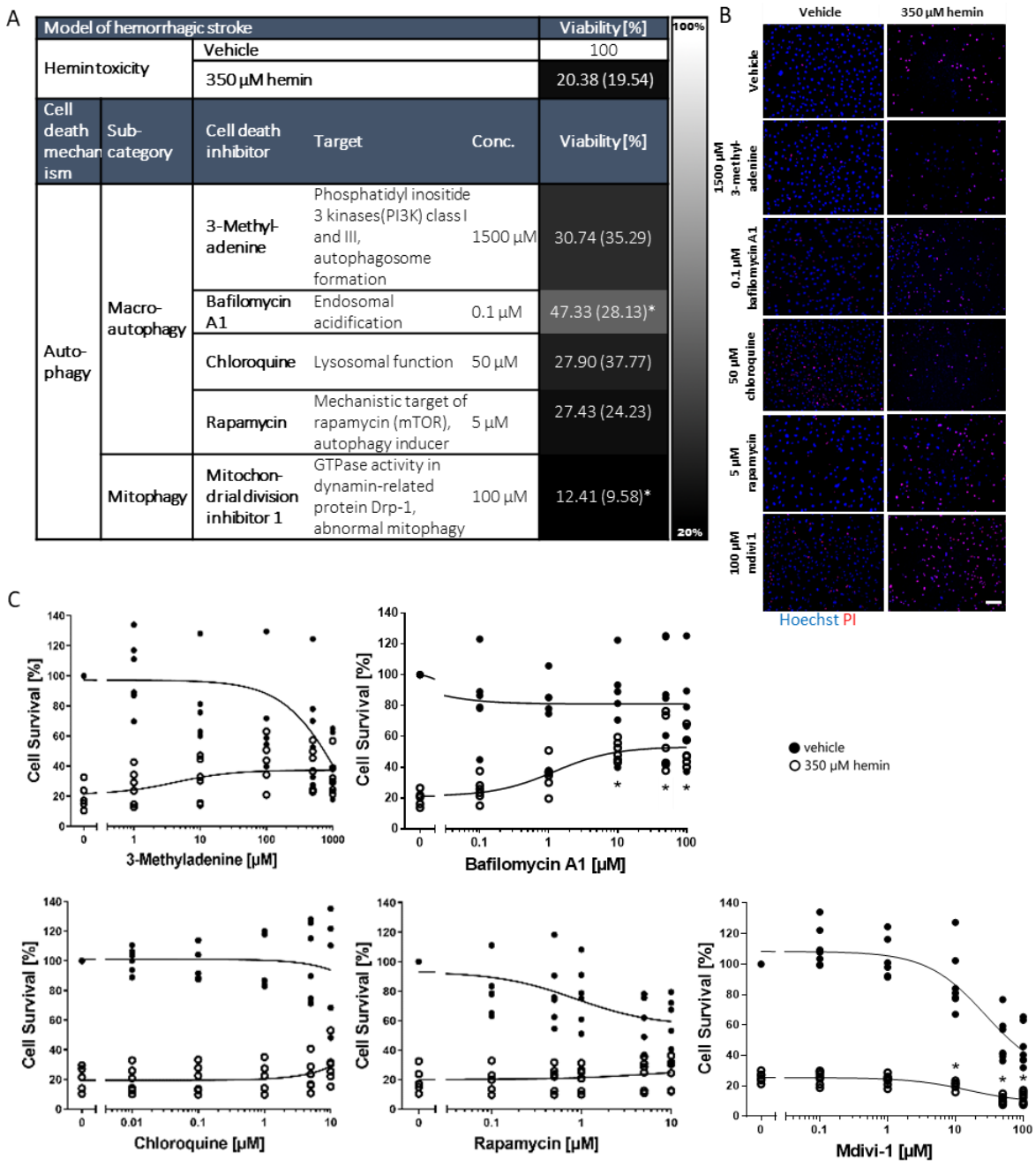

Figure 21. Autophagy inhibitors in hemin-induced cell death in bEnd.3 cells. A) bEnd.3 cells were treated with 350 µM hemin (EC_{50}) and chemical inhibitors of autophagy. Values show medians (interquartile range) at representative concentrations. Grayscale coding indicates the degree from no protection (black) to maximal cell viability (white) in the presence of hemin. **B**) Representative Hoechst/PI staining are shown. Scale bar = 200 µm. **C**) Concentration-responses of inhibitors hemin-induced death assessed by MTT assay. Lines indicate non-linear regressions. N = 6-7 biological replicates (means of four technical replicates per biological replicate). * P<0.05 versus hemin + vehicle. For detailed statistics, refer to **Table 11**.

Table 11. Statistical analysis of autophagy inhibitors in hemin-induced toxicity in bEnd.3 cells.

Cell death inhibitor	Kolmogorov-Smirnov test	Levené test	Omnibus test	Posthoc Mann-Whitney U with Bonferroni correction at α = 0.0083
3-Methyl-adenine	Z = 0.131, *P* = 0.04	F(11,60) = 5,630, *P* < 0.001	Kruskal-Wallis test, [chi]2(11,N = 72) = 47.673, *P* < 0.001, η^2 = 0.671	*P* = 0.002 for hemin vs. vehicle
Bafilo-mycin A1	Z = 0.117, *P* = 0.016	F(11,60) = 2.603, *P* = 0.009	Kruskal-Wallis test, [chi]2(11,N = 72) = 51.427, *P* < 0.001, η^2 = 0.724	*P* = 0.002 for hemin vs. vehicle*; P* = 0.002 for hemin + 0.01-0.1 µM bafilomycin A1 vs. hemin + vehicle
Chloro-quine	Z = 0.202, *P* < 0.001	F(11,60) = 13.039, *P* < 0.001	Kruskal-Wallis test, [chi]2(11,N = 72) = 54.264, *P* < 0.001, η^2 = 0.764	*P* = 0.002 for hemin vs. vehicle
Rapa-mycin	Z = 0.181, *P* < 0.001	F(11,60) = 2.543, *P* = 0.010	Kruskal-Wallis test, [chi]2(11,N = 72) = 56.747, *P* < 0.001, η^2 = 0.799	*P* = 0.002 for hemin vs. vehicle
Mdivi-1	Z = 0.210, *P* < 0.001	F(11,72) = 6.764, *P* < 0.001	Kruskal-Wallis test, [chi]2(11,N = 84) = 77.743, *P* < 0.001, η^2 = 0.937	*P* = 0.001 for 350 µM hemin vs. vehicle; *P* = 0.002 for hemin + 10 µM mdivi-1; *P* = 0.001 for 50-100 µM mdivi-1 vs hemin + vehicle

To assess the absence or presence of autophagy in hemin-induced endothelial cell death, I performed immunostaining of LC3. I first confirmed the specificity of the antibody using the autophagy inducer rapamycin in bEnd.3 cells as a positive control (Lei et al., 2012; Subirada et al., 2019). Rapamycin (0.5 µM) increased the number of LC3-positive cells, while the autophagosome formation inhibitor bafilomycin A1 abolished the activation of LC3 (**Figure 22**).

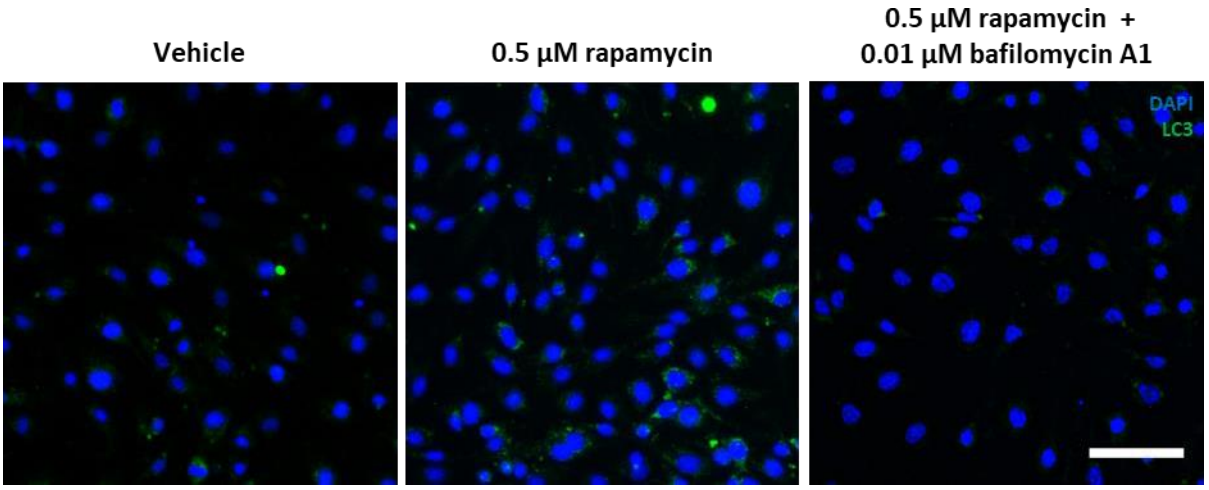

Figure 22. Validation of the autophagy marker LC3 in rapamycin-treated bEnd.3 cells. LC3 was expressed in bEnd.3 cells treated with 0.5 µM rapamycin for 4 hours. The expression was reduced by the co-administration of 0.01 µM bafilomycin A1. Scale bar = 50 µm.

Next, I assessed the LC3 expression in bEnd.3 cells exposed to hemin. The expression of LC3 increased at 300 µM after 24 hours of hemin application (**Figure 23A**). When investigating earlier time points, I observed an increase in LC3 expression starting from 4 hours of incubation of hemin (**Figure 23B**).

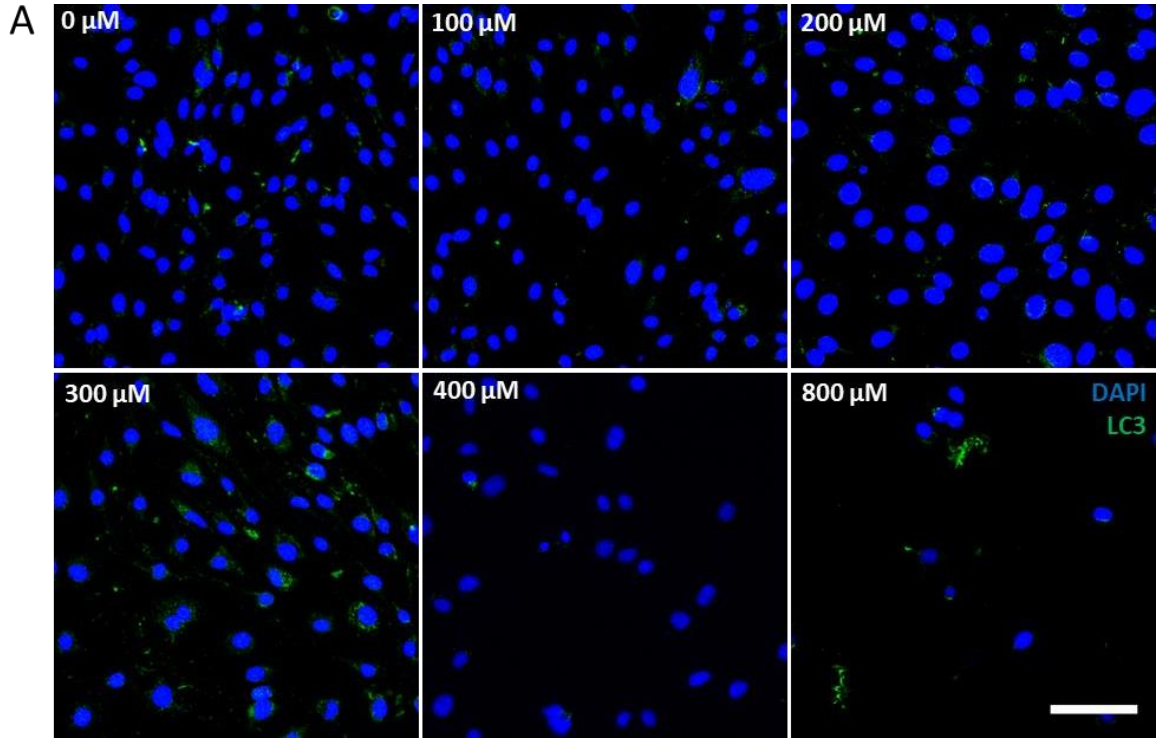

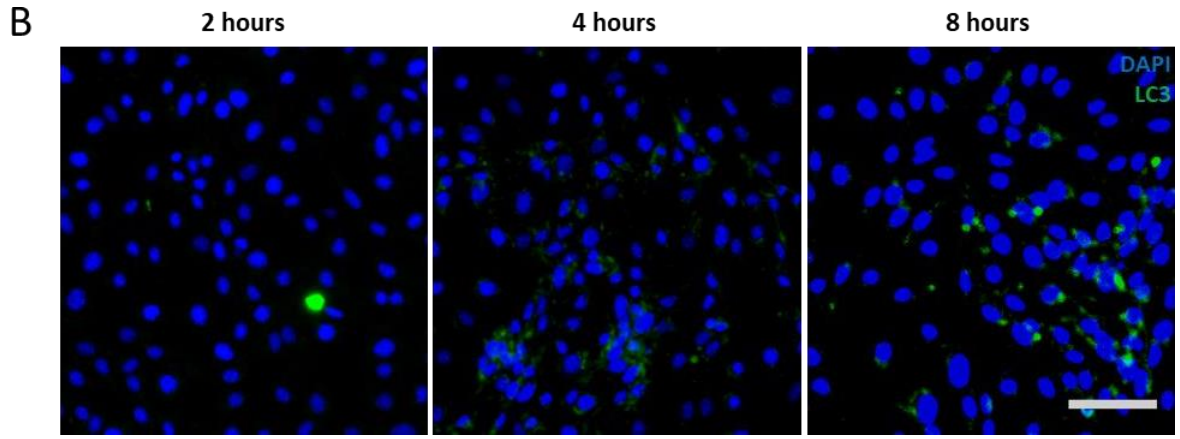

Figure 23. Expression of LC3 in hemin-treated bEnd.3 cells. A) LC3 levels increased in hemin-treated cells at 24 hours. **B**) The staining of bEnd.3 cells treated with 300 µM hemin at 2, 4, and 8 hours after hemin application also confirmed the presence of LC3 from 4 hours onwards. Scale bar = 50 µm.

In summary, the data suggest that autophagy plays a role in hemin-induced brain endothelial cell death.

4.1.3.4. Ferroptosis

To assess whether hemin induces ferroptosis in brain endothelial cells, I used several chemical inhibitors that together define ferroptosis (Dixon et al., 2012; Zille et al., 2017): a) the canonical ferroptosis inhibitor ferrostatin-1 that scavenges the initiation of alkoxyl radicals and other additional products that are generated by ferrous iron from lipid hydroperoxides (Miotto et al., 2020); b) deferoxamine, an iron chelator and inhibitor of HIF prolyl hydroxylases; c) N-acetylcysteine, a cysteine prodrug; d) the vitamin E analog Trolox, e) the MAP kinase kinase inhibitor U0126 compared to its inactive control U0124 (to ensure target specificity); f) actinomycin D, a transcription inhibitor and g) cycloheximide, a translation inhibitor.

N-acetylcysteine, deferoxamine, and Trolox, but not ferrostatin-1, U0126, actinomycin D or cyloheximide, inhibited hemin-induced cell death in bEnd.3 cells in a concentration-dependent manner. Actinomycin D and cycloheximide reduced the metabolic activity of the vehicle-treated cells (**Figure 24**).

A

Model of hemorrhagic stroke				Viability [%]
Hemin toxicity	Vehicle			100
	350 µM hemin			18.85 (17.84)
Cell death mechanism	Cell death inhibitor	Target	Conc.	Viability [%]
Ferroptosis	Actinomycin D	mRNA synthesis	1 µM	20.50 (20.38)
	Cycloheximide	Protein Synthesis	100 µM	16.36 (7.53)*
	Ferrostatin-1	Canonical ferroptosis inhibitor, reactive lipid species (RLS)	1 µM	20.17 (14.81)
	Deferoxamine	Iron, hypoxia induced factor (HIF) prolyl hydroxylase domain-containing inhibition	100 µM	42.60 (25.08)*
	N-Acetylcysteine	Reactive oxygen species (ROS), RLS	2000 µM	43.83 (17.14)*
	Trolox, vitamin E analog	RLS	100 µM	42.00 (31.09)*
	U0126	Mitogen activated protein kinase kinase 1/2 (MEK 1/2)	20 µM	23.83 (23.03)
	U0124	U0126 inactive control	20 µM	37.734 (13.924)

100%
20%

B

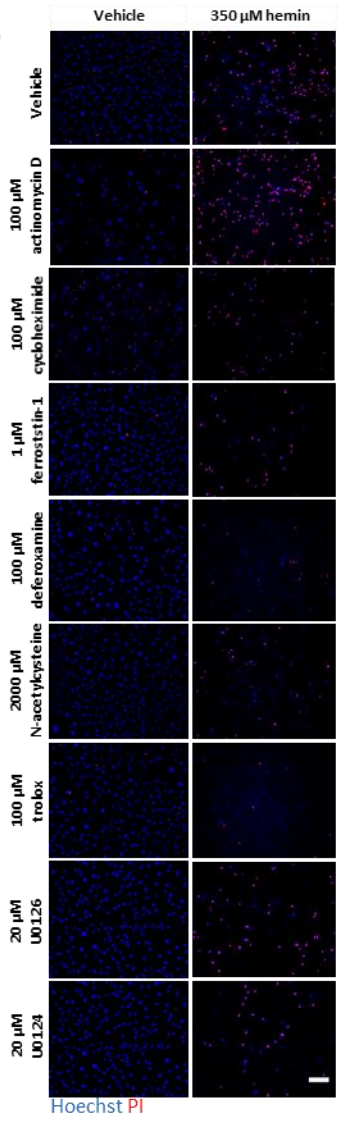

C

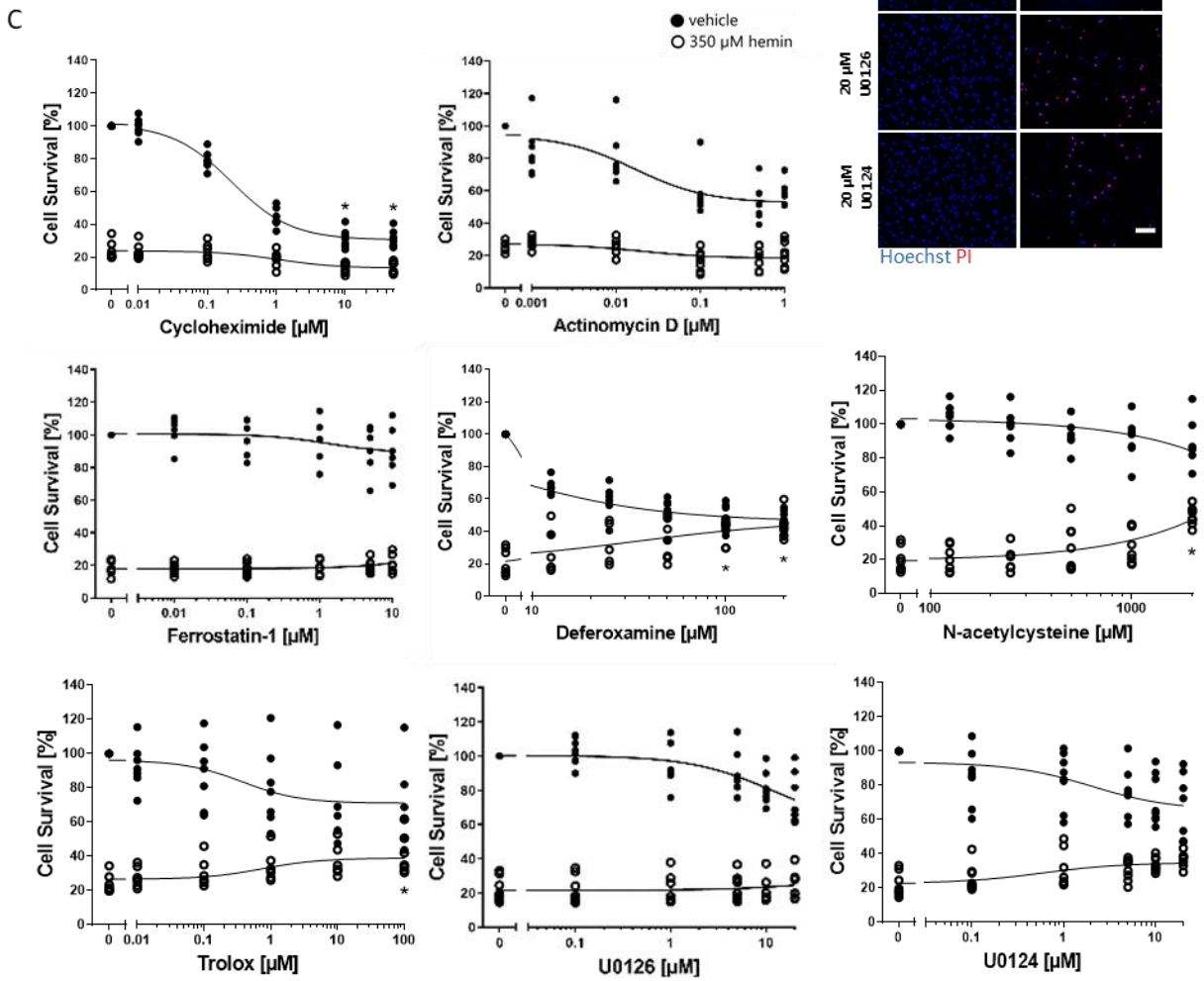

Figure 24. Ferroptosis inhibitors partially abrogate hemin-induced cell death in bEnd.3 cells. A) bEnd.3 cells were treated with 350 µM hemin (EC_{50}) and chemical inhibitors effective in blocking ferroptosis. Values show medians (interquartile range) at representative concentration. Grayscale coding indicates the degree from no protection (black) to maximal cell viability (white) in the presence of hemin. **B**) Representative Hoechst/PI staining are shown. Scale bar = 200 µm. **C**) Concentration-responses of inhibitors in hemin-induced death assessed by MTT assay. Lines indicate non-linear regressions. N = 6-8 biological replicates (means of four technical replicates per biological replicate). * P<0.05 versus hemin + vehicle. For detailed statistics, refer to **Table 12.**

Table 12. Statistical analysis of ferroptosis inhibitors in hemin-induced toxicity in bEnd.3 cells.

Cell death inhibitor	Kolmogorov-Smirnov test	Levené test	Omnibus test	Posthoc Mann-Whitney U
Actino-mycin D	Z = 0.197, P < 0.001	F(11,72) = 2.344, P = 0.016	Kruskal-Wallis test, [chi]2(11,N = 84) = 73.134, P < 0.001, η^2 = 0.881	with Bonferroni correction at α = 0.0083: P = 0.001 for hemin vs. vehicle
Cyclohexi-mide	Z = 0.230, P < 0.001	F(11,72) = 1.465, P = 0.164	Kruskal-Wallis test, [chi]2(11,N = 84) = 75.791, P < 0.001, η^2 = 0.913	P = 0.001 for hemin vs. vehicle, P = 0.01 for hemin + 10-50 µM cycloheximide vs. hemin + vehicle
Ferrostatin-1	Z = 0.267, P < 0.001	F(11,60) = 3.415, P = 0.001	Kruskal-Wallis test, [chi]2(11,N = 72) = 54.917, P < 0.001, η^2 = 0.773	with Bonferroni correction at α = 0.0083: P = 0.002 for hemin vs. vehicle
Deferoxa-mine	Z = 0.099, P = 0.039	F(11,72) = 2.698, P = 0.006	Kruskal-Wallis test, [chi]2(11,N = 84) = 57.810, P < 0.001, η^2 = 0.697	with Bonferroni correction at α = 0.0083: P = 0.001 for hemin vs. vehicle; P = 0.006 for hemin + 100 µM deferoxamine, P = 0.002 for hemin + 200 µM deferoxamine vs. hemin + vehicle

N-acetyl-cysteine	Z = 0.156, $P < 0.001$	F(11,72) = 2.472, $P = 0.011$	Kruskal-Wallis test, [chi]2(11,N = 84) = 69.156, $P < 0.001$, $\eta^2 = 0.833$	with Bonferroni correction at $\alpha = 0.0083$: $P = 0.001$ for hemin vs. vehicle; $P = 0.001$ for hemin + 2000 µM n-acetylcysteine vs. hemin + vehicle
Trolox	Z = 0.164, $P < 0.001$	F(11,72) = 3.409, $P = 0.001$	Kruskal-Wallis test, [chi]2(11,N = 84) = 68.164, $P < 0.001$, $\eta^2 = 0.821$	with Bonferroni correction at $\alpha = 0.0083$: $P = 0.001$ for hemin vs. vehicle; $P = 0.04$ for hemin + 100 µM trolox vs hemin + vehicle
U0126 + U0124 (inactive control)	Z = 0.167, $P < 0.001$	F(21,154) = 3.383, $P < 0.001$	Kruskal-Wallis test, [chi]2(21,N = 176) = 149.751, $P < 0.001$, $\eta^2 = 0.851$	with Bonferroni correction at $\alpha = 0.0031$: $P < 0.001$ for hemin vs. vehicle

Recently, TfR1 has been identified as a specific marker for ferroptosis along with MDA that is a secondary product of lipid peroxidation (Feng et al., 2020). I here assessed whether hemin induces the expression of these ferroptosis markers. To do so, I first verified the specificity of the TfR1 and MDA antibodies in a positive control, for which I incubated HT22 cells with the canonical ferroptosis inducer erastin (Zille et al., 2019b). Erastin treatment led to an increase in

TfR1 and MDA immunofluorescence, which was reduced by the ferroptosis inhibitor ferrostatin-1 (**Figure 25)**.

Figure 25. Validation of the ferroptosis markers TfR1 and MDA in erastin-treated HT22 cells. HT22 cells treated with erastin (0.5 µM) for 8 hours were positive for TfR1 and MDA. The ferroptosis inhibitor ferrostatin-1 abrogated the increase in TfR1 and MDA signal. Scale bar = 50 µm.

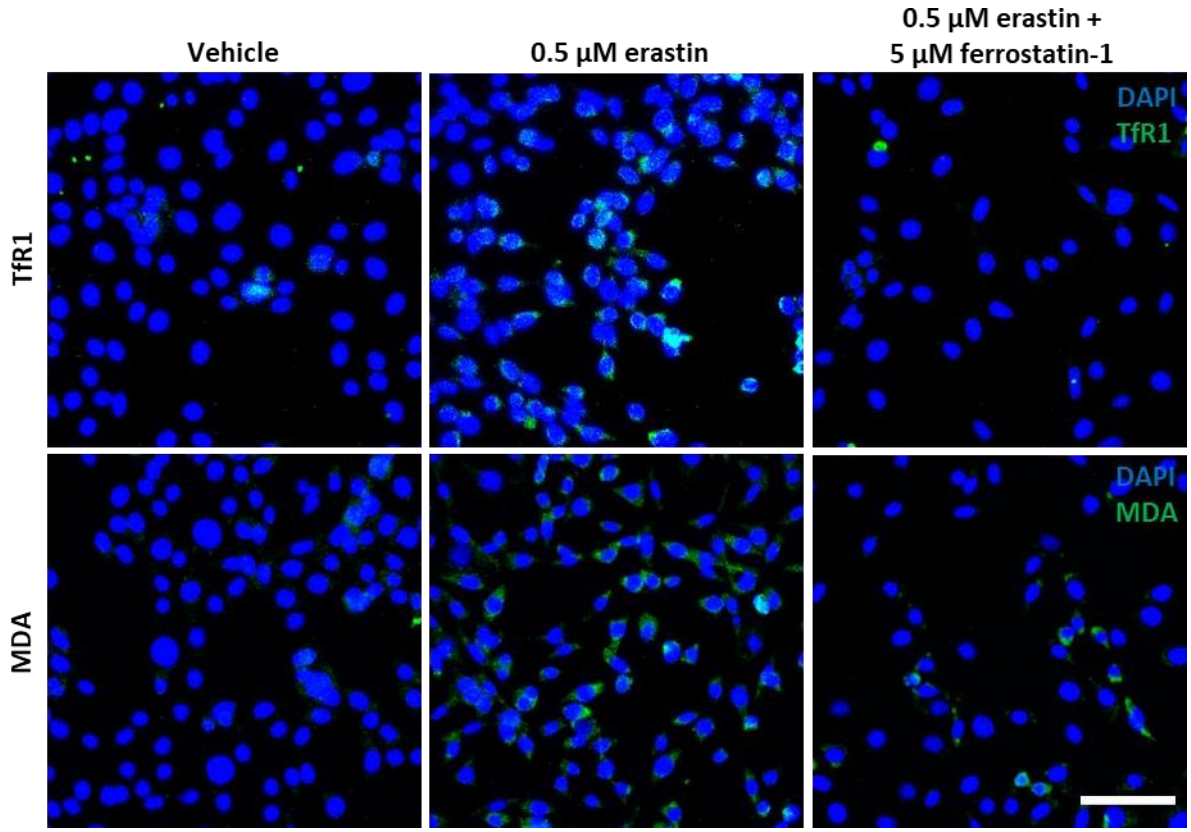

Next, I assessed the expression of TfR1 and MDA in bEnd.3 cells exposed to hemin. At 24 hours of hemin treatment, TfR1 and MDA were increased at 400 and 800 µM hemin (**Figure 26A-B**). Since the exact time point of the increase in expression in relation to cell death

is unknown, I also assessed both markers at different time points. I detected an increase in TfR1 and MDA immunofluorescence at 8 hours after hemin application (**Figure 26C**).

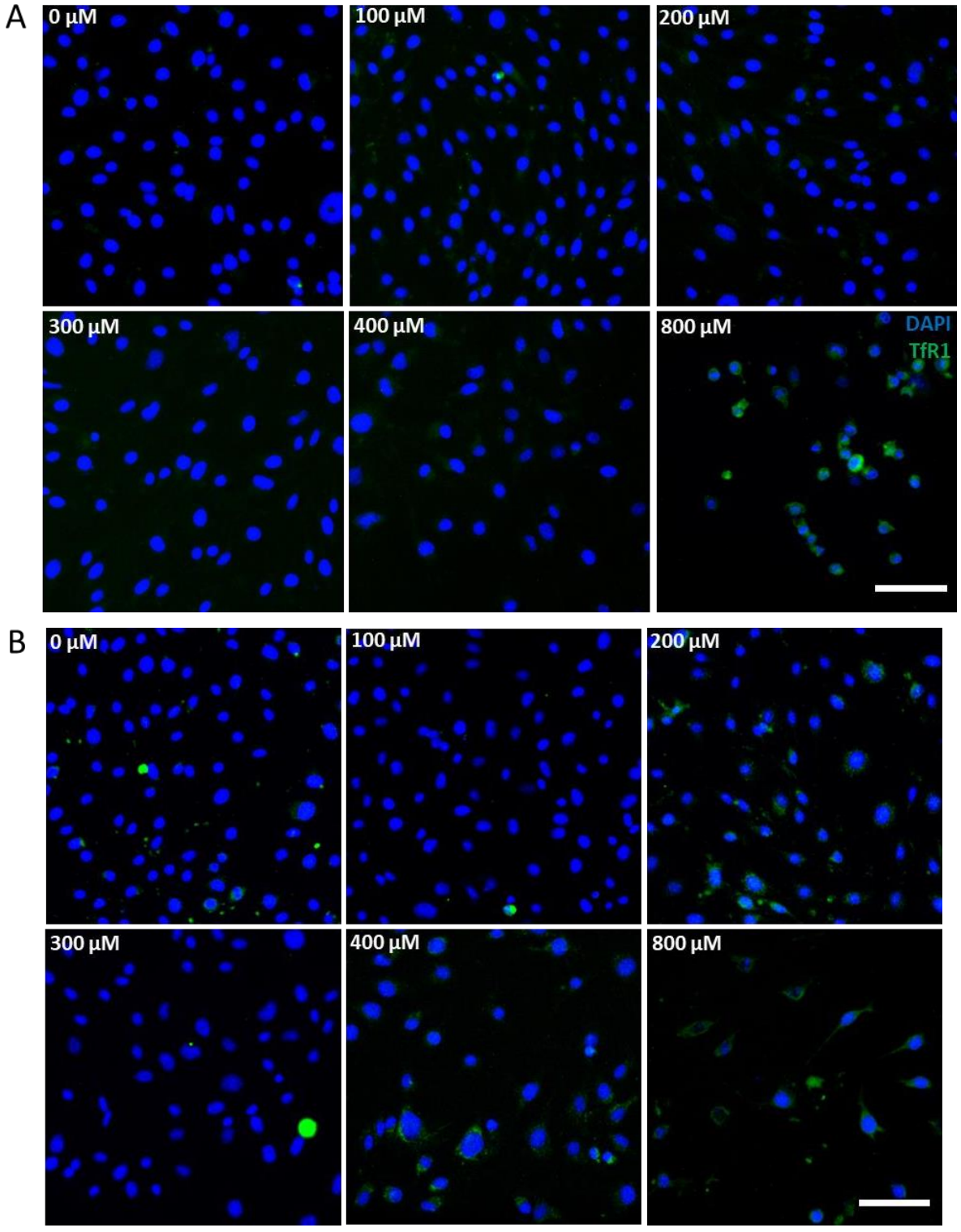

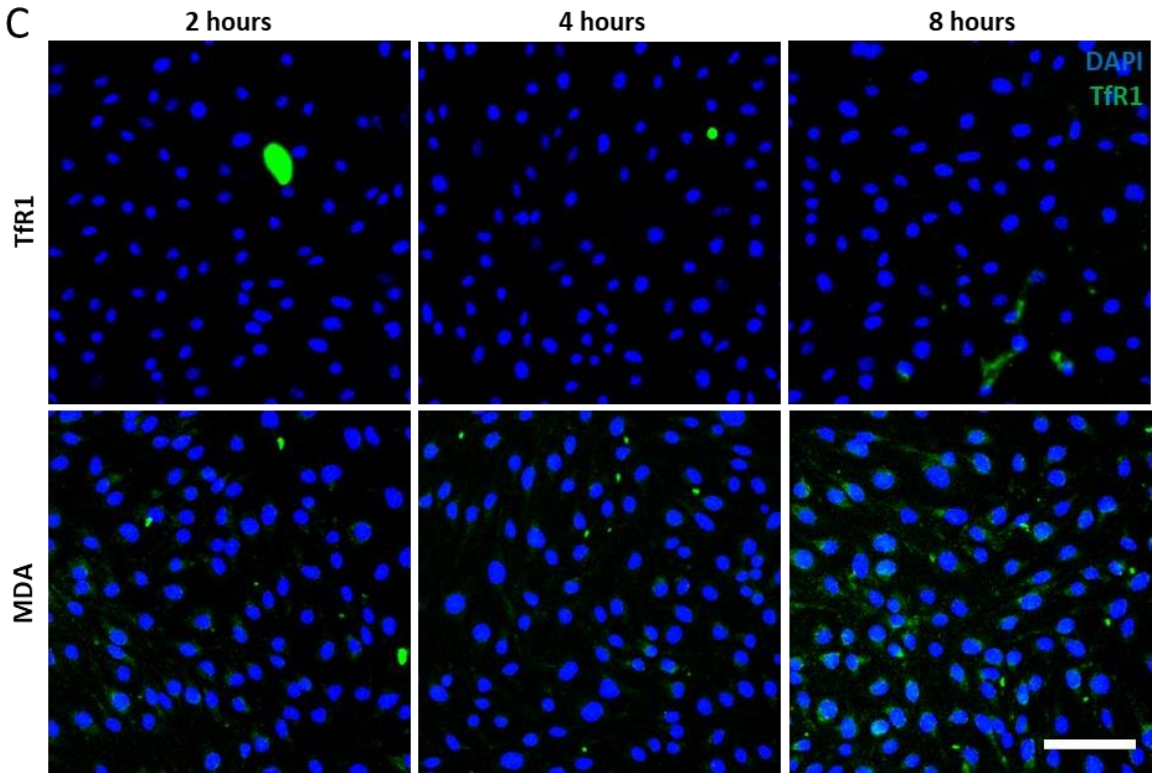

Figure 26. Expression of the ferroptosis markers TfR1 and MDA in hemin-treated bEnd.3 cells. A-B) Expression of TfR1 (**A**) and MDA (**B**) at different hemin concentration in bEnd.3 cells at 24 hours of exposure. **C**) Expression of TfR1 and MDA at 2, 4, and 8 hours of 400 µM hemin treatment in bEnd.3 cells. Scale bars = 50 µm.

In summary, these data suggest that ferroptosis plays a role in hemin-induced brain endothelial cel death, but that the inhibitors are only able to partially protect bEnd.3 cells from hemin toxicity.

4.1.3.5. Parthanatos

To investigate whether parthanatos is involved in hemin-induced brain endothelial cell death, I inhibited PARP1 and PARP2 with two inhibitors, DPQ and Olaparib. Olaparib is a market-approved PARP inhibitor and DPQ is only in laboratory use. Both of them target PARP1 and PARP2. I used two structurally different inhibitors that have the same target to ensure target specificity excluding off-target effects that may explain the effect of an inhibitor. I observed that neither DPQ nor Olaparib significantly inhibited brain endothelial cell death after hemin exposure (**Figure 27**).

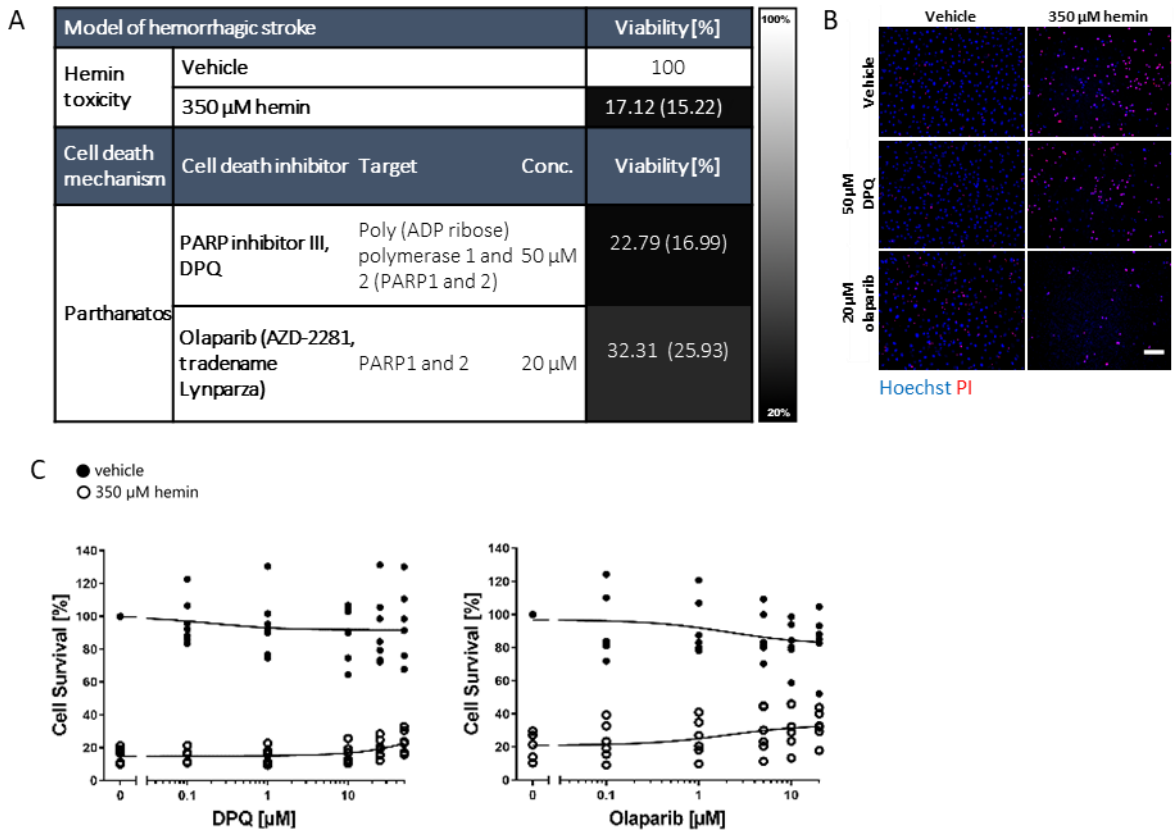

Figure 27. Parthanatos inhibitors in hemin-induced cell death in bEnd.3 cells. A) bEnd.3 cells were treated with 350 µM hemin (EC_{50}) and chemical inhibitors effective in parthanatos were observed. Values show medians (interquartile range) at representative concentrations. Grayscale coding indicates the degree from no protection (black) to maximal cell viability (white) in the presence of hemin. **B**) Representative Hoechst/PI staining are shown. Scale bar = 200 µm. **C**) Concentration-responses of inhibitors in hemin-induced death assessed by MTT assay. Lines indicate non-linear regressions. N = 6-7 biological replicates (means of four technical replicates per biological replicate). For detailed statistics, refer to **Table 13.**

Table 13. Statistical analysis of parthanatos inhibitors in hemin-induced toxicity in bEnd.3 cells

Cell death inhibitor	Kolmogorov-Smirnov test	Levené test	Omnibus test	Posthoc Mann-Whitney U with Bonferroni correction at α = 0.0083
DPQ	Z = 0.235, $P < 0.001$	F(11,72) = 4.654, $P < 0.001$	Kruskal-Wallis test, [chi]2(11,N = 84) = 64.996, $P < 0.001$, $\eta^2 = 0.783$	$P = 0.001$ for hemin vs. vehicle

Olaparib	Z = 0.162, *P* < 0.001	F(11,60) = 1.985, *P* = 0.046	Kruskal-Wallis test, [chi]2(11,N = 72) = 56.264, *P* < 0.001, η^2 = 0.792	*P* = 0.002 for hemin vs. vehicle

4.1.4. The effect of cell death inhibitors on hemin-induced cell death in pBCECs

Primary brain endothelial cell cells such as pBCECs are more similar to brain ECs in humans in terms of their BBB properties, demonstrating higher transendothelial resistance (Patabendige et al., 2013). Hence, it is important to establish that the results I obtained in bEnd.3 cells are reproducible in pBCECs. Therefore, I first determined the EC_{50} of hemin in pBCECs. I found that EC_{50} of hemin in pBCECs is 441.1 µM hemin (**Figure 28**).

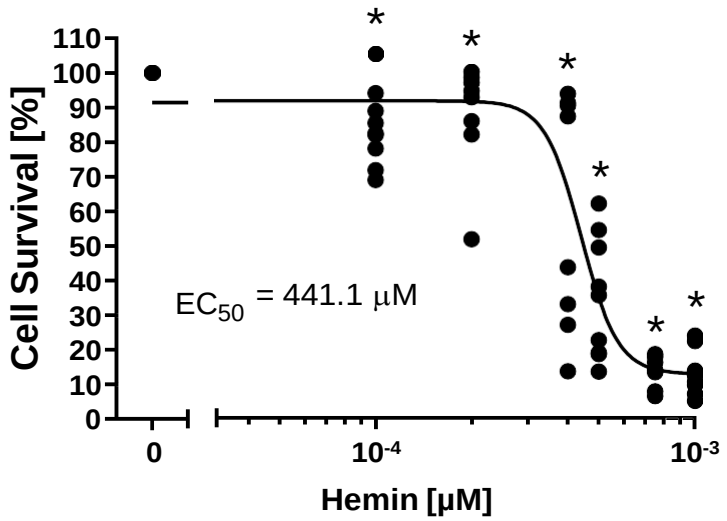

Figure 28. Hemin concentration-response in pBCECs. pBCECs were seeded in 96-well plates and treated with hemin. The cell survival was measured using the MTT assay. N = 9 biological replicates (means of four technical replicates per biological replicate). Kolmogorov-smirnov test, Z = 0.184, *P* < 0.001; Levene test, F(6,55) = 17.177, *P* < 0.001; Kruskal-Wallis test, [chi]2(6,N = 62) = 48.077, *P* < 0.001, η^2 = 0.788; posthoc Mann-Whitney U with Bonferroni correction at α = 0.007, * *P* = 0.004 for 100-400 µM hemin, *P* < 0.001 for 500-1000 µM hemin vs. vehicle.

Next, I assessed some of the cell death inhibitors that I used in bEnd.3 cells in pBCECs. The two ferroptosis inhibitors that were protective in bEnd.3 cells, N-acetylcysteine and deferoxamine, also abrogated hemin-induced cell death in pBCECs, while ferrostatin-1 and U0126 both had no effect similar to my findings in bEnd.3 cells (**Figure 29**). I also evaluated

Z-VAD-FMK trying to understand the involvement of apoptosis in hemin-induced toxicity as the pan-caspase inhibitor partially protected bEnd.3 cells, while I did not observe cleaved caspase-3 at the different time points investigated. Interestingly, Z-VAD-FMK did not protect pBCECs from hemin-induced cell death, suggesting that apoptosis is likely not involved in brain endothelial cell death after brain hemorrhage.

A

Model of hemorrhagic stroke				Viability [%]
Hemin toxicity	Vehicle			100
	300-400 µM hemin			61.10 (47.89)
Cell death mechanism	Cell death inhibitor	Target	Conc.	Viability [%]
Ferroptosis	Ferrostatin-1	Canonical ferroptosis inhibitor, reactive lipid species (RLS)	1 µM	49.05 (34.43)
	Deferoxamine	Iron, hypoxia induced factor (HIF) prolyl hydroxylase domain-containing (PHD) inhibition	100 µM	82.92 (59.66)
	N-acetylcysteine	Reacitve Oxygen Species (ROS), RLS	2000 µM	75.92 (29.60)
	U0126	Mitogen activated protein kinase kinase ½ (MEK ½)	20 µM	24.17 (13.98)
Apoptosis	Z-VAD-FMK	Caspases	100 µM	54.38 (32.96)

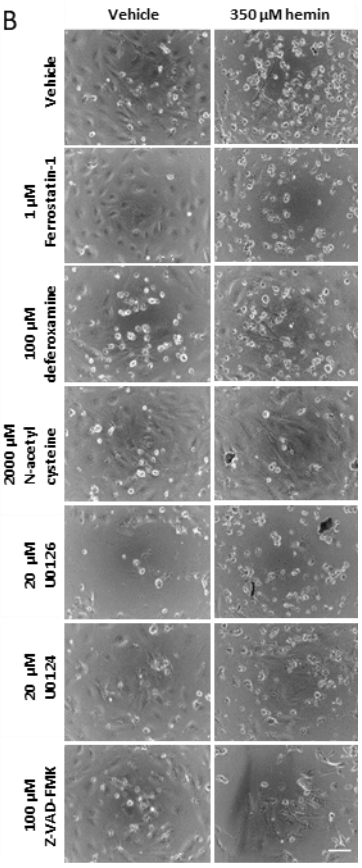

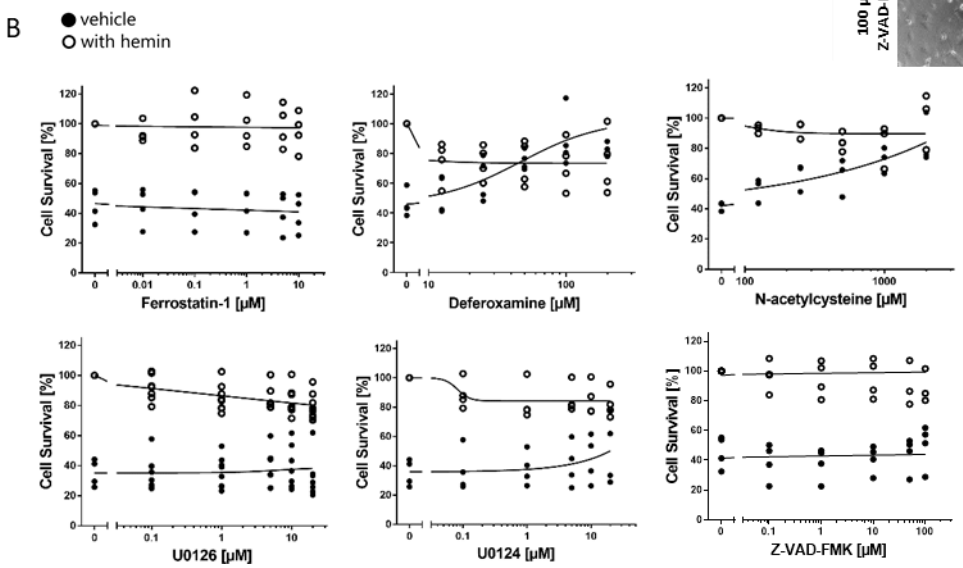

Figure 29. Selected cell death inhibitors in hemin-treated pBCECs. A) pBCEC cells were treated with 350-400 µM hemin (EC_{50}, determined the day prior to the inhibitor experiments for each culture as I observed differences between the different primary cultures) and the

different cell death inhibitors. Values show median (interquartile range) at representative concentrations. Grayscale coding indicates the degree from no protection (black) to maximal cell viability (white) in the presence of hemin. **B**) Representative phase-contrast images are shown. Scale bar = 200 µm. **C**) Concentration-responses of inhibitors in the MTT assay. Lines indicate non-linear regressions. N = 3-4 biological replicates (means of four technical replicates per biological replicate). Statistics were not performed due to the low sample size.

4.1.5. Differential involvement of cell death pathways in brain endothelial cells compared to neurons

To summarize, I statistically compared whether cell death in primary neurons and brain endothelial cells exposed to hemin is similar or different (**Table 14**). I observed a large overlap; statistical analysis did not reveal that they were different (Fisher's exact test, two-tailed $P = 0.7281$, **Table 15**).

Table 14. Comparison of the effectiveness of cell death inhibitors in neurons and brain endothelial cells treated with hemin. Comparison to previously published results in primary neurons exposed to hemin (Zille et al., 2017). Data on GSK872 and necrosulfonamide in neurons is from Dr. Marietta Zille, but has not been published so far.

Criterion	Z-VAD-FMK	Cycloheximide	Cyclosporine A	SB203380	SP600125	GSK872	Necrostatin-1	Necrosulfonamide	3-methyl adenine	Bafilomycin A1	Chloroquine	Mdivi-1	Ferrostatin-1	Deferoxamine	N-acetylcysteine	Trolox	U0126	DPQ	Olaparib
Neurons	-	-	-	-	-	+	+	-	-	-	-	-	+	+	+	+	+	-	-
Brain endo-thelial cells	-	-	-	-	-	+	-	-	-	+	-	-	-	+	+	+	-	-	-

Table 15. Statistical analysis of the profile of protective inhibitors in primary cortical neurons and brain endothelial cells. Fisher's exact test, two-sided $P = 0.7281$.

2x2 contingency table	Protective	Not protective	Total
Neurons	7	12	19
Brain endothelial cells	5	14	19
Total	11	27	38

4.2. Systematic review on stem cells and drug interactions

4.2.1. Interactions between NSCs and drugs commonly used in the elderly

To assess the effects of drugs commonly used in the elderly on NSCs, I performed a systematic pubmed search and identified 5954 publications. First, 582 duplicates were removed. After screening 5372 abstracts, I excluded 4865 abstracts because they were not relevant to the topic of my systematic review. Of the remaining 507 manuscripts that were assessed based on their full-texts, I excluded further 293 manuscripts (**Supplemental Table 1**). The exclusions were based on the following criteria: no adequate method provided, the use of another type of stem cells, the use of drugs that were not available on the market, no direct interaction between the drug and stem cells assessed, the use of non-mammalian species, the use of the drug only as a part of the procedure and other technical reasons such as review articles, non-English manuscripts or withdrawn articles. Eventually, 214 papers were available for quality synthesis (**Supplemental Table 2**).

Among those, 115 were records about the physiologic state of NSCs, 69 records reported the use of NSCs in the context of neurological disorders/injury, and 32 records studied NSCs under modified conditions such as in transgenic animals, enriched environment or the combination of drugs (**Figure 30, Table 16**).

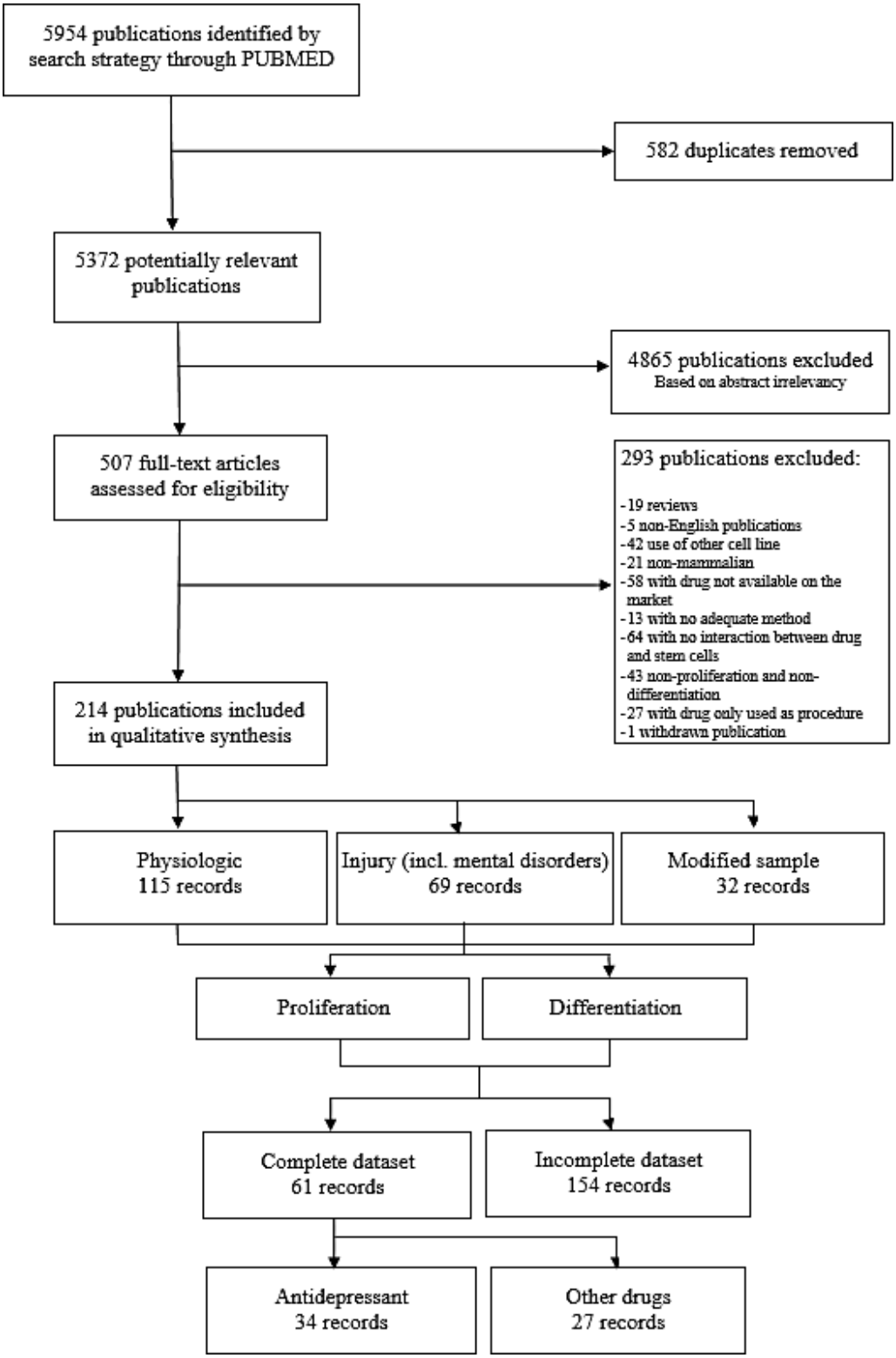

Figure 30. PRISMA Flow diagram of NSC interactions with drugs commonly used in the elderly. The number of "records" represents the number of experiments in all publications, because some publications describe multiple experiments covering different conditions (physiologic, injury or modified). Studies were included for meta-analysis if the complete dataset including sample size, mean, and standard deviation were accessible.

Table 16. Distribution of the records of drug classes and subclasses.

Drug class	Drug subclass	Number of records
Analgesic	Opioid	25
	Nonsteroidal anti-inflammatory drug	15
	Total	**40**
Antibiotic	Aminoglycoside	9
	Macrolide	9
	Quinolone	6
	Tetracycline	4
	Cephalosporin	2
	Nitroimidazol	1
	Total	**31**
Antidepressant	Selective serotonin reuptake inhibitor	54
	Tricyclic antidepressant	22
	Monoamine oxidases inhibitor	5
	Atypical antidepressant	1
	Selective serotonin-norephinephrine reuptake inhibitor	1
	Total	**83**
Antidiabetic	Insulin	9
	Thiazolidinedione	9
	Incretin mimetic	3
	Biguanide	1
	Total	**22**
Antihyperlipidemic	Statin	6
	Total	**6**
Antihypertensive	Loop diuretic	4
	Aldosterone receptor inhibitor	3
	Alpha 2 adrenergic agonist	3
	Beta blocker	3
	Calcium channel antagonist	3
	Ace inhibitor	2
	Angiotensin II receptor inhibitor	1
	Total	**19**
Other drugs	Phosphodiesterase type-5	6
	Corticosteroid	4
	Hormonal therapy	2
	Rho-Kinase inhibitor	2
	Supplement	2
	Antihelminthic	1
	Atypical antipsychotic	1
	Cytosine arabinoside	1
	Triazole derivative	1
	Total	**20**

Most of the publications investigated antidepressants and analgesics (83 and 40 records, respectively; **Table 17-18**). 69.2 % of the publications assessed the interaction between hippocampal stem cells and drugs. I did not find any record on NSC transplantation in combination with drugs nor clinical trials (**Table 13**).

Table 17. The six most frequently used drugs identified by the systematic search. To note, although rapamycin has been classified as an antibiotic, it is not in clinical use in humans as antibiotic.

Drug class	Drug subclass	Drug	Number of records
Antidepressant	Selective serotonin reuptake inhibitor	Fluoxetine	44
Analgesic	Opioid	Morphine	19
Antidepressant	Tricyclic antidepressant	Imipramine	18
Antidiabetic	Insulin	Insulin	12
Antibiotic	Macrolide	Rapamycin	8
Antidiabetic	Thiazolidinedione	Rosiglitazone	6

4.2.1.1. Drug effects on NSCs

I assessed the effect of the drugs on stem cells based on the drug classes and subclasses. Some of the drug classes were reported to stimulate or inhibit cell proliferation and/or differentiation (**Table 18)**. For instance, antidepressants had a predominantly stimulating effect on NSC proliferation and differentiation. In contrast, analgesics showed a predominantly inhibitory effect. Other drug classes had no predominant effect.

Table 18. Distribution of the drug classes based on the effect on NSCs.

Drug class	**Proliferation**			**Differentiation**		
	Stimulating	Neutral	Inhibiting	Stimulating	Neutral	Inhibiting
Analgesic	2 (14.3 %)	2 (14.3 %)	10 (71.4 %)	5 (26.3 %)	2 (10.5 %)	12 (63.2 %)
Antibiotic	5 (35.7 %)	3 (21.4 %)	6 (42.9 %)	3 (20 %)	6 (40 %)	6 (40 %)
Antidepressant	21 (56.7 %)	11 (29.8 %)	5 (13.5 %)	16 (51.6 %)	11 (35.5 %)	4 (12.9 %)
Antidiabetic	2 (50 %)	1 (25 %)	1 (25 %)	4 (50 %)	2 (25 %)	2 (25 %)
Antihypertensive	4 (57.1 %)	3 (42.9 %)	0	5 (45.5 %)	2 (18.2 %)	4(36.3 %)

I further separated the drug classes into different subclasses to understand whether some of the opposing effects may be due to individual classes. However, I did not identify specific drugs or subclasses that mediated the different effects within a drug class (**Table 19)**.

Table 19. Distribution of the drug subclasses based on the effect on NSCs.

Drug class	Drug subclass	Proliferation			Differentiation		
		Stimulating	Neutral	Inhibiting	Stimulating	Neutral	Inhibiting
Analgesic	NSAID	6	2	8	0	1	3
	Opioid	0	3	12	6	1	10
Antibiotic	Aminoglycoside	0	2	6	0	2	6
	Macrolide	2	2	3	2	2	4
	Quinolone	4	0	0	2	1	0
	Tetracycline	2	1	1	2	2	2
Antidepressant	MAO Inhibitor	0	1	2	1	2	3
	SNRI	0	0	0	1	0	1
	SSRI	27	11	4	16	10	5
	Tricyclic Antidepressant	12	3	0	12	1	1
Antidiabetic	Incretin mimetic	1	0	0	2	0	0
	Insulin	2	2	1	4	2	2
	Non sulfonylurea	0	0	0	1	0	0
	Thiazolidinediones	0	1	1	2	2	4
Antihypertensive	Aldosterone receptor inhibitor	1	1	1	1	0	0
	Alpha blocker	3	0	0	1	0	0
	Beta bloker	1	0	0	1	1	0
	Calcium channel blocker	0	1	0	2	1	2
	Loop diuretic	2	1	0	2	0	0

4.2.2. Meta-analysis

Meta-analysis is a statistical method to derive a specific estimate of the effect of a treatment from multiple studies with contradictory results. Descriptive data such as the sample size, mean, and standard deviation are required to perform meta-analysis. I extracted these data from the studies included in the “physiologic” condition. Only 18 records stated the complete dataset in the publication. I then contacted the authors of the studies with missing information to complete the dataset and obtained 19 additional datasets. Further 24 datasets were obtained by manually measuring the mean and standard deviations from the graphs using ImageJ.

From all collected datasets, only the data of the antidepressant drug class were sufficient to perform a meta-analysis. Twenty-one records reported effects on NSC proliferation (**Supplemental Table 3**) and 7 records on NSC differentiation in the physiologic condition (**Supplemental Table 4**), whereas 6 records were obtained describing effects on NSC proliferation in models of depression (**Supplemental Table 5**). Using meta-analysis, I confirmed that antidepressants significantly stimulated neuronal stem cell proliferation in the physiologic condition (Hedges' g SMD, 0.66; 95 % CI, 0.20 to 1.12; $P = 0.005$, **Figure 31A**). Selective serotonin reuptake inhibitors (SSRIs) were the most frequently studied drugs in the antidepressant drug class (**Table 19)**. They significantly induced the proliferation of NSCs (Hedges' g SMD, 0.72; 95 % CI, 0.17 to 1.27; $P = 0.01 < 0.017$ (Holm-Bonferroni cutoff *P*-value), **Figure 31A**). On the other hand, the effect of antidepressants on differentiation was neutral (Hedges' g SMD, 0.23; 95 % CI, -0.68 to 1.13; $P = 0.63$, **Figure 31B**).

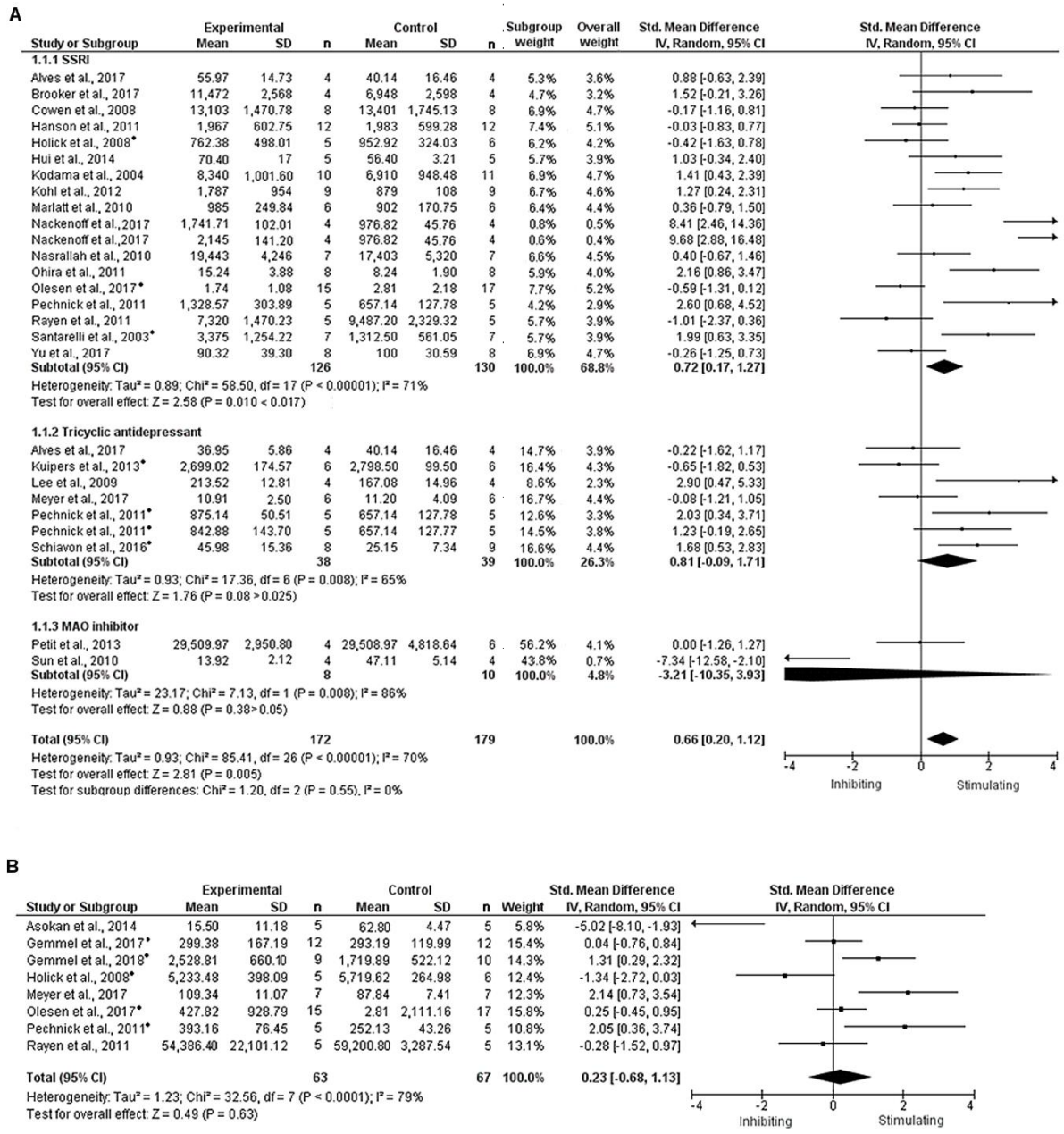

Figure 31. Forest plot of the effect of antidepressants under physiologic conditions. A) Antidepressant increased NSC proliferation (Hedges' *g* standardized mean difference (SMD), 0.66; 95% CI, 0.20 to 1.12; *P* = 0.005). The weights are given for both subgroup and the overall analysis. The *P*-values in the subgroup analysis were compared with the cutoff *P*-value calculated by the Holm-Bonferroni method, a sequential method of testing *P*-values (from smallest to largest) to correct for multiplicity. **B**) Antidepressants had an overall neutral effect on NSC differentiation. Hedges' *g* SMD, 0.23; 95 % CI, -0.68 to 1.13; *P* = 0.63). * indicates publications from which SDs and means were derived by manual graphical measurement using ImageJ.

I further performed meta-analysis on NSC proliferation in models of depression, which was nonsignificantly increased by the use of antidepressants (Hedges' g SMD, 1.14; 95% CI, -0.03 to 2.32; *P* = 0.06, **Figure 32**).

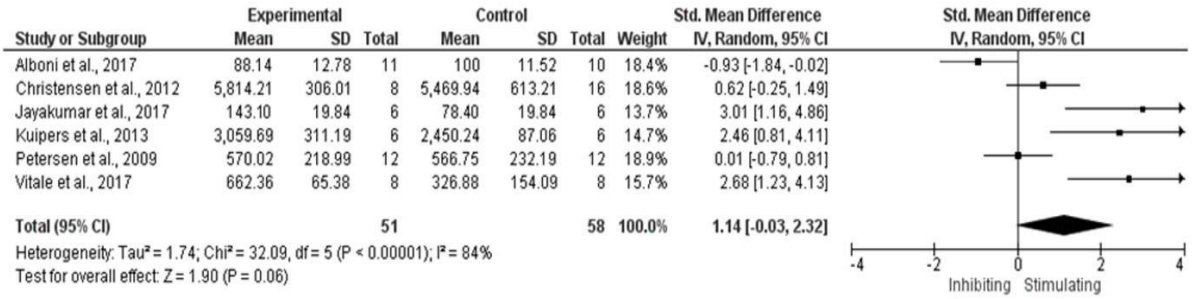

Figure 32. Forest plot of the effect of antidepressants in models of depression. Antidepressants stimulated NSC proliferation in models of depression, but the effect was not statistically significant (Hedges' *g* standardized mean difference (SMD), 1.14; 95 % CI, -0.03 to 2.32; *P* = 0.06). * indicates publications from which SDs and means were derived by manual graphical measurement using ImageJ.

4.2.3. Potential effect of drugs on NSCs in the context of brain injury

Although the number of studies investigating the interactions of drugs on NSCs in brain injury was very low, the few studies still offer potential insights that may be useful for future study design. For instance, the phosphodiesterase type 5 inhibitor sildenafil increased the proliferation of NSCs in the context of ischemia/hypoxia (Engels et al., 2017; Zhang et al., 2002; Zhang et al., 2012; Zhang et al., 2006). However, the overall number of publications with complete datasets were too low and the heterogeneous effects were too high to perform robust meta-analysis in the brain injury subgroup (will be discussed later, see section **5.2.1. Systematic review on NSCs and drug interactions**))

4.2.4. Interactions between EPCs and drugs commonly used in the elderly

EPCs play a pivotal role in repairing the vascular damage and inducing angiogenesis. This may be crucial in ICH which is caused by the rupture of a blood vessel and hence, vascular damage occurs. Here, I systematically searched the literature to investigate the effect of drugs that are commonly used in the elderly on EPCs in the context of the brain (**Figure 33**). I identified 47

publications, removed five duplicates, and excluded 14 publications based on their abstracts that were irrelevant to the topic, leaving 28 publications for full-text assessment. Of those, I excluded 22 publications according to the predetermined inclusion and exclusion criteria (**Supplemental Table 6**). The remaining six publications (**Supplemental Table 7**) will be discussed below (see section **5.2.2. Systematic review on EPCs and drug interactions)**. Since the number of studies was too low, I did not perform meta-analysis.

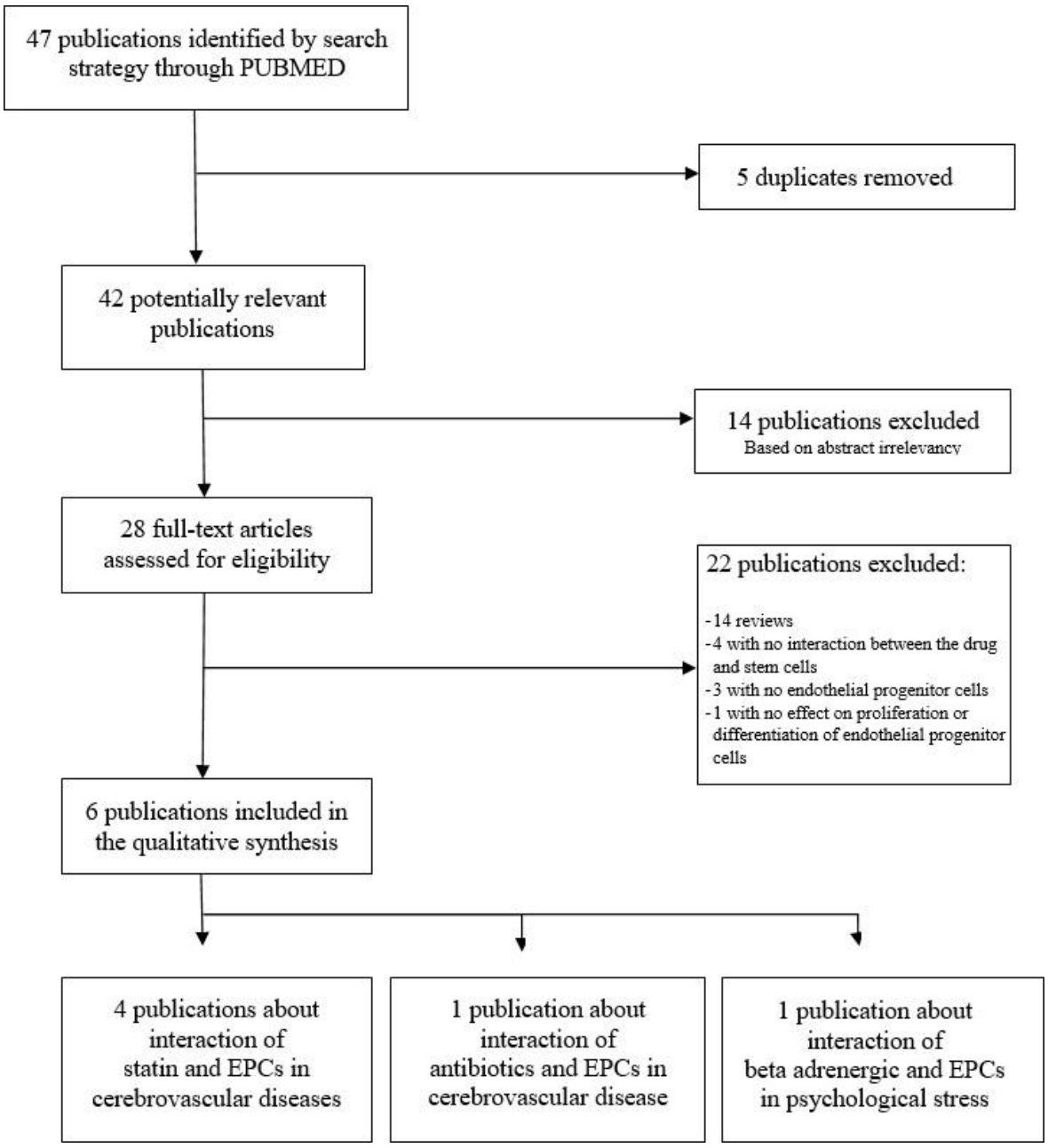

Figure 33. PRISMA Flow diagram of the interactions of EPCs with drugs commonly used in the elderly in the context of the brain.

5. Discussion

5.1. Characterization of brain endothelial cell death in ICH

Understanding secondary damage mechanisms caused by hemolysis products in the hematoma after ICH is important for the development of treatment options because surgical removal of the hematoma is of limited benefit. Although the cell death mechanisms in neurons (Kwon et al., 2013; Su et al., 2018; Zille et al., 2017) and astrocytes (Chen & Regan, 2004, 2005; Laird et al., 2008; Owen et al., 2014; Regan et al., 2001) have been comparably well studied, the mechanisms underlying brain endothelial cell death still remain to be elucidated. In this thesis, I demonstrated that brain endothelial cell death after hemin treatment is not different from neuronal cell death overall, but that some cell death inhibitors effective against neuronal cell death do not protect brain endothelial cells from hemin-induced cell death.

First of all, it was important to establish that hemin induces brain endothelial cell death. There has been previous evidence in the literature assessing brain endothelial cells *in vitro* (Higdon et al., 2012; Imai et al., 2019; Sukumari-Ramesh et al., 2010; Vigne et al., 1995; Xu et al., 2019a), *in vivo* (Cui et al., 2016; Zhou et al., 2014), and in human tissue from subarachnoid hemorrhage (Friedrich et al., 2012) and ICH (Shtaya et al., 2019). In particular, Sukumari-Ramesh and colleagues observed that hemin decreased the cell viability of bEnd.3 cells (Sukumari-Ramesh et al., 2010). This is in line with my findings. However, I observed that only higher concentrations of hemin (350 µM compared to 75 µM) and longer time periods (24 hours compared to 18 hours) were sufficient to reduce the cell viability by 50 % (**Figure 15**). This was further substantiated by the time-lapse experiments showing that hemin affected the bEnd.3 cells in a time- and concentration-dependent manner (**Figure 16**).

Only very few studies investigated the underlying cell death mechanisms. To distinguish these mechanisms, various biochemical tools and markers have been reported for the use in cell death research, although some of them have been identified to be involved in different modes of regulated cell death. Therefore, the Nomenclature Committee on Cell Death recommends the use of at least two independent markers or criteria to validate the cell death mechanism (Galluzzi et al., 2009; Galluzzi et al., 2018; Kroemer et al., 2009). Here, I applied chemical inhibitors of different cell death mechanisms including apoptosis, necroptosis, autophagy, ferroptosis, and parthanatos. I also used biochemical markers of some of these pathways as a second measure of their involvement. To ensure target specificity, I used several additional controls where possible. For instance, I used inactive controls of some of the drugs or

structurally diverse drugs that have the same target to see whether the drug affects the pathway not simply because of its off-target effects. I also used multiple inhibitors to block different targets in the same pathway.

5.1.2. Apoptosis

Apoptosis has been previously demonstrated to be involved in ICH pathophysiology (Fan & Mu, 2017). The pan-caspase inhibitor Z-VAD-FMK decreased the number of dead cells in a rat collagenase model of ICH (Matsushita et al., 2000). However, *in vitro* experiments in neurons demonstrated that Z-FAD-FMK did not protect the cells from hemin toxicity (Goldstein et al., 2003; Su et al., 2018; Zille et al., 2017). In endothelial cells, hemin-induced cell death of bEnd.3 cells was partially abrogated by the apoptosis inhibitor Z-VAD-FMK (Sukumari-Ramesh et al., 2010). In my systematic analysis, I also demonstrated that Z-VAD-FMK partially blocked hemin-induced cell death in bEnd.3 cells (**Figure 17**). However, when I tested Z-VAD-FMK on pBCECs, cell death was not abrogated (**Figure 29**).

I also assessed other drugs that inhibit different players of the apoptosis cascade. It has been reported previously that the c-Jun-terminal kinase inhibitor SP600125 and the protein synthesis inhibitor cycloheximide abrogate ICH-induced neuronal injury in rats by inhibiting c-Jun-terminal kinase (Ohnishi et al., 2007). The P38 MAPK inhibitor SB203580 is able to decrease neurological deficits in ICH in mice via the suppression of platelet-derived growth factor receptor alpha (Ma et al., 2011). However, none of these three inhibitors protected bEnd.3 cells from hemin-induced toxicity (**Figure 17**).

As a second measure of apoptosis, I sought to assess a biochemical marker of apoptosis. The expression of annexin V has been previously reported in hemin-treated bEnd.3 cells (Sukumari-Ramesh et al., 2010). However, the presence of annexin V is not specific to apoptosis. For instance, annexin V can be expressed in secondary necrosis where phosphatidylserine is exposed for binding at the inner leaflet of the cell (Zille et al., 2012). Another apoptosis marker that has been used to investigate apoposis in ICH is TUNEL and an increase of the number of TUNEL-positive cells was detected in the autologous blood injection model of ICH in rats (Fan & Mu, 2017; Matsushita et al., 2000). Although TUNEL is able to detect DNA fragmentation, some TUNEL-positive cells have been reported to be necrotic cells (Duan et al., 2003). Cleaved caspase-3 is a more reliable marker of apoptosis since both intrinsic and extrinsic apoptosis pathways converge onto it (Ashkenazi et al., 2017; Wong, 2011). Enhanced caspase-3 activity

has also been demonstrated in the autologous blood injection model of ICH in rats (Fan & Mu, 2017; Matsushita et al., 2000).

Therefore, I decided to investigate the cleavage of caspase-3 at different time points after hemin treatment as caspase-3 activation may be transient and investigating single time points may lead to false-negatives. In the positive control, the treatment of the cells with the apoptosis inducer staurosporine, I was able to demonstrate the specificity of the antibody as well as that Z-VAD-FMK reduces caspase-3 cleavage (**Figure 18**). Based on this result, my finding that bEnd.3 cells treated with hemin did not indicate an increase of cleaved caspase-3 at any of the investigated time points (**Figure 19**) suggests that caspase-dependent apoptosis is not involved in hemin toxicity in brain endothelial cells.

However, what may be the reason for Z-VAD-FMK to lead to partial protection? One possibility is that the caspase-3 was cleaved at a certain time point besides 2, 4, 8 or 24 hours. The time when the cell death happened is one of the stumbling blocks of cell death detection since the exact time for measuring cell death is not known. Another possibility is that the cell death mechanism in hemin-treated endothelial cells involves many pathways. This explanation may fit with the fact that Z-VAD-FMK only led to a partial blocking of the cell death. It could be that the cells undergo other pathways beside caspase-dependent apoptosis. Further experiments such as the detection of other markers of apoptosis, e.g. BCL-2, and testing the application of combinations of cell death inhibitors is important to investigate these hypotheses.

5.1.3. Necroptosis

It is known that in the presence of apoptosis inhibitors or caspase-8 inactivity, cells can switch from apoptosis to necroptosis to execute cell death eventually (Degterev et al., 2005). In neurons, necroptosis has been observed after hemin exposure. The RIPK1 inhibitor necrostatin-1 significantly protected neurons and astrocytes from hemin toxicity (Su et al., 2018; Zille et al., 2017). In addition, necrostatin-1 has been shown to protect in the *in vivo* model of ICH (Chang et al., 2014; Chu et al., 2018; Su et al., 2015). Necroptosis has also been detected in astrocytes under hemin exposure (Laird et al., 2008). Furthermore, an increase in *Ripk1* and *Ripk3* gene expression was observed after hemin application, along with an increase in RIPK1 phosphorylation at serine 166, indicative of necroptosis (Zille et al., 2017). In addition, antibodies against phospho-RIPK3 and phospho-MLKL may help to specify the necroptosis finding (Zille et al., 2019a). In electron microscopy, it is not possible to differentiate

between necrosis and necroptosis, but morphological signs of necrosis support the notion of an involvement of necroptosis in hemin-induced neuronal cell death (Zille et al., 2017).

In this study, I observed that neither the RIPK1 inhibitor necrostatin-1 compared to its inactive analog nor the MLKL inhibitor necrosulfonamide protected bEnd.3 cells from hemin-induced cell death. However, the RIPK3 inhibitor GSK872 partially abrogated the cell death (**Figure 20**). Taken together, my data is insufficient to verify that necroptosis plays a role in hemin-induced cell death in brain endothelial cell because only one inhibitor was effective, which may be an off-target effect. Future studies using molecular knockdown of the key necroptosis proteins or demonstrating necrosome formation are required to accept or refute the involvement of necroptosis.

5.1.3. Autophagy

Autophagy is a complex mechanism that may also result in cell death (Denton & Kumar, 2019). The co-existence of autophagy, ferroptosis, and necrosis has been demonstrated in neurons after ICH using electron microscopy (Li et al., 2018a). Iron overload may force the conversion of LC3-I to LC3-II which mediates autophagosome formation (He et al., 2008a). Besides iron, thrombin has been suggested to be involved in autophagy in ICH (Zhang & Liu, 2020). Furthermore, heme was reported to mediate autophagy via endoplasmic reticulum stress in neurons (Yang et al., 2020). In addition, autophagy was also observed in microglia exposed to erythrocyte lysis, involving the beclin-1-ATG pathway (Yuan et al., 2017). Pretreatment with 3-methyladenine, that blocks autophagosome formation, decreased brain edema, cell death, LC3 expression, but also caspase-3 cleavage in a mouse collagenase model of ICH, while the autophagy inducer rapamycin reversed these effects (Shen et al., 2016). Furthermore, the presence of LC3 has been observed in ICH patients and was correlated with ICH severity (Wu et al., 2019). Autophagosomes and autophagic genes have also been detected in the perihematoma area of ICH patients (Durocher et al., 2020).

I used different autophagy blockers in hemin-treated bEnd.3 cells, namely 3-methyladenine, bafilomycin A1, chloroquine and mdivi-1 as well as rapamycin as an autophagy inducer. All the inhibitors have been previously tested in hemin-treated neurons, but were ineffective in blocking cell death (Zille et al., 2017). In my study, only bafilomycin A1 showed a protective effect (**Figure 21**). Interestingly, bafilomycin A1 also inhibited cell death under the exposure of the ferroptosis inducer erastin in cancer cells but not in neurons (Zille et al., 2019b). Bafilomycin A1 works by inhibiting the fusion of the autophagosome and the lysosome.

However, bafilomycin A1 has been demonstrated to be specific only for a short time period, beyond which it has undesirable effects such as the inhibition of endosome transport proteosomal blockage. Furthermore, one of the targets of bafilomycin A1, the V-ATPase, is expressed not only on lysosomes, but also on endosomes and the plasma membrane. V-ATPases play an important role in maintaining a slightly alkaline pH in the cytosol, which prevents acid-induced apoptosis and promotes antitumor drug resistance (Vinod et al., 2014).

Another drug, chloroquine, that inhibits the transfer of materials inside the lysosome to the autophagosome after fusion, did not protect hemin-treated bEnd.3 cells. The inability of chloroquine to block cell death despite the significant inhibition by its upstream inhibitor bafilomycin A1 indicates that the protective effect of bafilomycin A1 may be independent of the autophagosome formation. Alternatively, bafilomycin A1 may also block mitochondria and lysosome destruction after the formation of the autophagosome, which has been demonstrated in staurosporine-induced neuronal death (Shacka et al., 2006).

Of note, mdivi-1 decreased the metabolic activity of vehicle-treated cells. However, there was no increase in the number of PI-positive cells, indicating that the cells are not dead. An alternative possibility for its effect on reducing metabolic activity may be because mdivi-1 inhibits mitochondrial complex I, thereby altering the NAD^+/NADH ratio (Dai et al., 2020), which would affect the conversion of MTT to formazan.

As a second, independent measure of autophagy, I evaluated LC3 in hemin-treated bEnd.3 cells, which was increased in a concentration-dependent manner (**Figure 23**). I further observed that the expression of LC3 started to increase at 4 hours after the start of hemin incubation. Together, this data demonstrates that autophagy plays a role in hemin-induced brain endothelial cell death. However, further experiments need to be performed to identify how autophagy may interact with other cell death pathways.

5.1.4. Ferroptosis

Another cell death mechanism shown to be involved in hemin-induced neuronal cell death is ferroptosis (Zille et al., 2017). We used seven chemical inhibitors that collectively define ferroptosis (Dixon et al., 2012; Zille et al., 2017):

1) N-acetylcysteine is a precursor of cysteine (a building block of GSH). GSH is needed to induce GPX4 that is able to reduce the lipid peroxides in ferroptosis (Alim et al., 2019). N-acetylcysteine administration improved functional recovery in the collagenase-induced mouse model of ICH (Karuppagounder et al., 2018) and abrogated hemin-induced toxicity in primary

neurons (Zille et al., 2017). In endothelial cells, N-acetylcysteine has been shown to prevent hemin toxicity (Sukumari-Ramesh et al., 2010). In this study, I also observed that N-acetylcysteine protected brain endothelial cells from hemin-induced toxicity (**Figure 24**).

2) Deferoxamine, an iron chelator, is able to inhibit hemin-related cell death via HIF prolyl hydroxylase domain enzymes that are involved in cell death transcription (Karuppagounder et al., 2016). Deferoxamine has been demonstrated to inhibit cell death in neurons (Hatakeyama et al., 2013; Karuppagounder et al., 2016; Zille et al., 2017), abrogate microglia activation (Sun et al., 2016) and protect endothelial cells from heme toxicity (Sukumari-Ramesh et al., 2010). Deferoxamine has also attenuated cell injury in animal models of ICH (Cui et al., 2015; Hu et al., 2019; Xie et al., 2014). Moderate doses of deferoxamine have been demonstrated to be safe for the treatment of ICH patients, but further studies are needed to establish efficacy (Selim et al., 2019). Deferoxamine may also be involved in autophagy via its iron scavenging function by preventing the conversion of LC3-I to LC3-II and thereby autophagosome formation (He et al., 2008b). In my study, deferoxamine also protected brain endothelial cells from hemin-induced toxicity (**Figure 24**). Of note, deferoxamine also reduced the metabolic activity of the cells, which seemed to be due to decreased cell proliferation, potentially by reducing iron storages in the cells (Foa et al., 1986).

3) The lipid peroxide inhibitor and canonical ferroptosis inhibitor ferrostatin-1 has been reported to inhibit neuronal cell death upon hemin treatment (Zille et al., 2017). Ferrostatin-1 also attenuated hemoglobin-induced neuronal cell death in organotypic hippocampal slice of mice and reduced neurological deficits, injury volume, and iron deposition in the collagenase-induced ICH model in mice (Li et al., 2017). The protective effect of ferrostatin-1 has been observed to also promote long-term functional outcome of mice subjected to aulogous blood infusion as a model of ICH (Chen et al., 2019) . However, I did not observe a protective effect of ferrostatin-1 in hemin-treated brain endothelial cells (**Figure 24**).

4) Trolox, a vitamin E analog, is an antioxidant that inhibits cell death in erastin-treated (Zille et al., 2019b) and hemin-treated neurons (Zille et al., 2017). It has been suggested that the protective effect of Trolox is not related to iron-dependent oxidative neurotoxicity, but that Trolox protects the plasma membrane due to its lipid solubility (Jaremko et al., 2010). Trolox has already been demonstrated to abrogate hemin-induced endothelial cell death (Sukumari-Ramesh et al., 2010). In line with these results, I observed that trolox abrogated hemin-induced cell death of bEnd.3 cells (**Figure 24**).

5) U0126, a MAPK kinase inhibitor, has been demonstrated to prevent erastin-induced (Zille et al., 2019b) and hemin-induced neuronal cell death (Zille et al., 2017). It has been suggested to work by reducing HO-1 activity (Chen-Roetling et al., 2009). The phosphorylation of extracellular signal-regulated kinase, downstream of MAPK kinase, is increased in neurons (Ohnishi et al., 2007; Zille et al., 2017) and astrocytes in the context of ICH (Regan et al., 2001). Conversely, other MAPK inhibitors have been demonstrated to decrease cell death (Ohnishi et al., 2007; Regan et al., 2001). In my study, I used U0124, an analog of U0126 that cannot inhibit MAPK kinase at concentrations below 100 µM, which is helpful to define whether the effect of U0126 is based on MAPK kinase inhibition or a potential off-target effect (Favata et al., 1998). Both U0126 and U0124 were not able to inhibit brain endothelial cell death under hemin exposure (**Figure 24 and 29**).

6) Cycloheximide, a protein synthesis inhibitor, and 7) actinomycin D, a transcription inhibitor, originally were used to define erastin-mediated cell death as ferroptotic (Dixon et al., 2012). However, hemin-induced ferroptosis has been shown to be independent of transcription and translation (Zille et al., 2017). The presence of these two inhibitors in classical ferroptosis (Ratan, 2020)is the main reason for their inclusion in this experiment. However, none of them prevented hemin-induced brain endothelial cell death (**Figure 24**). On the other hand, both decreased the metabolic activity of vehicle-treated cells, while there was no increase in PI indicating that this effect was independent of cell death. A potential reason may be that the general inhibition of gene transcription or protein translation affects the availability of enzymes including mitochondrial reductase that converts MTT into formazan.

Besides those seven putative ferroptosis inhibitors, I investigated TfR1, an iron transporter and newly described ferroptosis biomarker, as well as the presence of lipid peroxides using MDA (Feng et al., 2020). TfR1 is crucial for iron homeostatis. It binds to transferrin, a major iron distributor in the cells, and controls the transport of iron into the cells (Gamella et al., 2017). The expression of TfR1 is altered in the context of neurodegenerative diseases (Wu et al., 2003). In ICH, TfR1 expression increased due to iron accumulation in the brain of the rat model (Chen et al., 2015; Zhou et al., 2017). MDA is a well-studied lipid peroxide breakdown product (Gaschler & Stockwell, 2017) that can be used as a marker for ferroptosis (Feng et al., 2020). The level of MDA peaked at 3 days after ICH in mice (Chen et al., 2019; Mao et al., 2017; Wang et al., 2017a). It has also been reported that serum MDA levels increased significantly in ICH patients and were correlated with the mortality of the patients (Lorente et al., 2018).

In my study, the expression of TfR1 or MDA increased in a concentration-dependent manner upon hemin exposure (**Figure 26**). But the administration of ferrostatin-1, a lipid peroxide inhibitor, failed to abrogate cell death. Thus, it indicates that N-acetylcysteine and deferoxamine may inhibit the toxic effect of hemin not by blocking ferroptosis. To note, there is also a basal expression of TfR1 and MDA under physiological conditions.

5.1.5. Parthanatos

Parthanatos has been reported to be involved in nervous system diseases (for review, see (Wang & Ge, 2020)). In the context of ICH, parthanatos inhibitors did not protect neurons from hemin-induced toxicity (Zille et al., 2017). In my study, there was no indication of the involvement of parthanatos in hemin-induced brain endothelial cell death. I used two different inhibitors that work on the same target, PARP1 and PARP2. Both did not abrogate cell death (**Figure 27**). Further investigations of parthanatos including the detection of PAR oligomers or macrophage migration inhibitory factor are needed to further confirm this finding.

5.1.6. Conclusions of the experimental research

In conclusion, my data indicate that brain endothelial cell death after hemin exposure may be executed by different cell death mechanisms, including ferroptosis, necroptosis and autophagy. This is similar to what was observed in neurons (**Tables 14-15**) (Li et al., 2018a; Zille et al., 2017). The lack of effect of ferrostatin-1 may indicate that ferroptosis is not the main pathway in hemin-mediated cell death in brain endothelial cells. In fact, numerous studies point out the role of deferoxamine and N-acetylcysteine in autophagy in various cell types with many, sometimes contradictive, effects (Gutierez et al., 2014; Rakshit et al., 2020; Sahni et al., 2014; Sun et al., 2018; Wu et al., 2010). Further experiments to confirm this hypothesis are needed.

5.1.7. Limitations of the experimental research

My study had several limitations:

First, I cannot formally exclude that caspase-3 is not cleaved another time points than those I investigated in this study. Timing is one of the critical aspects of studying cell death since the exact timepoint when the cell deaths occur is unknown.

Second, the lack of well-established methods to determine some of the cell death mechanisms limits firm conclusions. Compared to apoptosis, the research on other cell death mechanisms is so far limited.

5.2. Systematic review on stem cells and drug interactions

Although knowing the cell death mechanism is of benefit to apply the cytoprotective agents to the cells in ICH, the hematoma will also cause immediate cell death in some part of the tissue. The conventional therapy aims to remove the hematoma, which will leave behind an empty cavity that will be filled by connective tissue. Stem cell therapy may help to fill this space and replace the dead cell (Zahra et al., 2020). However, the efficacy of stem cells therapy in ICH is still far from established (Gao et al., 2018b). In particular, polypharmacy is a confounding factor as elderly patients frequently suffer from comorbidities that require additional pharmaceutical intervention. Thus, we need to understand the effect of these drugs on the function of stem cells. This may provide the opportunity to specifically combine stem cells with drugs that can enhance stem cell function to achieve more efficient therapeutic interventions.

5.2.1. Systematic review on NSCs and drug interactions

Neuronal stem cells are a promising target for the therapy of neurodegenerative diseases. The exponential increase of studies in this field reflects an emerging hope. However, my systematic review revealed that multi-drug usage in the potential patient population, i.e. the elderly, is not sufficiently considered when designing research studies investigating the effect of endogenous stem cells as well as stem cell therapy. This raises concerns regarding the translational predictability of the respective studies. I therefore propose to consider drug-stem cell interactions in study design and to assess how pharmacological drugs and stem cells can be combined in more efficient, safe, and ultimately successful therapeutic strategies.

My systematic review on NSCs revealed 5954 papers over the last decade regarding drug-neuronal stem cell interactions. Only 214 studies were included in the qualitative synthesis after applying inclusion and exclusion criteria (**Figure 30**). I observed a large heterogeneity among the drugs used (**Table 16**). There was an unequal distribution of drugs and some drugs seemed to be more frequently studied as compared to their clinical representation. For example, fluoxetine dominated in the anti-depressants drug class. This may mislead the interpretation in case individual drugs within a drug class act differently. However, as can be seen from the analysis of the drug classes, respective subclasses, and individual drugs, the main effect on

proliferation and differentiation is similar (**Table 18-19**). My systematic literature reviews also revealed that the effects of drugs used in geriatric patients on NSCs have not been studied in much detail so far. In fact, the identified publications reported such interactions as auxiliary findings.

I observed that, although there were numerous studies using *in vitro* and *in vivo* models, there was no clinical trial investigating drug-stem cell interactions. Furthermore, endogenous stem cells investigated *in vivo* as well as NSCs evaluated *in vitro* dominated the identified studies (**Supplemental Table 2**).

I was able to show a clear interaction between antidepressants and NSCs in the physiologic condition and in models of depression (**Figures 31-32**). Although antidepressants are used in the treatment of post-stroke depression **(Robinson & Jorge, 2016)** and, based on my meta-analysis, stimulate NSC proliferation, the situation may be far more complex in human patients. For example, recent clinical trials demonstrated that while fluoxetine was effective in preventing post-stroke depression, there were no obvious effects on functional recovery, but a higher rate of bone fractures was observed **(AFFINITY trial collaboration., 2020a; EFFECTS trial collaboration., 2020b; FOCUS trial collaboration., 2019)**. Therefore, it is important to understand that my systematic review specifically investigated the effect of the drugs on NSC proliferation and differentiation. Although they are important for stem cell function, these parameters are neither the only ones indicating improved functional recovery after stroke, nor the most important ones.

To further understand how drugs used in the elderly affect stem cells, I elaborate the underlying mode of action of the drugs in the context of NSC differentiation and proliferation that have been investigated by several authors (**Figure 34**). This is an important step to develop more effective and specific drug-stem cell combination treatments and to minimize potential adverse effects. Among all records in the physiologic condition, the six most frequently utilized drugs (fluoxetine, imipramine, morphine, rosiglitazone, rapamycin, and insulin, **Table 11**) have been tested for their mechanism of action. However, the identified pathways were only described in a single publication each (**Figure 34**) and therefore still need to be verified.

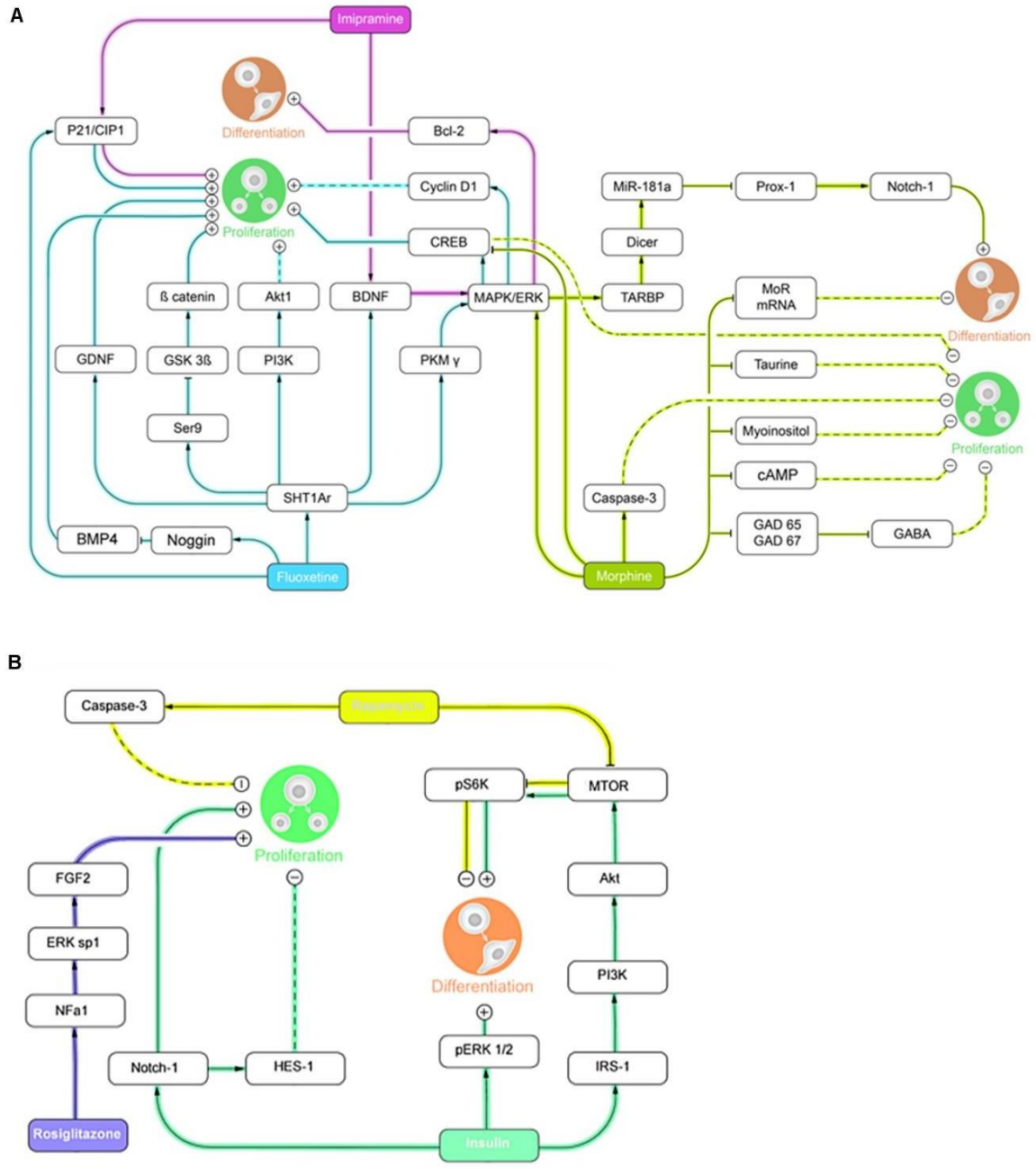

Figure 34. Recorded pathways from the selected publications in the NSC systematic review. The mechanisms of the drugs (**A**) imipramine, fluoxetine, morphine, and (**B**) rosiglitazone, rapamycin, and insulin on NSC proliferation and differentiation have been reported in a single publication each. Arrows indicate stimulation and T-shapes indicate inhibition of the subsequent substance. Positive signs indicate stimulation and negative signs indicate inhibition of the end effects (proliferation or differentiation). The straight lines indicate proven mechanisms and the dotted lines indicate assumed mechanisms. Abbreviations: Bcl-2, B-cell lymphoma-2; BDNF, brain-derived neurotrophic factor; BMP4, bone morphogenetic protein 4; cAMP, cyclic adenosine monophosphate; CIP1, cyclin-dependent kinase (CDK) inhibitor protein 1; CREB, cAMP response element-binding protein; FGF2, fibroblast growth

factor-2; GABA, γ-aminobutyric acid; GAD, glutamic acid decarboxylase; GDNF, glial cell-derived neurotrophic factor; GSK3β, glycogen synthase kinase 3β; HES-1, hairy and enhancer of split-1; IRS-1, insulin receptor substrate-1; MAPK, mitogen-activated protein kinase; NF-α-1, nuclear factor-α-1; pERK/ERK, phosphorylated extracellular signal-regulated kinases; PI3K, phosphatidylinositol-4,5-biphosphate 3-kinase; PKM, protein kinase M; SHT1Ar, serotonin-1-agonist receptor.

Fluoxetine, imipramine, and morphine affect the mitogen-activated protein kinase/extracellular signal-regulated kinase (MAPK/ERK) pathway (Xu et al., 2015). This is one of the key signaling pathways modulating neuronal stem cell proliferation and differentiation (Jiang et al., 2015; Peng et al., 2008). MAPK signaling contributes to synaptic plasticity and long-term memory formation (Impey et al., 1999). It is also supposed to be neuroprotective (Davis, 2000).

The antidepressant fluoxetine increased the proliferation of NSCs. This is likely mediated by the activation of serotonin-1-agonist receptor (SHT1Ar, **Figure 34**) (Hui et al., 2014; Zusso et al., 2008). SHT1Ar activated phosphatidylinositol-4,5-biphosphate 3-kinase (PI3K), followed by an increase of AKT1 that in turn increased neuronal stem cell proliferation (Rahmani et al., 2013). Moreover, SHT1Ar triggered the MAPK/ERK cascade which increased neurogenesis by stimulating cyclin D1 (Zusso et al., 2008). Hui and colleagues reported that SHT1Ar induced ser9, which inhibited glycogen synthase kinase 3β (GSK3ß) followed by the activation of β-catenin (Hui et al., 2014). Another potential mechanism is that SHT1Ar stimulated the cAMP response element-binding (CREB) protein by activating MAPK/ERK (Wang et al., 2014b). In a study unrelated to SHT1Ar, fluoxetine stimulated cyclin-dependent kinase (CDK) inhibitor protein 1 (P21/CIP1) leading to increased neurogenesis (Pechnick et al., 2011).

Rapamycin and insulin affect the mTOR signaling pathway in different ways. Insulin stimulated serine/threonine and subsequently enhance mTOR and rapamycin inhibited it (Hancer et al., 2014; Lee et al., 2016a; Lee et al.,2016b). mTOR is a receptor tyrosine kinase that is pivotal in regulating cell proliferation and differentiation (Yu et al., 2017). Inhibition of mTOR blocked p70 ribosomal S6 Kinase (S6K) which then led to the inhibition of stem cell differentiation via telomerase activity reduction (Dogan et al., 2018; Lee et al., 2016b).

An antidiabetic drug from the subclass of thiazolidinediones, rosiglitazone, stimulated the neurotrophic factor α1 (NF-α1) which then upregulated the fibroblast growth factor-2 (FGF-2). FGF-2 induced neurogenesis in the hippocampus (Cheng et al., 2015). Another study

demonstrated that FGF-2 needs cystatin C to induce its mitogenic activity (Taupin et al., 2000). However, this has not yet been confirmed by the identified publications.

Taken together, although they are potential therapeutic targets, these pathways also control many very fundamental cell processes. Modulating these pathways may therefore cause interference with important basic cellular functions. Hence, it would be necessary to find more specific targets avoiding adverse side effects and/or supporting positive effects. In addition, prospective research should validate each pathway in the particular cell type and source of interest.

5.2.2. Systematic review on EPCs and drug interactions

For the EPCs literature review, the number of studies investigating the effects of drugs used in the elderly on EPCs in the brain is low (**Figure 33**). Among the identified studies (**Supplemental Table 7**), four studies focused on the effect of statins on EPCs in the context of stroke or traumatic brain injury. They demonstrate that statins can increase the number of EPCs, enhance their migration in the blood after ischemic stroke (Golab-Janowska et al., 2018; Marti-Fabregas et al., 2013; Meamar et al., 2016), and improve functional outcome in traumatic brain injury (Wang et al., 2012). One study assessed the effect of chronic subtherapeutic antibiotics treatment at doses that are commonly used in agriculture on the therapeutic efficacy of EPC transplantation in ischemic stroke in mice. Antibiotics treatment abrogated the beneficial effects ofEPC transplantation on cerebral ischemic injury, including infarct size reduction, functional outcome improvement, and angiogenesis promotion. Similar effects were also observed when the authors used EPC-conditioned culture medium and levels of secreted vascular endothelial growth factor and platelet-derived growth factor were reduced (Dong et al., 2017). Another study reported that the administration of the beta-adrenergic receptor agonist isoproterenol failed to mobilize the progenitor cells in human blood in response to acute psychological stress (Riddell et al., 2015).

I identified only two studies about EPCs in the context of ICH that demonstrated an improvement of ICH prognosis via several effects, including reendothelialization, vasculogenesis, paracrine-related angiogenesis, and BBB protection (Li et al., 2015a; Pias-Peleteiro et al., 2017).

The number of studies was insufficient to perform meta-analysis. Nonetheless, the use of EPCs in brain injury, especially in cerebrovascular disease has been proposed as a potential novel therapy (Bayraktutan, 2019; Esquiva et al., 2018).

5.2.3. Unmet research needs identified in the systematic review

It is important to investigate the effect of the combination of stem cells and drugs under physiologic conditions to comprehend the basic interactions of the drugs with NSCs. In addition, the underlying mechanisms should be assessed in injury conditions, e.g., in animal models of neurodegenerative diseases. Another point to be scrutinized is that drug metabolism (pharmacokinetics and dynamics) is distinct between rodents and humans. Hence, further studies to ensure the translatability need to be performed.

Endogenous EPC therapy, in contrast, is well studied as a stem cell therapy for cardiovascular disease (Bianconi et al., 2018; Chong et al., 2016). Since we want to focus only on the effect of EPC on the brain, we decided to specify the keywords of the screening by including “brain” in front of “EPC”. In contrast to the cardiovascular field, the number of studies on the underlying mechanisms of how EPCs improve functional outcome after cerebrovascular disease are still limited. Furthermore, the underlying mechanisms for the effect of EPCs on cerebrovascular disease are still unclear (Lapergue et al., 2007). Several studies suggest the use of EPCs for the treatment of neurological diseases such as stroke (Bayraktutan, 2019; Esquiva et al., 2018; Lapergue et al., 2007; Pias-Peleteiro et al., 2017). Although it has been demonstrated that the transplantation of EPCs into the brain can promote atherosclerotic plaque formation and abnormal intima hyperplasia (Decano et al., 2013), other studies report that EPC transplantation inhibits neointima hyperplasia when transfected with angiotpoietin-1 (Wang et al., 2014a). Thus, the transplantation of EPC may still be promising for the treatment of cerebrovascular disease (Li et al., 2015a).

5.2.4. Limitations of the systematic reviews and meta-analysis

My analysis has several limitations:

i) I only focused on proliferation and differentiation, which does not cover all aspects of stem cells therapy. I did not investigate migration and survival because migration is difficult to measure *in vivo* and it has different effects based on species differences (Srivastave et al., 2018) and survival after transplantation is more the result of durability against a toxic environment. Other functions of stem cells such as integration into the neuronal network is only applicable to differentiated cells, therefore it was included in my study.

ii) The meta-analysis on NSCs needs more studies to be more robust. Despite the small sample size, I identified an important interaction of drugs and stem cells, which indicates its relevancy. Nevertheless, more studies on frequently used stem cells are needed.

iii) I did not identify any studies on drug interaction upon NSC transplantation. Further studies investigating the effect of drugs on transplanted NSCs are necessary.

iv) The heterogeneity of the samples (**Table 16**) limits general conclusions.

v) Some drugs were dominantly studied (**Table 17**) which can lead to a bias due to overrepresentation within a drug class. For example, in the NSC review, fluoxetine dominated among the antidepressants (53.01 %) followed by imipramine (21.69 %). However, when comparing the effect of the main drug classes with their subclasses, we did not reveal any differences (**Table 18-19**).

vi) The overall quality of the publications was relatively poor. Publications that provided underlying mechanisms were scarce (41 records out of 115 records in the physiologic condition, 35.7%). Basic statistical data such as mean and standard deviation were difficult to extract.

6. Conclusions and outlook

In conclusion, I was able to demonstrate that hemin-induced endothelial cell death involves ferroptosis, necroptosis, and autophagy. These findings intersect with what has been observed in neurons (Li et al., 2018b; Zille et al., 2017). Some ferroptosis inhibitors such as N-acetylcysteine, deferoxamine, and Trolox are protective for both brain endothelial cells and neurons, while the ferroptosis inhibitor ferrostatin-1 is only beneficial for neurons and the autophagy inhibitor bafilomycin A1 for endothelial cells. This suggests that different cell death inhibitors targeting the different brain cell types may be needed to improve the functional outcome of ICH patients. Further experiments to substantiate this hypothesis are needed. On the other hand, the loss of the brain cells in ICH is inevitable. Therefore, stem cell therapies, including EPCs and NSCs, are a promising intervention for brain cell restoration. While the overall knowledge about the interactions of drugs commonly used in the elderly and stem cells is still limited, my meta-analysis highlights that these interactions exist and that they are relevant to consider in stem cell therapy. To overcome one of the crucial limitations of cell therapy, i.e. the availability of the stem cells, understanding how to induce the proliferation of the stem cells *in vivo* through drug interactions may be beneficial.

Together, cell protection and stem cell therapy can be supportive treatments of ICH. They can be combined with the primary intervention of evacuating the hematoma and help fill the cavity. For example, the combination of hematoma evacuation with minimally invasive surgery and bone marrow stem cell therapy has recently been demonstrated to be safe and may even increase neurological function in a phase I clinical trial (Zahra et al., 2020). Other approaches besides stem cell therapy and cytoproctive drugs should also be considered such as biomaterials (Lim et al., 2020; Zhang et al., 2016) and immunomodulatory agents (Fu et al., 2014; Li et al., 2015b) (**Figure 35**).

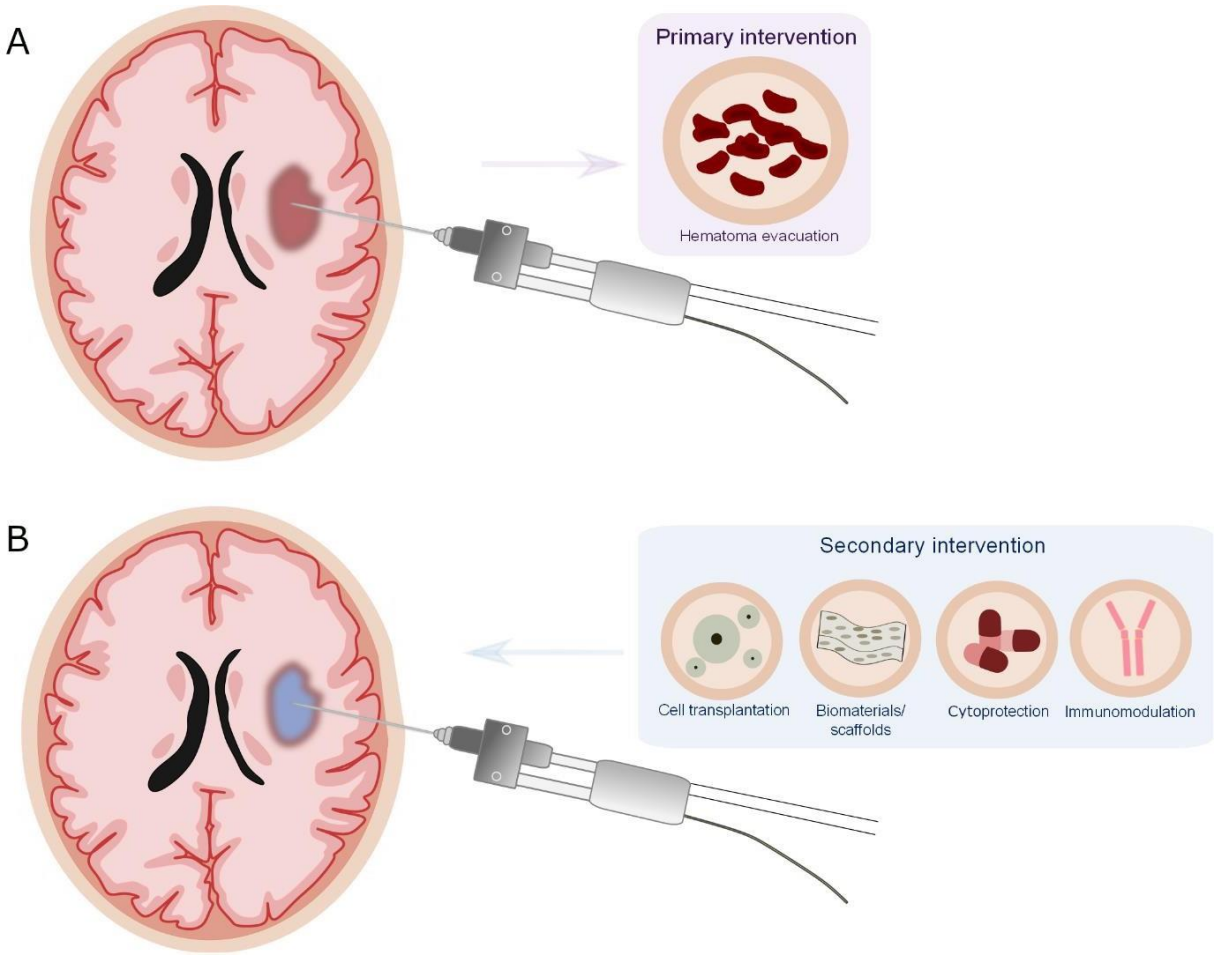

Figure 35. Possible therapeutic interventions for ICH. **A**) Primary intervention aims to remove the hematoma to decrease intracranial pressure and to remove the toxic hemolysis products. **B**) Secondary intervention targets the remaining tissue for cytoprotection and regeneration.

References

Alim, I., Caulfield, J. T., Chen, Y., Swarup, V., Geschwind, D. H., Ivanova, E., Seravalli, J., Ai, Y., Sansing, L. H., Ste Marie, E. J., Hondal, R. J., Mukherjee, S., Cave, J. W., Sagdullaev, B. T., Karuppagounder, S. S., & Ratan, R. R. (2019). Selenium Drives a Transcriptional Adaptive Program to Block Ferroptosis and Treat Stroke. *Cell, 177*(5), 1262-1279 e1225. doi: 10.1016/j.cell.2019.03.032

Alvarado-Kristensson, M., Melander, F., Leandersson, K., Ronnstrand, L., Wernstedt, C., & Andersson, T. (2004). p38-MAPK signals survival by phosphorylation of caspase-8 and caspase-3 in human neutrophils. *J Exp Med, 199*(4), 449-458. doi: 10.1084/jem.20031771

An, S. J., Kim, T. J., & Yoon, B. W. (2017). Epidemiology, Risk Factors, and Clinical Features of Intracerebral Hemorrhage: An Update. *J Stroke, 19*(1), 3-10. doi: 10.5853/jos.2016.00864

Anthonymuthu, T. S., Tyurina, Y. Y., Sun, W. Y., Mikulska-Ruminska, K., Shrivastava, I. H., Tyurin, V. A., Cinemre, F. B., Dar, H. H., VanDemark, A. P., Holman, T. R., Sadovsky, Y., Stockwell, B. R., He, R. R., Bahar, I., Bayir, H., & Kagan, V. E. (2020). Resolving the paradox of ferroptotic cell death: Ferrostatin-1 binds to 15LOX/PEBP1 complex, suppresses generation of peroxidized ETE-PE, and protects against ferroptosis. *Redox Biol, 38*, 101744. doi: 10.1016/j.redox.2020.101744

Aoki, H., Kang, P. M., Hampe, J., Yoshimura, K., Noma, T., Matsuzaki, M., & Izumo, S. (2002). Direct activation of mitochondrial apoptosis machinery by c-Jun N-terminal kinase in adult cardiac myocytes. *J Biol Chem, 277*(12), 10244-10250. doi: 10.1074/jbc.M112355200

Ashkenazi, A., Fairbrother, W. J., Leverson, J. D., & Souers, A. J. (2017). From basic apoptosis discoveries to advanced selective BCL-2 family inhibitors. *Nat Rev Drug Discov, 16*(4), 273-284. doi: 10.1038/nrd.2016.253

Askenase, M. H., & Sansing, L. H. (2016). Stages of the Inflammatory Response in Pathology and Tissue Repair after Intracerebral Hemorrhage. *Semin Neurol, 36*(3), 288-297. doi: 10.1055/s-0036-1582132

Babu, R., Bagley, J. H., Di, C., Friedman, A. H., & Adamson, C. (2012). Thrombin and hemin as central factors in the mechanisms of intracerebral hemorrhage-induced secondary brain injury and as potential targets for intervention. *Neurosurg Focus, 32*(4), E8. doi: 10.3171/2012.1.FOCUS11366

Baehrecke, E. H. (2005). Autophagy: dual roles in life and death? *Nat Rev Mol Cell Biol, 6*(6), 505-510. doi: 10.1038/nrm1666

Bamm, V. V., Tsemakhovich, V. A., Shaklai, M., & Shaklai, N. (2004). Haptoglobin phenotypes differ in their ability to inhibit heme transfer from hemoglobin to LDL. *Biochemistry, 43*(13), 3899-3906. doi: 10.1021/bi0362626

Bayraktutan, U. (2019). Endothelial progenitor cells: Potential novel therapeutics for ischaemic stroke. *Pharmacol Res, 144*, 181-191. doi: 10.1016/j.phrs.2019.04.017

Bedini, G., Bersano, A., Zanier, E. R., Pischiutta, F., & Parati, E. A. (2018). Mesenchymal Stem Cell Therapy in Intracerebral Haemorrhagic Stroke. *Curr Med Chem, 25*(19), 2176-2197. doi: 10.2174/0929867325666180111101410

Bennett, B. L., Sasaki, D. T., Murray, B. W., O'Leary, E. C., Sakata, S. T., Xu, W., Leisten, J. C., Motiwala, A., Pierce, S., Satoh, Y., Bhagwat, S. S., Manning, A. M., & Anderson, D. W. (2001). SP600125, an anthrapyrazolone inhibitor of Jun N-terminal kinase. *Proc Natl Acad Sci U S A, 98*(24), 13681-13686. doi: 10.1073/pnas.251194298

Berridge, M. V., & Tan, A. S. (1993). Characterization of the cellular reduction of 3-(4,5-dimethylthiazol-2-yl)-2,5-diphenyltetrazolium bromide (MTT): subcellular localization, substrate dependence, and involvement of mitochondrial electron transport in MTT reduction. *Arch Biochem Biophys, 303*(2), 474-482. doi: 10.1006/abbi.1993.1311

Bianconi, V., Sahebkar, A., Kovanen, P., Bagaglia, F., Ricciuti, B., Calabro, P., Patti, G., & Pirro, M. (2018). Endothelial and cardiac progenitor cells for cardiovascular repair: A controversial

paradigm in cell therapy. *Pharmacol Ther, 181*, 156-168. doi: 10.1016/j.pharmthera.2017.08.004

Brott, T., Broderick, J., Kothari, R., Barsan, W., Tomsick, T., Sauerbeck, L., Spilker, J., Duldner, J., & Khoury, J. (1997). Early hemorrhage growth in patients with intracerebral hemorrhage. *Stroke, 28*(1), 1-5. doi: 10.1161/01.str.28.1.1

Cao, S., Zheng, M., Hua, Y., Chen, G., Keep, R. F., & Xi, G. (2016). Hematoma Changes During Clot Resolution After Experimental Intracerebral Hemorrhage. *Stroke, 47*(6), 1626-1631. doi: 10.1161/STROKEAHA.116.013146

Chang, P., Dong, W., Zhang, M., Wang, Z., Wang, Y., Wang, T., Gao, Y., Meng, H., Luo, B., Luo, C., Chen, X., & Tao, L. (2014). Anti-necroptosis chemical necrostatin-1 can also suppress apoptotic and autophagic pathway to exert neuroprotective effect in mice intracerebral hemorrhage model. *J Mol Neurosci, 52*(2), 242-249. doi: 10.1007/s12031-013-0132-3

Chen-Roetling, J., Cai, Y., Lu, X., & Regan, R. F. (2014). Hemin uptake and release by neurons and glia. *Free Radic Res, 48*(2), 200-205. doi: 10.3109/10715762.2013.859386

Chen-Roetling, J., Li, Z., Chen, M., Awe, O. O., & Regan, R. F. (2009). Heme oxygenase activity and hemoglobin neurotoxicity are attenuated by inhibitors of the MEK/ERK pathway. *Neuropharmacology, 56*(5), 922-928. doi: 10.1016/j.neuropharm.2009.01.022

Chen, B., Chen, Z., Liu, M., Gao, X., Cheng, Y., Wei, Y., Wu, Z., Cui, D., & Shang, H. (2019). Inhibition of neuronal ferroptosis in the acute phase of intracerebral hemorrhage shows long-term cerebroprotective effects. *Brain Res Bull, 153*, 122-132. doi: 10.1016/j.brainresbull.2019.08.013

Chen, J., & Regan, R. F. (2004). Heme oxygenase-2 gene deletion increases astrocyte vulnerability to hemin. *Biochem Biophys Res Commun, 318*(1), 88-94. doi: 10.1016/j.bbrc.2004.03.187

Chen, J., & Regan, R. F. (2005). Increasing expression of heme oxygenase-1 by proteasome inhibition protects astrocytes from heme-mediated oxidative injury. *Curr Neurovasc Res, 2*(3), 189-196.

Chen, L., Jin, X. G., Zhu, J. F., Li, H. J., Wang, Y. P., Zhou, Y. X., Wang, J., & Wang, W. H. (2015). Expression of transferrin in hematoma brain tissue at different stages after intra cerebral hemorrhage in rats. *Asian Pac J Trop Med, 8*(7), 574-577. doi: 10.1016/j.apjtm.2015.06.002

Cheng, Y., Rodriguiz, R. M., Murthy, S. R., Senatorov, V., Thouennon, E., Cawley, N. X., Aryal, D. K., Ahn, S., Lecka-Czernik, B., Wetsel, W. C., & Loh, Y. P. (2015). Neurotrophic factor-alpha1 prevents stress-induced depression through enhancement of neurogenesis and is activated by rosiglitazone. [Neurotrophic factor-alpha1 prevents stress-induced depression through enhancement of neurogenesis and is activated by rosiglitazone.In NF-alpha1-knockout mice, hippocampal FGF2 levels and neurogenesis are reduced.Rosiglitazone upregulates FGF2 expression in a NF-alpha1-dependent manner in hippocampal neurons]. *Mol Psychiatry, 20*(6), 744-754. doi: 10.1038/mp.2014.136

mp2014136 [pii]

Chong, M. S., Ng, W. K., & Chan, J. K. (2016). Concise Review: Endothelial Progenitor Cells in Regenerative Medicine: Applications and Challenges. *Stem Cells Transl Med, 5*(4), 530-538. doi: 10.5966/sctm.2015-0227

Chu, X., Wu, X., Feng, H., Zhao, H., Tan, Y., Wang, L., Ran, H., Yi, L., Peng, Y., Tong, H., Liu, R., Bai, W., Shi, H., Li, L., & Huo, D. (2018). Coupling Between Interleukin-1R1 and Necrosome Complex Involves in Hemin-Induced Neuronal Necroptosis After Intracranial Hemorrhage. *Stroke, 49*(10), 2473-2482. doi: 10.1161/STROKEAHA.117.019253

Clarke, P. G. (1990). Developmental cell death: morphological diversity and multiple mechanisms. *Anat Embryol (Berl), 181*(3), 195-213. doi: 10.1007/BF00174615

Cohen-Kashi Malina, K., Cooper, I., & Teichberg, V. I. (2009). Closing the gap between the in-vivo and in-vitro blood-brain barrier tightness. *Brain Res, 1284*, 12-21. doi: 10.1016/j.brainres.2009.05.072

Collaboration, A. T. (2020a). Safety and efficacy of fluoxetine on functional outcome after acute stroke (AFFINITY): a randomised, double-blind, placebo-controlled trial. *Lancet Neurol, 19*(8), 651-660. doi: 10.1016/S1474-4422(20)30207-6

Collaboration, E. T. (2020b). Safety and efficacy of fluoxetine on functional recovery after acute stroke (EFFECTS): a randomised, double-blind, placebo-controlled trial. *Lancet Neurol, 19*(8), 661-669. doi: 10.1016/S1474-4422(20)30219-2

Collaboration, F. T. (2019). Effects of fluoxetine on functional outcomes after acute stroke (FOCUS): a pragmatic, double-blind, randomised, controlled trial. *Lancet, 393*(10168), 265-274. doi: 10.1016/S0140-6736(18)32823-X

Cordeiro, M. F., & Horn, A. P. (2015). Stem cell therapy in intracerebral hemorrhage rat model. *World J Stem Cells, 7*(3), 618-629. doi: 10.4252/wjsc.v7.i3.618

Cordonnier, C., Demchuk, A., Ziai, W., & Anderson, C. S. (2018). Intracerebral haemorrhage: current approaches to acute management. *Lancet, 392*(10154), 1257-1268. doi: 10.1016/S0140-6736(18)31878-6

Crowley, L. C., Marfell, B. J., & Waterhouse, N. J. (2016a). Analyzing Cell Death by Nuclear Staining with Hoechst 33342. *Cold Spring Harb Protoc, 2016*(9). doi: 10.1101/pdb.prot087205

Crowley, L. C., Scott, A. P., Marfell, B. J., Boughaba, J. A., Chojnowski, G., & Waterhouse, N. J. (2016b). Measuring Cell Death by Propidium Iodide Uptake and Flow Cytometry. *Cold Spring Harb Protoc, 2016*(7). doi: 10.1101/pdb.prot087163

Cuenda, A., Rouse, J., Doza, Y. N., Meier, R., Cohen, P., Gallagher, T. F., Young, P. R., & Lee, J. C. (1995). SB 203580 is a specific inhibitor of a MAP kinase homologue which is stimulated by cellular stresses and interleukin-1. *FEBS Lett, 364*(2), 229-233. doi: 10.1016/0014-5793(95)00357-f

Cuenda, A., & Rousseau, S. (2007). p38 MAP-kinases pathway regulation, function and role in human diseases. *Biochim Biophys Acta, 1773*(8), 1358-1375. doi: 10.1016/j.bbamcr.2007.03.010

Cui, C., Cui, Y., Gao, J., Li, R., Jiang, X., Tian, Y., Wang, K., & Cui, J. (2017). Intraparenchymal treatment with bone marrow mesenchymal stem cell-conditioned medium exerts neuroprotection following intracerebral hemorrhage. *Mol Med Rep, 15*(4), 2374-2382. doi: 10.3892/mmr.2017.6223

Cui, H. J., He, H. Y., Yang, A. L., Zhou, H. J., Wang, C., Luo, J. K., Lin, Y., & Tang, T. (2015). Efficacy of deferoxamine in animal models of intracerebral hemorrhage: a systematic review and stratified meta-analysis. *PLoS One, 10*(5), e0127256. doi: 10.1371/journal.pone.0127256

Cui, Y., Duan, X., Li, H., Dang, B., Yin, J., Wang, Y., Gao, A., Yu, Z., & Chen, G. (2016). Hydrogen Sulfide Ameliorates Early Brain Injury Following Subarachnoid Hemorrhage in Rats. *Mol Neurobiol, 53*(6), 3646-3657. doi: 10.1007/s12035-015-9304-1

Dai, W., Wang, G., Chwa, J., Oh, M. E., Abeywardana, T., Yang, Y., Wang, Q. A., & Jiang, L. (2020). Mitochondrial division inhibitor (mdivi-1) decreases oxidative metabolism in cancer. *Br J Cancer, 122*(9), 1288-1297. doi: 10.1038/s41416-020-0778-x

Dang, G., Yang, Y., Wu, G., Hua, Y., Keep, R. F., & Xi, G. (2017). Early Erythrolysis in the Hematoma After Experimental Intracerebral Hemorrhage. *Transl Stroke Res, 8*(2), 174-182. doi: 10.1007/s12975-016-0505-3

Dang, T. N., Bishop, G. M., Dringen, R., & Robinson, S. R. (2011). The metabolism and toxicity of hemin in astrocytes. *Glia, 59*(10), 1540-1550. doi: 10.1002/glia.21198

Dang, T. N., Robinson, S. R., Dringen, R., & Bishop, G. M. (2011). Uptake, metabolism and toxicity of hemin in cultured neurons. *Neurochem Int, 58*(7), 804-811. doi: 10.1016/j.neuint.2011.03.006

Davis, A. E. (2000). Cognitive impairments following traumatic brain injury. Etiologies and interventions. *Crit Care Nurs Clin North Am, 12*(4), 447-456.

Decano, J. L., Moran, A. M., Giordano, N., Ruiz-Opazo, N., & Herrera, V. L. (2013). Analysis of CD45-[CD34+/KDR+] endothelial progenitor cells as juvenile protective factors in a rat model of ischemic-hemorrhagic stroke. *PLoS One, 8*(1), e55222. doi: 10.1371/journal.pone.0055222

Degterev, A., Huang, Z., Boyce, M., Li, Y., Jagtap, P., Mizushima, N., Cuny, G. D., Mitchison, T. J., Moskowitz, M. A., & Yuan, J. (2005). Chemical inhibitor of nonapoptotic cell death with therapeutic potential for ischemic brain injury. *Nat Chem Biol, 1*(2), 112-119. doi: 10.1038/nchembio711

Delehouze, C., Leverrier-Penna, S., Le Cann, F., Comte, A., Jacquard-Fevai, M., Delalande, O., Desban, N., Baratte, B., Gallais, I., Faurez, F., Bonnet, M. C., Hauteville, M., Goekjian, P. G., Thuillier, R., Favreau, F., Vandenabeele, P., Hauet, T., Dimanche-Boitrel, M. T., & Bach, S. (2017). 6E11, a highly selective inhibitor of Receptor-Interacting Protein Kinase 1, protects cells against cold hypoxia-reoxygenation injury. *Sci Rep, 7*(1), 12931. doi: 10.1038/s41598-017-12788-4

Demeuse, P., Fragner, P., Leroy-Noury, C., Mercier, C., Payen, L., Fardel, O., Couraud, P. O., & Roux, F. (2004). Puromycin selectively increases mdr1a expression in immortalized rat brain endothelial cell lines. *J Neurochem, 88*(1), 23-31. doi: 10.1046/j.1471-4159.2003.02071.x

Denton, D., & Kumar, S. (2019). Autophagy-dependent cell death. *Cell Death Differ, 26*(4), 605-616. doi: 10.1038/s41418-018-0252-y

Denton, D., Nicolson, S., & Kumar, S. (2012). Cell death by autophagy: facts and apparent artefacts. *Cell Death Differ, 19*(1), 87-95. doi: 10.1038/cdd.2011.146

Diederichs, C., Berger, K., & Bartels, D. B. (2011). The measurement of multiple chronic diseases--a systematic review on existing multimorbidity indices. *J Gerontol A Biol Sci Med Sci, 66*(3), 301-311. doi: 10.1093/gerona/glq208

Ding, R., Chen, Y., Yang, S., Deng, X., Fu, Z., Feng, L., Cai, Y., Du, M., Zhou, Y., & Tang, Y. (2014). Blood-brain barrier disruption induced by hemoglobin in vivo: Involvement of up-regulation of nitric oxide synthase and peroxynitrite formation. *Brain Res, 1571*, 25-38. doi: 10.1016/j.brainres.2014.04.042

Dixon, S. J., Lemberg, K. M., Lamprecht, M. R., Skouta, R., Zaitsev, E. M., Gleason, C. E., Patel, D. N., Bauer, A. J., Cantley, A. M., Yang, W. S., Morrison, B., 3rd, & Stockwell, B. R. (2012). Ferroptosis: an iron-dependent form of nonapoptotic cell death. *Cell, 149*(5), 1060-1072. doi: 10.1016/j.cell.2012.03.042

Dogan, F., Ozates, N. P., Bagca, B. G., Abbaszadeh, Z., Sogutlu, F., Gasimli, R., Gunduz, C., & Biray Avci, C. (2018). Investigation of the effect of telomerase inhibitor BIBR1532 on breast cancer and breast cancer stem cells. *J Cell Biochem*. doi: 10.1002/jcb.27089

Dondelinger, Y., Declercq, W., Montessuit, S., Roelandt, R., Goncalves, A., Bruggeman, I., Hulpiau, P., Weber, K., Sehon, C. A., Marquis, R. W., Bertin, J., Gough, P. J., Savvides, S., Martinou, J. C., Bertrand, M. J., & Vandenabeele, P. (2014). MLKL compromises plasma membrane integrity by binding to phosphatidylinositol phosphates. *Cell Rep, 7*(4), 971-981. doi: 10.1016/j.celrep.2014.04.026

Dong, X. H., Peng, C., Zhang, Y. Y., Tao, Y. L., Tao, X., Zhang, C., Chen, A. F., & Xie, H. H. (2017). Chronic Exposure to Subtherapeutic Antibiotics Aggravates Ischemic Stroke Outcome in Mice. *EBioMedicine, 24*, 116-126. doi: 10.1016/j.ebiom.2017.09.002

Dowlatshahi, D., Demchuk, A. M., Flaherty, M. L., Ali, M., Lyden, P. L., Smith, E. E., & Collaboration, V. (2011). Defining hematoma expansion in intracerebral hemorrhage: relationship with patient outcomes. *Neurology, 76*(14), 1238-1244. doi: 10.1212/WNL.0b013e3182143317

Duan, W. R., Garner, D. S., Williams, S. D., Funckes-Shippy, C. L., Spath, I. S., & Blomme, E. A. (2003). Comparison of immunohistochemistry for activated caspase-3 and cleaved cytokeratin 18 with the TUNEL method for quantification of apoptosis in histological sections of PC-3 subcutaneous xenografts. *J Pathol, 199*(2), 221-228. doi: 10.1002/path.1289

Durocher, M., Knepp, B., Yee, A., Jickling, G., Rodriguez, F., Ng, K., Zhan, X., Hamade, F., Ferino, E., Amini, H., Carmona-Mora, P., Hull, H., Ander, B. P., Sharp, F. R., & Stamova, B. (2020). Molecular Correlates of Hemorrhage and Edema Volumes Following Human Intracerebral Hemorrhage Implicate Inflammation, Autophagy, mRNA Splicing, and T Cell Receptor Signaling. *Transl Stroke Res*. doi: 10.1007/s12975-020-00869-y

Engels, J., Elting, N., Braun, L., Bendix, I., Herz, J., Felderhoff-Muser, U., & Dzietko, M. (2017). Sildenafil Enhances Quantity of Immature Neurons and Promotes Functional Recovery in the Developing Ischemic Mouse Brain. *Dev Neurosci, 39*(1-4), 287-297. doi: 10.1159/000457832

England, T. J., Abaei, M., Auer, D. P., Lowe, J., Jones, D. R., Sare, G., Walker, M., & Bath, P. M. (2012). Granulocyte-colony stimulating factor for mobilizing bone marrow stem cells in subacute stroke: the stem cell trial of recovery enhancement after stroke 2 randomized controlled trial. *Stroke, 43*(2), 405-411. doi: 10.1161/STROKEAHA.111.636449

Esquiva, G., Grayston, A., & Rosell, A. (2018). Revascularization and endothelial progenitor cells in stroke. *Am J Physiol Cell Physiol, 315*(5), C664-C674. doi: 10.1152/ajpcell.00200.2018

Fan, X., & Mu, L. (2017). The role of heme oxygenase-1 (HO-1) in the regulation of inflammatory reaction, neuronal cell proliferation and apoptosis in rats after intracerebral hemorrhage (ICH). *Neuropsychiatr Dis Treat, 13*, 77-85. doi: 10.2147/NDT.S120496

Fang, M. C., Coca Perraillon, M., Ghosh, K., Cutler, D. M., & Rosen, A. B. (2014). Trends in stroke rates, risk, and outcomes in the United States, 1988 to 2008. *Am J Med, 127*(7), 608-615. doi: 10.1016/j.amjmed.2014.03.017

Fatokun, A. A., Dawson, V. L., & Dawson, T. M. (2014). Parthanatos: mitochondrial-linked mechanisms and therapeutic opportunities. *Br J Pharmacol, 171*(8), 2000-2016. doi: 10.1111/bph.12416

Favata, M. F., Horiuchi, K. Y., Manos, E. J., Daulerio, A. J., Stradley, D. A., Feeser, W. S., Van Dyk, D. E., Pitts, W. J., Earl, R. A., Hobbs, F., Copeland, R. A., Magolda, R. L., Scherle, P. A., & Trzaskos, J. M. (1998). Identification of a novel inhibitor of mitogen-activated protein kinase kinase. *J Biol Chem, 273*(29), 18623-18632. doi: 10.1074/jbc.273.29.18623

Feigin, V. L., Lawes, C. M., Bennett, D. A., Barker-Collo, S. L., & Parag, V. (2009). Worldwide stroke incidence and early case fatality reported in 56 population-based studies: a systematic review. *Lancet Neurol, 8*(4), 355-369. doi: 10.1016/S1474-4422(09)70025-0

Feng, H., Schorpp, K., Jin, J., Yozwiak, C. E., Hoffstrom, B. G., Decker, A. M., Rajbhandari, P., Stokes, M. E., Bender, H. G., Csuka, J. M., Upadhyayula, P. S., Canoll, P., Uchida, K., Soni, R. K., Hadian, K., & Stockwell, B. R. (2020). Transferrin Receptor Is a Specific Ferroptosis Marker. *Cell Rep, 30*(10), 3411-3423 e3417. doi: 10.1016/j.celrep.2020.02.049

Foa, P., Maiolo, A. T., Lombardi, L., Villa, L., & Polli, E. E. (1986). Inhibition of proliferation of human leukaemic cell populations by deferoxamine. *Scand J Haematol, 36*(1), 107-110. doi: 10.1111/j.1600-0609.1986.tb02659.x

Friedrich, V., Flores, R., & Sehba, F. A. (2012). Cell death starts early after subarachnoid hemorrhage. *Neurosci Lett, 512*(1), 6-11. doi: 10.1016/j.neulet.2012.01.036

Fu, Y., Hao, J., Zhang, N., Ren, L., Sun, N., Li, Y. J., Yan, Y., Huang, D., Yu, C., & Shi, F. D. (2014). Fingolimod for the treatment of intracerebral hemorrhage: a 2-arm proof-of-concept study. *JAMA Neurol, 71*(9), 1092-1101. doi: 10.1001/jamaneurol.2014.1065

Galluzzi, L., Aaronson, S. A., Abrams, J., Alnemri, E. S., Andrews, D. W., Baehrecke, E. H., Bazan, N. G., Blagosklonny, M. V., Blomgren, K., Borner, C., Bredesen, D. E., Brenner, C., Castedo, M., Cidlowski, J. A., Ciechanover, A., Cohen, G. M., De Laurenzi, V., De Maria, R., Deshmukh, M., Dynlacht, B. D., El-Deiry, W. S., Flavell, R. A., Fulda, S., Garrido, C., Golstein, P., Gougeon, M. L., Green, D. R., Gronemeyer, H., Hajnoczky, G., Hardwick, J. M., Hengartner, M. O., Ichijo, H., Jaattela, M., Kepp, O., Kimchi, A., Klionsky, D. J., Knight, R. A., Kornbluth, S., Kumar, S., Levine, B., Lipton, S. A., Lugli, E., Madeo, F., Malomi, W., Marine, J. C., Martin, S. J., Medema, J. P., Mehlen, P., Melino, G., Moll, U. M., Morselli, E., Nagata, S., Nicholson, D. W., Nicotera, P., Nunez, G., Oren, M., Penninger, J., Pervaiz, S., Peter, M. E., Piacentini, M., Prehn, J. H., Puthalakath, H., Rabinovich, G. A., Rizzuto, R., Rodrigues, C. M., Rubinsztein, D. C., Rudel, T., Scorrano, L., Simon, H. U., Steller, H., Tschopp, J., Tsujimoto, Y., Vandenabeele, P., Vitale, I., Vousden, K. H., Youle, R. J., Yuan, J., Zhivotovsky, B., & Kroemer, G. (2009). Guidelines for the use and interpretation of assays for monitoring cell death in higher eukaryotes. *Cell Death Differ, 16*(8), 1093-1107. doi: 10.1038/cdd.2009.44

Galluzzi, L., Vitale, I., Aaronson, S. A., Abrams, J. M., Adam, D., Agostinis, P., Alnemri, E. S., Altucci, L., Amelio, I., Andrews, D. W., Annicchiarico-Petruzzelli, M., Antonov, A. V., Arama, E., Baehrecke, E. H., Barlev, N. A., Bazan, N. G., Bernassola, F., Bertrand, M. J. M., Bianchi, K., Blagosklonny, M. V., Blomgren, K., Borner, C., Boya, P., Brenner, C., Campanella, M., Candi, E., Carmona-Gutierrez, D., Cecconi, F., Chan, F. K., Chandel, N. S., Cheng, E. H., Chipuk, J. E., Cidlowski, J. A., Ciechanover, A., Cohen, G. M., Conrad, M., Cubillos-Ruiz, J. R., Czabotar, P. E., D'Angiolella, V., Dawson, T. M., Dawson, V. L., De Laurenzi, V., De Maria, R., Debatin, K. M., DeBerardinis, R. J., Deshmukh, M., Di Daniele, N., Di Virgilio, F., Dixit, V. M., Dixon, S. J., Duckett, C. S., Dynlacht, B. D., El-Deiry, W. S., Elrod, J. W., Fimia, G. M., Fulda, S., Garcia-Saez,

A. J., Garg, A. D., Garrido, C., Gavathiotis, E., Golstein, P., Gottlieb, E., Green, D. R., Greene, L. A., Gronemeyer, H., Gross, A., Hajnoczky, G., Hardwick, J. M., Harris, I. S., Hengartner, M. O., Hetz, C., Ichijo, H., Jaattela, M., Joseph, B., Jost, P. J., Juin, P. P., Kaiser, W. J., Karin, M., Kaufmann, T., Kepp, O., Kimchi, A., Kitsis, R. N., Klionsky, D. J., Knight, R. A., Kumar, S., Lee, S. W., Lemasters, J. J., Levine, B., Linkermann, A., Lipton, S. A., Lockshin, R. A., Lopez-Otin, C., Lowe, S. W., Luedde, T., Lugli, E., MacFarlane, M., Madeo, F., Malewicz, M., Malorni, W., Manic, G., Marine, J. C., Martin, S. J., Martinou, J. C., Medema, J. P., Mehlen, P., Meier, P., Melino, S., Miao, E. A., Molkentin, J. D., Moll, U. M., Munoz-Pinedo, C., Nagata, S., Nunez, G., Oberst, A., Oren, M., Overholtzer, M., Pagano, M., Panaretakis, T., Pasparakis, M., Penninger, J. M., Pereira, D. M., Pervaiz, S., Peter, M. E., Piacentini, M., Pinton, P., Prehn, J. H. M., Puthalakath, H., Rabinovich, G. A., Rehm, M., Rizzuto, R., Rodrigues, C. M. P., Rubinsztein, D. C., Rudel, T., Ryan, K. M., Sayan, E., Scorrano, L., Shao, F., Shi, Y., Silke, J., Simon, H. U., Sistigu, A., Stockwell, B. R., Strasser, A., Szabadkai, G., Tait, S. W. G., Tang, D., Tavernarakis, N., Thorburn, A., Tsujimoto, Y., Turk, B., Vanden Berghe, T., Vandenabeele, P., Vander Heiden, M. G., Villunger, A., Virgin, H. W., Vousden, K. H., Vucic, D., Wagner, E. F., Walczak, H., Wallach, D., Wang, Y., Wells, J. A., Wood, W., Yuan, J., Zakeri, Z., Zhivotovsky, B., Zitvogel, L., Melino, G., & Kroemer, G. (2018). Molecular mechanisms of cell death: recommendations of the Nomenclature Committee on Cell Death 2018. *Cell Death Differ, 25*(3), 486-541. doi: 10.1038/s41418-017-0012-4

Gammella, E., Buratti, P., Cairo, G., & Recalcati, S. (2017). The transferrin receptor: the cellular iron gate. *Metallomics, 9*(10), 1367-1375. doi: 10.1039/c7mt00143f

Gao, H., Bai, Y., Jia, Y., Zhao, Y., Kang, R., Tang, D., & Dai, E. (2018a). Ferroptosis is a lysosomal cell death process. *Biochem Biophys Res Commun, 503*(3), 1550-1556. doi: 10.1016/j.bbrc.2018.07.078

Gao, L., Xu, W., Li, T., Chen, J., Shao, A., Yan, F., & Chen, G. (2018b). Stem Cell Therapy: A Promising Therapeutic Method for Intracerebral Hemorrhage. *Cell Transplant, 27*(12), 1809-1824. doi: 10.1177/0963689718773363

Gaschler, M. M., & Stockwell, B. R. (2017). Lipid peroxidation in cell death. *Biochem Biophys Res Commun, 482*(3), 419-425. doi: 10.1016/j.bbrc.2016.10.086

Glick, D., Barth, S., & Macleod, K. F. (2010). Autophagy: cellular and molecular mechanisms. *J Pathol, 221*(1), 3-12. doi: 10.1002/path.2697

Golab-Janowska, M., Paczkowska, E., Machalinski, B., Meller, A., Kotlega, D., Safranow, K., Wankowicz, P., & Nowacki, P. (2018). Statins Therapy is Associated with Increased Populations of Early Endothelial Progenitor (CD133+/VEGFR2+) and Endothelial (CD34-/CD133- /VEGFR2+) Cells in Patients with Acute Ischemic Stroke. *Curr Neurovasc Res, 15*(2), 120-128. doi: 10.2174/1567202615666180611120546

Goldstein, L., Teng, Z. P., Zeserson, E., Patel, M., & Regan, R. F. (2003). Hemin induces an iron-dependent, oxidative injury to human neuron-like cells. *J Neurosci Res, 73*(1), 113-121. doi: 10.1002/jnr.10633

Gomez-Crisostomo, N. P., Lopez-Marure, R., Zapata, E., Zazueta, C., & Martinez-Abundis, E. (2013). Bax induces cytochrome c release by multiple mechanisms in mitochondria from MCF7 cells. *J Bioenerg Biomembr, 45*(5), 441-448. doi: 10.1007/s10863-013-9508-x

Goodell, M. A., & Rando, T. A. (2015). Stem cells and healthy aging. *Science, 350*(6265), 1199-1204. doi: 10.1126/science.aab3388

Gutierrez, E., Richardson, D. R., & Jansson, P. J. (2014). The anticancer agent di-2-pyridylketone 4,4-dimethyl-3-thiosemicarbazone (Dp44mT) overcomes prosurvival autophagy by two mechanisms: persistent induction of autophagosome synthesis and impairment of lysosomal integrity. *J Biol Chem, 289*(48), 33568-33589. doi: 10.1074/jbc.M114.599480

Hancer, N. J., Qiu, W., Cherella, C., Li, Y., Copps, K. D., & White, M. F. (2014). Insulin and metabolic stress stimulate multisite serine/threonine phosphorylation of insulin receptor substrate 1 and inhibit tyrosine phosphorylation. *J Biol Chem, 289*(18), 12467-12484. doi: 10.1074/jbc.M114.554162

Hanley, D. F., Thompson, R. E., Rosenblum, M., Yenokyan, G., Lane, K., McBee, N., Mayo, S. W., Bistran-Hall, A. J., Gandhi, D., Mould, W. A., Ullman, N., Ali, H., Carhuapoma, J. R., Kase, C. S., Lees, K. R., Dawson, J., Wilson, A., Betz, J. F., Sugar, E. A., Hao, Y., Avadhani, R., Caron, J. L., Harrigan, M. R., Carlson, A. P., Bulters, D., LeDoux, D., Huang, J., Cobb, C., Gupta, G., Kitagawa, R., Chicoine, M. R., Patel, H., Dodd, R., Camarata, P. J., Wolfe, S., Stadnik, A., Money, P. L., Mitchell, P., Sarabia, R., Harnof, S., Barzo, P., Unterberg, A., Teitelbaum, J. S., Wang, W., Anderson, C. S., Mendelow, A. D., Gregson, B., Janis, S., Vespa, P., Ziai, W., Zuccarello, M., Awad, I. A., & Investigators, M. I. (2019). Efficacy and safety of minimally invasive surgery with thrombolysis in intracerebral haemorrhage evacuation (MISTIE III): a randomised, controlled, open-label, blinded endpoint phase 3 trial. *Lancet, 393*(10175), 1021-1032. doi: 10.1016/S0140-6736(19)30195-3

Hatakeyama, T., Okauchi, M., Hua, Y., Keep, R. F., & Xi, G. (2013). Deferoxamine reduces neuronal death and hematoma lysis after intracerebral hemorrhage in aged rats. *Transl Stroke Res, 4*(5), 546-553. doi: 10.1007/s12975-013-0270-5

He, C., & Klionsky, D. J. (2009). Regulation mechanisms and signaling pathways of autophagy. *Annu Rev Genet, 43*, 67-93. doi: 10.1146/annurev-genet-102808-114910

He, Y., Hua, Y., Song, S., Liu, W., Keep, R. F., & Xi, G. (2008a). Induction of autophagy in rat hippocampus and cultured neurons by iron. *Acta Neurochir Suppl, 105*, 29-32. doi: 10.1007/978-3-211-09469-3_6

He, Y., Wan, S., Hua, Y., Keep, R. F., & Xi, G. (2008b). Autophagy after experimental intracerebral hemorrhage. *J Cereb Blood Flow Metab, 28*(5), 897-905. doi: 10.1038/sj.jcbfm.9600578

Helms, H. C., Abbott, N. J., Burek, M., Cecchelli, R., Couraud, P. O., Deli, M. A., Forster, C., Galla, H. J., Romero, I. A., Shusta, E. V., Stebbins, M. J., Vandenhaute, E., Weksler, B., & Brodin, B. (2016). In vitro models of the blood-brain barrier: An overview of commonly used brain endothelial cell culture models and guidelines for their use. *J Cereb Blood Flow Metab, 36*(5), 862-890. doi: 10.1177/0271678X16630991

Hemorrhagic Stroke Academia Industry Roundtable, P. (2018). Basic and Translational Research in Intracerebral Hemorrhage: Limitations, Priorities, and Recommendations. *Stroke, 49*(5), 1308-1314. doi: 10.1161/STROKEAHA.117.019539

Higdon, A. N., Benavides, G. A., Chacko, B. K., Ouyang, X., Johnson, M. S., Landar, A., Zhang, J., & Darley-Usmar, V. M. (2012). Hemin causes mitochondrial dysfunction in endothelial cells through promoting lipid peroxidation: the protective role of autophagy. *Am J Physiol Heart Circ Physiol, 302*(7), H1394-1409. doi: 10.1152/ajpheart.00584.2011

Hu, S., Hua, Y., Keep, R. F., Feng, H., & Xi, G. (2019). Deferoxamine therapy reduces brain hemin accumulation after intracerebral hemorrhage in piglets. *Exp Neurol, 318*, 244-250. doi: 10.1016/j.expneurol.2019.05.003

Hua, Y., Xi, G., Keep, R. F., & Hoff, J. T. (2000). Complement activation in the brain after experimental intracerebral hemorrhage. *J Neurosurg, 92*(6), 1016-1022. doi: 10.3171/jns.2000.92.6.1016

Huang, A. P., Hsu, Y. H., Wu, M. S., Tsai, H. H., Su, C. Y., Ling, T. Y., Hsu, S. H., & Lai, D. M. (2020). Potential of stem cell therapy in intracerebral hemorrhage. *Mol Biol Rep, 47*(6), 4671-4680. doi: 10.1007/s11033-020-05457-9

Huang, F. P., Xi, G., Keep, R. F., Hua, Y., Nemoianu, A., & Hoff, J. T. (2002). Brain edema after experimental intracerebral hemorrhage: role of hemoglobin degradation products. *J Neurosurg, 96*(2), 287-293. doi: 10.3171/jns.2002.96.2.0287

Hui, J., Zhang, J., Kim, H., Tong, C., Ying, Q., Li, Z., Mao, X., Shi, G., Yan, J., Zhang, Z., & Xi, G. (2014). Fluoxetine regulates neurogenesis in vitro through modulation of GSK-3beta/beta-catenin signaling. *Int J Neuropsychopharmacol, 18*(5). doi: 10.1093/ijnp/pyu099

Imai, T., Iwata, S., Hirayama, T., Nagasawa, H., Nakamura, S., Shimazawa, M., & Hara, H. (2019). Intracellular Fe(2+) accumulation in endothelial cells and pericytes induces blood-brain barrier dysfunction in secondary brain injury after brain hemorrhage. *Sci Rep, 9*(1), 6228. doi: 10.1038/s41598-019-42370-z

Impey, S., Obrietan, K., & Storm, D. R. (1999). Making new connections: role of ERK/MAP kinase signaling in neuronal plasticity. *Neuron, 23*(1), 11-14. doi: 10.1016/s0896-6273(00)80747-3

Jacobsen, M. D., Weil, M., & Raff, M. C. (1996). Role of Ced-3/ICE-family proteases in staurosporine-induced programmed cell death. *J Cell Biol, 133*(5), 1041-1051. doi: 10.1083/jcb.133.5.1041

Jaffe, E. R. (1981). Methemoglobin pathophysiology. *Prog Clin Biol Res, 51*, 133-151.

Jaremko, K. M., Chen-Roetling, J., Chen, L., & Regan, R. F. (2010). Accelerated hemolysis and neurotoxicity in neuron-glia-blood clot co-cultures. *J Neurochem, 114*(4), 1063-1073. doi: 10.1111/j.1471-4159.2010.06826.x

Jeong, S. W., Chu, K., Jung, K. H., Kim, S. U., Kim, M., & Roh, J. K. (2003). Human neural stem cell transplantation promotes functional recovery in rats with experimental intracerebral hemorrhage. *Stroke, 34*(9), 2258-2263. doi: 10.1161/01.STR.0000083698.20199.1F

Jiang, P., Zhu, T., Xia, Z., Gao, F., Gu, W., Chen, X., Yuan, T., & Yu, H. (2015). Inhibition of MAPK/ERK signaling blocks hippocampal neurogenesis and impairs cognitive performance in prenatally infected neonatal rats. *Eur Arch Psychiatry Clin Neurosci, 265*(6), 497-509. doi: 10.1007/s00406-015-0588-y

Karuppagounder, S. S., Alim, I., Khim, S. J., Bourassa, M. W., Sleiman, S. F., John, R., Thinnes, C. C., Yeh, T. L., Demetriades, M., Neitemeier, S., Cruz, D., Gazaryan, I., Killilea, D. W., Morgenstern, L., Xi, G., Keep, R. F., Schallert, T., Tappero, R. V., Zhong, J., Cho, S., Maxfield, F. R., Holman, T. R., Culmsee, C., Fong, G. H., Su, Y., Ming, G. L., Song, H., Cave, J. W., Schofield, C. J., Colbourne, F., Coppola, G., & Ratan, R. R. (2016). Therapeutic targeting of oxygen-sensing prolyl hydroxylases abrogates ATF4-dependent neuronal death and improves outcomes after brain hemorrhage in several rodent models. *Sci Transl Med, 8*(328), 328ra329. doi: 10.1126/scitranslmed.aac6008

Karuppagounder, S. S., Alin, L., Chen, Y., Brand, D., Bourassa, M. W., Dietrich, K., Wilkinson, C. M., Nadeau, C. A., Kumar, A., Perry, S., Pinto, J. T., Darley-Usmar, V., Sanchez, S., Milne, G. L., Pratico, D., Holman, T. R., Carmichael, S. T., Coppola, G., Colbourne, F., & Ratan, R. R. (2018). N-acetylcysteine targets 5 lipoxygenase-derived, toxic lipids and can synergize with prostaglandin E2 to inhibit ferroptosis and improve outcomes following hemorrhagic stroke in mice. *Ann Neurol, 84*(6), 854-872. doi: 10.1002/ana.25356

Kerr, J. F., Wyllie, A. H., & Currie, A. R. (1972). Apoptosis: a basic biological phenomenon with wide-ranging implications in tissue kinetics. *Br J Cancer, 26*(4), 239-257. doi: 10.1038/bjc.1972.33

King, M. D., Whitaker-Lea, W. A., Campbell, J. M., Alleyne, C. H., Jr., & Dhandapani, K. M. (2014). Necrostatin-1 reduces neurovascular injury after intracerebral hemorrhage. *Int J Cell Biol, 2014*, 495817. doi: 10.1155/2014/495817

Koeppen, A. H., Dickson, A. C., & McEvoy, J. A. (1995). The cellular reactions to experimental intracerebral hemorrhage. *J Neurol Sci, 134 Suppl*, 102-112. doi: 10.1016/0022-510x(95)00215-n

Krafft, P. R., Rolland, W. B., Duris, K., Lekic, T., Campbell, A., Tang, J., & Zhang, J. H. (2012). Modeling intracerebral hemorrhage in mice: injection of autologous blood or bacterial collagenase. *J Vis Exp*(67), e4289. doi: 10.3791/4289

Kroemer, G., Galluzzi, L., Vandenabeele, P., Abrams, J., Alnemri, E. S., Baehrecke, E. H., Blagosklonny, M. V., El-Deiry, W. S., Golstein, P., Green, D. R., Hengartner, M., Knight, R. A., Kumar, S., Lipton, S. A., Malorni, W., Nunez, G., Peter, M. E., Tschopp, J., Yuan, J., Piacentini, M., Zhivotovsky, B., Melino, G., & Nomenclature Committee on Cell, D. (2009). Classification of cell death: recommendations of the Nomenclature Committee on Cell Death 2009. *Cell Death Differ, 16*(1), 3-11. doi: 10.1038/cdd.2008.150

Kroemer, G., Marino, G., & Levine, B. (2010). Autophagy and the integrated stress response. *Mol Cell, 40*(2), 280-293. doi: 10.1016/j.molcel.2010.09.023

Kuhn, H. G., Dickinson-Anson, H., & Gage, F. H. (1996). Neurogenesis in the dentate gyrus of the adult rat: age-related decrease of neuronal progenitor proliferation. *J Neurosci, 16*(6), 2027-2033.

Kwon, K. J., Kim, J. N., Kim, M. K., Kim, S. Y., Cho, K. S., Jeon, S. J., Kim, H. Y., Ryu, J. H., Han, S. Y., Cheong, J. H., Ignarro, L. J., Han, S. H., & Shin, C. Y. (2013). Neuroprotective effects of valproic acid against hemin toxicity: possible involvement of the down-regulation of heme oxygenase-1 by regulating ubiquitin-proteasomal pathway. *Neurochem Int, 62*(3), 240-250. doi: 10.1016/j.neuint.2012.12.019

Laird, M. D., Wakade, C., Alleyne, C. H., Jr., & Dhandapani, K. M. (2008). Hemin-induced necroptosis involves glutathione depletion in mouse astrocytes. *Free Radic Biol Med, 45*(8), 1103-1114. doi: 10.1016/j.freeradbiomed.2008.07.003

Lapergue, B., Mohammad, A., & Shuaib, A. (2007). Endothelial progenitor cells and cerebrovascular diseases. *Prog Neurobiol, 83*(6), 349-362. doi: 10.1016/j.pneurobio.2007.08.001

Lauretani, F., Ceda, G. P., Pelliccioni, P., Ruffini, L., Nardelli, A., Cherubini, A., & Maggio, M. (2014). Approaching neurological diseases to reduce mobility limitations in older persons. *Curr Pharm Des, 20*(19), 3149-3164. doi: 10.2174/13816128113196660687

Lee, H. J., Kim, K. S., Kim, E. J., Choi, H. B., Lee, K. H., Park, I. H., Ko, Y., Jeong, S. W., & Kim, S. U. (2007). Brain transplantation of immortalized human neural stem cells promotes functional recovery in mouse intracerebral hemorrhage stroke model. *Stem Cells, 25*(5), 1204-1212. doi: 10.1634/stemcells.2006-0409

Lee, H. J., Park, I. H., Kim, H. J., & Kim, S. U. (2009). Human neural stem cells overexpressing glial cell line-derived neurotrophic factor in experimental cerebral hemorrhage. *Gene Ther, 16*(9), 1066-1076. doi: 10.1038/gt.2009.51

Lee, J. A., & Gao, F. B. (2009). Inhibition of autophagy induction delays neuronal cell loss caused by dysfunctional ESCRT-III in frontotemporal dementia. *J Neurosci, 29*(26), 8506-8511. doi: 10.1523/JNEUROSCI.0924-09.2009

Lee, J. E., Lim, M. S., Park, J. H., Park, C. H., & Koh, H. C. (2016a). PTEN Promotes Dopaminergic Neuronal Differentiation Through Regulation of ERK-Dependent Inhibition of S6K Signaling in Human Neural Stem Cells. [Insulin Activates S6K Through PI3K/Akt/mTOR Signaling Pathways in hNSCs.mTORplays a positive role in the insulin-induced differentiation of hNSCs into dopaminergic neurons. inhibitionof

mTOR by rapamycin did not affect proliferation, and proliferating hNSCsmaintained the capacity for self-renewal even under conditions of mTOR inhibition. We found that rapamycin treatment decreased dopaminergic neuronal differentiation even in the absence of insulin.]. *Stem Cells Transl Med, 5*(10), 1319-1329. doi: sctm.2015-0200 [pii]

10.5966/sctm.2015-0200

Lee, J. E., Lim, M. S., Park, J. H., Park, C. H., & Koh, H. C. (2016b). S6K Promotes Dopaminergic Neuronal Differentiation Through PI3K/Akt/mTOR-Dependent Signaling Pathways in Human Neural Stem Cells. [same as lee other paper. rapamycin, a specific inhibitor of mTOR, significantly reduced neuronal differentiation without affecting proliferation]. *Mol Neurobiol, 53*(6), 3771-3782. doi: 10.1007/s12035-015-9325-9

10.1007/s12035-015-9325-9 [pii]

Lei, B., Sheng, H., Wang, H., Lascola, C. D., Warner, D. S., Laskowitz, D. T., & James, M. L. (2014). Intrastriatal injection of autologous blood or clostridial collagenase as murine models of intracerebral hemorrhage. *J Vis Exp*(89). doi: 10.3791/51439

Lei, F. R., Li, X. Q., Liu, H., Zhu, R. D., Meng, Q. Y., & Rong, J. J. (2012). Rapamycin and 3-methyladenine regulate apoptosis and autophagy in bone-derived endothelial progenitor cells. *Chin Med J (Engl), 125*(22), 4076-4082.

Letarte, P. B., Lieberman, K., Nagatani, K., Haworth, R. A., Odell, G. B., & Duff, T. A. (1993). Hemin: levels in experimental subarachnoid hematoma and effects on dissociated vascular smooth-muscle cells. *J Neurosurg, 79*(2), 252-255. doi: 10.3171/jns.1993.79.2.0252

Li, B., Bai, W., Sun, P., Zhou, B., Hu, B., & Ying, J. (2015a). The effect of CXCL12 on endothelial progenitor cells: potential target for angiogenesis in intracerebral hemorrhage. *J Interferon Cytokine Res, 35*(1), 23-31. doi: 10.1089/jir.2014.0004

Li, Q., Han, X., Lan, X., Gao, Y., Wan, J., Durham, F., Cheng, T., Yang, J., Wang, Z., Jiang, C., Ying, M., Koehler, R. C., Stockwell, B. R., & Wang, J. (2017). Inhibition of neuronal ferroptosis protects hemorrhagic brain. *JCI Insight, 2*(7), e90777. doi: 10.1172/jci.insight.90777

Li, Q., Weiland, A., Chen, X., Lan, X., Han, X., Durham, F., Liu, X., Wan, J., Ziai, W. C., Hanley, D. F., & Wang, J. (2018a). Ultrastructural Characteristics of Neuronal Death and White Matter Injury

in Mouse Brain Tissues After Intracerebral Hemorrhage: Coexistence of Ferroptosis, Autophagy, and Necrosis. *Front Neurol, 9*, 581. doi: 10.3389/fneur.2018.00581

Li, Q. Q., Li, L. J., Wang, X. Y., Sun, Y. Y., & Wu, J. (2018b). Research Progress in Understanding the Relationship Between Heme Oxygenase-1 and Intracerebral Hemorrhage. *Front Neurol, 9*, 682. doi: 10.3389/fneur.2018.00682

Li, Y. J., Chang, G. Q., Liu, Y., Gong, Y., Yang, C., Wood, K., Shi, F. D., Fu, Y., & Yan, Y. (2015b). Fingolimod alters inflammatory mediators and vascular permeability in intracerebral hemorrhage. *Neurosci Bull, 31*(6), 755-762. doi: 10.1007/s12264-015-1532-2

Lim, T. C., Mandeville, E., Weng, D., Wang, L. S., Kurisawa, M., Leite-Morris, K., Selim, M. H., Lo, E. H., & Spector, M. (2020). Hydrogel-Based Therapy for Brain Repair After Intracerebral Hemorrhage. *Transl Stroke Res, 11*(3), 412-417. doi: 10.1007/s12975-019-00721-y

Linkermann, A., & Green, D. R. (2014). Necroptosis. *N Engl J Med, 370*(5), 455-465. doi: 10.1056/NEJMra1310050

Liu, M., Wilson, N. O., Hibbert, J. M., & Stiles, J. K. (2013). STAT3 regulates MMP3 in heme-induced endothelial cell apoptosis. *PLoS One, 8*(8), e71366. doi: 10.1371/journal.pone.0071366

Liu, R., Li, H., Hua, Y., Keep, R. F., Xiao, J., Xi, G., & Huang, Y. (2019). Early Hemolysis Within Human Intracerebral Hematomas: an MRI Study. *Transl Stroke Res, 10*(1), 52-56. doi: 10.1007/s12975-018-0630-2

Lorente, L., Martin, M. M., Abreu-Gonzalez, P., Sabatel, R., Ramos, L., Argueso, M., Sole-Violan, J., Riano-Ruiz, M., Jimenez, A., & Garcia-Marin, V. (2018). Serum Malondialdehyde Levels and Mortality in Patients with Spontaneous Intracerebral Hemorrhage. *World Neurosurg, 113*, e542-e547. doi: 10.1016/j.wneu.2018.02.085

Ma, Q., Huang, B., Khatibi, N., Rolland, W., 2nd, Suzuki, H., Zhang, J. H., & Tang, J. (2011). PDGFR-alpha inhibition preserves blood-brain barrier after intracerebral hemorrhage. *Ann Neurol, 70*(6), 920-931. doi: 10.1002/ana.22549

Ma, W., Halweg, C. J., Menendez, D., & Resnick, M. A. (2012). Differential effects of poly(ADP-ribose) polymerase inhibition on DNA break repair in human cells are revealed with Epstein-Barr virus. *Proc Natl Acad Sci U S A, 109*(17), 6590-6595. doi: 10.1073/pnas.1118078109

Ma, X., Qin, J., Song, B., Shi, C., Zhang, R., Liu, X., Ji, Y., Ji, W., Gong, G., & Xu, Y. (2015). Stem cell-based therapies for intracerebral hemorrhage in animal model: a meta-analysis. *Neurol Sci, 36*(8), 1311-1317. doi: 10.1007/s10072-015-2238-6

Madangarli, N., Bonsack, F., Dasari, R., & Sukumari-Ramesh, S. (2019). Intracerebral Hemorrhage: Blood Components and Neurotoxicity. *Brain Sci, 9*(11). doi: 10.3390/brainsci9110316

Malsy, M., Bitzinger, D., Graf, B., & Bundscherer, A. (2019). Staurosporine induces apoptosis in pancreatic carcinoma cells PaTu 8988t and Panc-1 via the intrinsic signaling pathway. *Eur J Med Res, 24*(1), 5. doi: 10.1186/s40001-019-0365-x

Mao, L. L., Yuan, H., Wang, W. W., Wang, Y. J., Yang, M. F., Sun, B. L., Zhang, Z. Y., & Yang, X. Y. (2017). Adoptive Regulatory T-cell Therapy Attenuates Perihematomal Inflammation in a Mouse Model of Experimental Intracerebral Hemorrhage. *Cell Mol Neurobiol, 37*(5), 919-929. doi: 10.1007/s10571-016-0429-1

Marti-Fabregas, J., Crespo, J., Delgado-Mederos, R., Martinez-Ramirez, S., Pena, E., Marin, R., Dinia, L., Jimenez-Xarrie, E., Fernandez-Arcos, A., Perez-Perez, J., Querol, L., Suarez-Calvet, M., & Badimon, L. (2013). Endothelial progenitor cells in acute ischemic stroke. *Brain Behav, 3*(6), 649-655. doi: 10.1002/brb3.175

Matsushita, K., Meng, W., Wang, X., Asahi, M., Asahi, K., Moskowitz, M. A., & Lo, E. H. (2000). Evidence for apoptosis after intercerebral hemorrhage in rat striatum. *J Cereb Blood Flow Metab, 20*(2), 396-404. doi: 10.1097/00004647-200002000-00022

McGuinness, O., Yafei, N., Costi, A., & Crompton, M. (1990). The presence of two classes of high-affinity cyclosporin A binding sites in mitochondria. Evidence that the minor component is involved in the opening of an inner-membrane Ca(2+)-dependent pore. *Eur J Biochem, 194*(2), 671-679. doi: 10.1111/j.1432-1033.1990.tb15667.x

Meamar, R., Nikyar, H., Dehghani, L., Talebi, M., Dehghani, M., Ghasemi, M., Ansari, B., & Saadatnia, M. (2016). The role of endothelial progenitor cells in transient ischemic attack patients for future cerebrovascular events. *J Res Med Sci, 21*, 47. doi: 10.4103/1735-1995.183995

Mendelow, A. D., Gregson, B. A., Rowan, E. N., Murray, G. D., Gholkar, A., Mitchell, P. M., & Investigators, S. I. (2013). Early surgery versus initial conservative treatment in patients with spontaneous supratentorial lobar intracerebral haematomas (STICH II): a randomised trial. *Lancet, 382*(9890), 397-408. doi: 10.1016/S0140-6736(13)60986-1

Miotto, G., Rossetto, M., Di Paolo, M. L., Orian, L., Venerando, R., Roveri, A., Vuckovic, A. M., Bosello Travain, V., Zaccarin, M., Zennaro, L., Maiorino, M., Toppo, S., Ursini, F., & Cozza, G. (2020). Insight into the mechanism of ferroptosis inhibition by ferrostatin-1. *Redox Biol, 28*, 101328. doi: 10.1016/j.redox.2019.101328

Moher, D., Liberati, A., Tetzlaff, J., Altman, D. G., & Group, P. (2009). Preferred reporting items for systematic reviews and meta-analyses: the PRISMA statement. *BMJ, 339*, b2535. doi: 10.1136/bmj.b2535

Napoli, E., & Borlongan, C. V. (2016). Recent Advances in Stem Cell-Based Therapeutics for Stroke. *Transl Stroke Res, 7*(6), 452-457. doi: 10.1007/s12975-016-0490-6

Nonaka, M., Yoshikawa, M., Nishimura, F., Yokota, H., Kimura, H., Hirabayashi, H., Nakase, H., Ishizaka, S., Wanaka, A., & Sakaki, T. (2004). Intraventricular transplantation of embryonic stem cell-derived neural stem cells in intracerebral hemorrhage rats. *Neurol Res, 26*(3), 265-272. doi: 10.1179/016164104225014049

Ohnishi, M., Katsuki, H., Fujimoto, S., Takagi, M., Kume, T., & Akaike, A. (2007). Involvement of thrombin and mitogen-activated protein kinase pathways in hemorrhagic brain injury. *Exp Neurol, 206*(1), 43-52. doi: 10.1016/j.expneurol.2007.03.030

Oliveira, S. R., Amaral, J. D., & Rodrigues, C. M. P. (2018). Mechanism and disease implications of necroptosis and neuronal inflammation. *Cell Death Dis, 9*(9), 903. doi: 10.1038/s41419-018-0872-7

Omidi, Y., Campbell, L., Barar, J., Connell, D., Akhtar, S., & Gumbleton, M. (2003). Evaluation of the immortalised mouse brain capillary endothelial cell line, b.End3, as an in vitro blood-brain barrier model for drug uptake and transport studies. *Brain Res, 990*(1-2), 95-112. doi: 10.1016/s0006-8993(03)03443-7

Onorati, A. V., Dyczynski, M., Ojha, R., & Amaravadi, R. K. (2018). Targeting autophagy in cancer. *Cancer, 124*(16), 3307-3318. doi: 10.1002/cncr.31335

Owen, J. E., Bishop, G. M., & Robinson, S. R. (2014). Phenanthrolines protect astrocytes from hemin without chelating iron. *Neurochem Res, 39*(4), 693-699. doi: 10.1007/s11064-014-1256-8

Owen, J. E., Bishop, G. M., & Robinson, S. R. (2016). Uptake and Toxicity of Hemin and Iron in Cultured Mouse Astrocytes. *Neurochem Res, 41*(1-2), 298-306. doi: 10.1007/s11064-015-1795-7

Park, K. S., Kim, M. J., Ho, J. S., Ryu, C. K., & Chung, J. H. (1996). Effect of glutathione depletion on haemoglobin and membrane integrity of red blood cells of rats. *J Int Med Res, 24*(1), 40-46. doi: 10.1177/030006059602400106

Patabendige, A., Skinner, R. A., & Abbott, N. J. (2013). Establishment of a simplified in vitro porcine blood-brain barrier model with high transendothelial electrical resistance. *Brain Res, 1521*, 1-15. doi: 10.1016/j.brainres.2012.06.057

Pechnick, R. N., Zonis, S., Wawrowsky, K., Cosgayon, R., Farrokhi, C., Lacayo, L., & Chesnokova, V. (2011). Antidepressants stimulate hippocampal neurogenesis by inhibiting p21 expression in the subgranular zone of the hipppocampus. *PLoS One, 6*(11), e27290. doi: 10.1371/journal.pone.0027290

Peng, C. H., Chiou, S. H., Chen, S. J., Chou, Y. C., Ku, H. H., Cheng, C. K., Yen, C. J., Tsai, T. H., Chang, Y. L., & Kao, C. L. (2008). Neuroprotection by Imipramine against lipopolysaccharide-induced apoptosis in hippocampus-derived neural stem cells mediated by activation of BDNF and the MAPK pathway. *Eur Neuropsychopharmacol, 18*(2), 128-140. doi: 10.1016/j.euroneuro.2007.05.002

Pero, M. E., Zullo, G., Esposito, L., Iannuzzi, A., Lombardi, P., De Canditiis, C., Neglia, G., & Gasparrini, B. (2018). Inhibition of apoptosis by caspase inhibitor Z-VAD-FMK improves cryotolerance of in vitro derived bovine embryos. *Theriogenology, 108*, 127-135. doi: 10.1016/j.theriogenology.2017.11.031

Pias-Peleteiro, J., Campos, F., Castillo, J., & Sobrino, T. (2017). Endothelial progenitor cells as a therapeutic option in intracerebral hemorrhage. *Neural Regen Res, 12*(4), 558-561. doi: 10.4103/1673-5374.205085

Qin, J., Song, B., Zhang, H., Wang, Y., Wang, N., Ji, Y., Qi, J., Chandra, A., Yang, B., Zhang, Y., Gong, G., & Xu, Y. (2013). Transplantation of human neuro-epithelial-like stem cells derived from induced pluripotent stem cells improves neurological function in rats with experimental intracerebral hemorrhage. *Neurosci Lett, 548*, 95-100. doi: 10.1016/j.neulet.2013.05.007

Rahmani, A., Kheradmand, D., Keyhanvar, P., Shoae-Hassani, A., & Darbandi-Azar, A. (2013). Neurogenesis and increase in differentiated neural cell survival via phosphorylation of Akt1 after fluoxetine treatment of stem cells. *Biomed Res Int, 2013*, 582526. doi: 10.1155/2013/582526

Rakshit, J., Priyam, A., Gowrishetty, K. K., Mishra, S., & Bandyopadhyay, J. (2020). Iron chelator Deferoxamine protects human neuroblastoma cell line SH-SY5Y from 6-Hydroxydopamine-induced apoptosis and autophagy dysfunction. *J Trace Elem Med Biol, 57*, 126406. doi: 10.1016/j.jtemb.2019.126406

Ratan, R. R. (2020). The Chemical Biology of Ferroptosis in the Central Nervous System. *Cell Chem Biol, 27*(5), 479-498. doi: 10.1016/j.chembiol.2020.03.007

Regan, R. F., Wang, Y., Ma, X., Chong, A., & Guo, Y. (2001). Activation of extracellular signal-regulated kinases potentiates hemin toxicity in astrocyte cultures. *J Neurochem, 79*(3), 545-555. doi: 10.1046/j.1471-4159.2001.00590.x

Riddell, N. E., Burns, V. E., Wallace, G. R., Edwards, K. M., Drayson, M., Redwine, L. S., Hong, S., Bui, J. C., Fischer, J. C., Mills, P. J., & Bosch, J. A. (2015). Progenitor cells are mobilized by acute psychological stress but not beta-adrenergic receptor agonist infusion. *Brain Behav Immun, 49*, 49-53. doi: 10.1016/j.bbi.2015.02.028

Robinson, N., Ganesan, R., Hegedus, C., Kovacs, K., Kufer, T. A., & Virag, L. (2019). Programmed necrotic cell death of macrophages: Focus on pyroptosis, necroptosis, and parthanatos. *Redox Biol, 26*, 101239. doi: 10.1016/j.redox.2019.101239

Robinson, R. G., & Jorge, R. E. (2016). Post-Stroke Depression: A Review. *Am J Psychiatry, 173*(3), 221-231. doi: 10.1176/appi.ajp.2015.15030363

Robinson, S. R., Dang, T. N., Dringen, R., & Bishop, G. M. (2009). Hemin toxicity: a preventable source of brain damage following hemorrhagic stroke. *Redox Rep, 14*(6), 228-235. doi: 10.1179/135100009X12525712409931

Ryter, S. W., & Tyrrell, R. M. (2000). The heme synthesis and degradation pathways: role in oxidant sensitivity. Heme oxygenase has both pro- and antioxidant properties. *Free Radic Biol Med, 28*(2), 289-309. doi: 10.1016/s0891-5849(99)00223-3

Sahni, S., Bae, D. H., Lane, D. J., Kovacevic, Z., Kalinowski, D. S., Jansson, P. J., & Richardson, D. R. (2014). The metastasis suppressor, N-myc downstream-regulated gene 1 (NDRG1), inhibits stress-induced autophagy in cancer cells. *J Biol Chem, 289*(14), 9692-9709. doi: 10.1074/jbc.M113.529511

Schulman, I. H., Balkan, W., & Hare, J. M. (2018). Mesenchymal Stem Cell Therapy for Aging Frailty. *Front Nutr, 5*, 108. doi: 10.3389/fnut.2018.00108

Selim, M., Foster, L. D., Moy, C. S., Xi, G., Hill, M. D., Morgenstern, L. B., Greenberg, S. M., James, M. L., Singh, V., Clark, W. M., Norton, C., Palesch, Y. Y., Yeatts, S. D., & i, D. E. F. I. (2019). Deferoxamine mesylate in patients with intracerebral haemorrhage (i-DEF): a multicentre, randomised, placebo-controlled, double-blind phase 2 trial. *Lancet Neurol, 18*(5), 428-438. doi: 10.1016/S1474-4422(19)30069-9

Shacka, J. J., Klocke, B. J., & Roth, K. A. (2006). Autophagy, bafilomycin and cell death: the "a-B-cs" of plecomacrolide-induced neuroprotection. *Autophagy, 2*(3), 228-230. doi: 10.4161/auto.2703

Sharrief, A., & Grotta, J. C. (2019). Stroke in the elderly. *Handb Clin Neurol, 167*, 393-418. doi: 10.1016/B978-0-12-804766-8.00021-2

Shen, X., Ma, L., Dong, W., Wu, Q., Gao, Y., Luo, C., Zhang, M., Chen, X., & Tao, L. (2016). Autophagy regulates intracerebral hemorrhage induced neural damage via apoptosis and NF-kappaB pathway. *Neurochem Int, 96*, 100-112. doi: 10.1016/j.neuint.2016.03.004

Shtaya, A., Bridges, L. R., Esiri, M. M., Lam-Wong, J., Nicoll, J. A. R., Boche, D., & Hainsworth, A. H. (2019). Rapid neuroinflammatory changes in human acute intracerebral hemorrhage. *Ann Clin Transl Neurol, 6*(8), 1465-1479. doi: 10.1002/acn3.50842

Sommer, C. J., & Schabitz, W. R. (2017). Fostering Poststroke Recovery: Towards Combination Treatments. *Stroke, 48*(4), 1112-1119. doi: 10.1161/STROKEAHA.116.013324

Sotthibundhu, A., McDonagh, K., von Kriegsheim, A., Garcia-Munoz, A., Klawiter, A., Thompson, K., Chauhan, K. D., Krawczyk, J., McInerney, V., Dockery, P., Devine, M. J., Kunath, T., Barry, F., O'Brien, T., & Shen, S. (2016). Rapamycin regulates autophagy and cell adhesion in induced pluripotent stem cells. *Stem Cell Res Ther, 7*(1), 166. doi: 10.1186/s13287-016-0425-x

Srivastava, R. K., Bulte, J. W. M., Walczak, P., & Janowski, M. (2018). Migratory potential of transplanted glial progenitors as critical factor for successful translation of glia replacement therapy: The gap between mice and men. *Glia, 66*(5), 907-919. doi: 10.1002/glia.23275

Stockwell, B. R., Friedmann Angeli, J. P., Bayir, H., Bush, A. I., Conrad, M., Dixon, S. J., Fulda, S., Gascon, S., Hatzios, S. K., Kagan, V. E., Noel, K., Jiang, X., Linkermann, A., Murphy, M. E., Overholtzer, M., Oyagi, A., Pagnussat, G. C., Park, J., Ran, Q., Rosenfeld, C. S., Salnikow, K., Tang, D., Torti, F. M., Torti, S. V., Toyokuni, S., Woerpel, K. A., & Zhang, D. D. (2017). Ferroptosis: A Regulated Cell Death Nexus Linking Metabolism, Redox Biology, and Disease. *Cell, 171*(2), 273-285. doi: 10.1016/j.cell.2017.09.021

Su, X., Wang, H., Kang, D., Zhu, J., Sun, Q., Li, T., & Ding, K. (2015). Necrostatin-1 ameliorates intracerebral hemorrhage-induced brain injury in mice through inhibiting RIP1/RIP3 pathway. *Neurochem Res, 40*(4), 643-650. doi: 10.1007/s11064-014-1510-0

Su, X., Wang, H., Lin, Y., & Chen, F. (2018). RIP1 and RIP3 mediate hemin-induced cell death in HT22 hippocampal neuronal cells. *Neuropsychiatr Dis Treat, 14*, 3111-3119. doi: 10.2147/NDT.S181074

Subirada, P. V., Paz, M. C., Ridano, M. E., Lorenc, V. E., Fader, C. M., Chiabrando, G. A., & Sanchez, M. C. (2019). Effect of Autophagy Modulators on Vascular, Glial, and Neuronal Alterations in the Oxygen-Induced Retinopathy Mouse Model. *Front Cell Neurosci, 13*, 279. doi: 10.3389/fncel.2019.00279

Sukumari-Ramesh, S., Laird, M. D., Singh, N., Vender, J. R., Alleyne, C. H., Jr., & Dhandapani, K. M. (2010). Astrocyte-derived glutathione attenuates hemin-induced apoptosis in cerebral microvascular cells. *Glia, 58*(15), 1858-1870. doi: 10.1002/glia.21055

Sun, Y., Zheng, Y., Wang, C., & Liu, Y. (2018). Glutathione depletion induces ferroptosis, autophagy, and premature cell senescence in retinal pigment epithelial cells. *Cell Death Dis, 9*(7), 753. doi: 10.1038/s41419-018-0794-4

Sun, Y. M., Wang, Y. T., Jiang, L., & Xue, M. Z. (2016). The effects of deferoxamine on inhibition for microglia activation and protection of secondary nerve injury after intracerebral hemorrhage in rats. *Pak J Pharm Sci, 29*(3 Suppl), 1087-1093.

Taupin, P., Ray, J., Fischer, W. H., Suhr, S. T., Hakansson, K., Grubb, A., & Gage, F. H. (2000). FGF-2-responsive neural stem cell proliferation requires CCg, a novel autocrine/paracrine cofactor. *Neuron, 28*(2), 385-397. doi: 10.1016/s0896-6273(00)00119-7

Theile, D., Staffen, B., & Weiss, J. (2010). ATP-binding cassette transporters as pitfalls in selection of transgenic cells. *Anal Biochem, 399*(2), 246-250. doi: 10.1016/j.ab.2009.12.014

Thuret, G., Chiquet, C., Herrag, S., Dumollard, J. M., Boudard, D., Bednarz, J., Campos, L., & Gain, P. (2003). Mechanisms of staurosporine induced apoptosis in a human corneal endothelial cell line. *Br J Ophthalmol, 87*(3), 346-352. doi: 10.1136/bjo.87.3.346

Tontsch, U., & Bauer, H. C. (1989). Isolation, characterization, and long-term cultivation of porcine and murine cerebral capillary endothelial cells. *Microvasc Res, 37*(2), 148-161. doi: 10.1016/0026-2862(89)90034-4

Venkatasubramanian, C., Mlynash, M., Finley-Caulfield, A., Eyngorn, I., Kalimuthu, R., Snider, R. W., & Wijman, C. A. (2011). Natural history of perihematomal edema after intracerebral hemorrhage measured by serial magnetic resonance imaging. *Stroke, 42*(1), 73-80. doi: 10.1161/STROKEAHA.110.590646

Vigne, P., Feolde, E., Ladoux, A., Duval, D., & Frelin, C. (1995). Contributions of NO synthase and heme oxygenase to cGMP formation by cytokine and hemin treated brain capillary endothelial cells. *Biochem Biophys Res Commun, 214*(1), 1-5. doi: 10.1006/bbrc.1995.2248

Vinod, V., Padmakrishnan, C. J., Vijayan, B., & Gopala, S. (2014). 'How can I halt thee?' The puzzles involved in autophagic inhibition. *Pharmacol Res, 82*, 1-8. doi: 10.1016/j.phrs.2014.03.005

Wakai, T., Sakata, H., Narasimhan, P., Yoshioka, H., Kinouchi, H., & Chan, P. H. (2014). Transplantation of neural stem cells that overexpress SOD1 enhances amelioration of intracerebral hemorrhage in mice. *J Cereb Blood Flow Metab, 34*(3), 441-449. doi: 10.1038/jcbfm.2013.215

Wang, B., Sun, L., Tian, Y., Li, Z., Wei, H., Wang, D., Yang, Z., Chen, J., Zhang, J., & Jiang, R. (2012). Effects of atorvastatin in the regulation of circulating EPCs and angiogenesis in traumatic brain injury in rats. *J Neurol Sci, 319*(1-2), 117-123. doi: 10.1016/j.jns.2012.04.015

Wang, G., Manaenko, A., Shao, A., Ou, Y., Yang, P., Budbazar, E., Nowrangi, D., Zhang, J. H., & Tang, J. (2017a). Low-density lipoprotein receptor-related protein-1 facilitates heme scavenging after intracerebral hemorrhage in mice. *J Cereb Blood Flow Metab, 37*(4), 1299-1310. doi: 10.1177/0271678X16654494

Wang, G., Wang, L., Sun, X. G., & Tang, J. (2018). Haematoma scavenging in intracerebral haemorrhage: from mechanisms to the clinic. *J Cell Mol Med, 22*(2), 768-777. doi: 10.1111/jcmm.13441

Wang, M., Hua, Y., Keep, R. F., Wan, S., Novakovic, N., & Xi, G. (2019). Complement Inhibition Attenuates Early Erythrolysis in the Hematoma and Brain Injury in Aged Rats. *Stroke, 50*(7), 1859-1868. doi: 10.1161/STROKEAHA.119.025170

Wang, X., & Ge, P. (2020). Parthanatos in the pathogenesis of nervous system diseases. *Neuroscience, 449*, 241-250. doi: 10.1016/j.neuroscience.2020.09.049

Wang, Y. Q., Song, J. J., Han, X., Liu, Y. Y., Wang, X. H., Li, Z. M., & Tzeng, C. M. (2014a). Effects of angiopoietin-1 on inflammatory injury in endothelial progenitor cells and blood vessels. *Curr Gene Ther, 14*(2), 128-135. doi: 10.2174/1566523214666140307111138

Wang, Y. X., Zhang, X. R., Zhang, Z. J., Li, L., Xi, G. J., Wu, D., & Wang, Y. J. (2014b). Protein kinase Mzeta is involved in the modulatory effect of fluoxetine on hippocampal neurogenesis in vitro. [fluoxetine increases hippocampal NSC neurogenesis via a PKMζ-mediated mechanism that links 5-HT1A receptor activation with the phosphorylation of the downstream MAPK signaling pathway. Fluoxetine significantly increased PKMζ expression in hippocampal NSCs in a 5-hydroxytryptamine-1A (5-HT1A) receptor-dependent manner in both the absence and presence of dexamethasone. The PKMζ peptide blocker ZIP and MEK inhibitor U0126 significantly inhibited the increase in extracellular signal-regulated kinase 1/2 and cyclic adenosine monophosphate response element binding protein phosphorylation in the mitogen-activated protein kinase (MAPK) pathway and hippocampal NSC neurogenesis in response to fluoxetine and the 5-HT1A receptor agonist 8-OH DPAT]. *Int J Neuropsychopharmacol, 17*(9), 1429-1441. doi: 10.1017/S1461145714000364

S1461145714000364 [pii]

Wang, Z., Yuan, B., Fu, F., Huang, S., & Yang, Z. (2017b). Hemoglobin enhances miRNA-144 expression and autophagic activation mediated inflammation of microglia via mTOR pathway. *Sci Rep, 7*(1), 11861. doi: 10.1038/s41598-017-12067-2

Wei, Y., Sinha, S., & Levine, B. (2008). Dual role of JNK1-mediated phosphorylation of Bcl-2 in autophagy and apoptosis regulation. *Autophagy, 4*(7), 949-951. doi: 10.4161/auto.6788

Wilkinson, D. A., Pandey, A. S., Thompson, B. G., Keep, R. F., Hua, Y., & Xi, G. (2018). Injury mechanisms in acute intracerebral hemorrhage. *Neuropharmacology, 134*(Pt B), 240-248. doi: 10.1016/j.neuropharm.2017.09.033

Willmore, L. J., & Triggs, W. J. (1991). Iron-induced lipid peroxidation and brain injury responses. *Int J Dev Neurosci, 9*(2), 175-180. doi: 10.1016/0736-5748(91)90009-b

Wong, R. S. (2011). Apoptosis in cancer: from pathogenesis to treatment. *J Exp Clin Cancer Res, 30*, 87. doi: 10.1186/1756-9966-30-87

Wu, C., Yan, X., Liao, Y., Liao, L., Huang, S., Zuo, Q., Zhou, L., Gao, L., Wang, Y., Lin, J., Li, S., Wang, K., Ge, X., Song, H., Yang, R., & Lu, F. (2019). Increased perihematomal neuron autophagy and plasma thrombin-antithrombin levels in patients with intracerebral hemorrhage: An observational study. *Medicine (Baltimore), 98*(39), e17130. doi: 10.1097/MD.0000000000017130

Wu, J., Hua, Y., Keep, R. F., Nakamura, T., Hoff, J. T., & Xi, G. (2003). Iron and iron-handling proteins in the brain after intracerebral hemorrhage. *Stroke, 34*(12), 2964-2969. doi: 10.1161/01.STR.0000103140.52838.45

Wu, Q., Gao, C., Wang, H., Zhang, X., Li, Q., Gu, Z., Shi, X., Cui, Y., Wang, T., Chen, X., Wang, X., Luo, C., & Tao, L. (2018). Mdivi-1 alleviates blood-brain barrier disruption and cell death in experimental traumatic brain injury by mitigating autophagy dysfunction and mitophagy activation. *Int J Biochem Cell Biol, 94*, 44-55. doi: 10.1016/j.biocel.2017.11.007

Wu, Y., Li, X., Xie, W., Jankovic, J., Le, W., & Pan, T. (2010). Neuroprotection of deferoxamine on rotenone-induced injury via accumulation of HIF-1 alpha and induction of autophagy in SH-SY5Y cells. *Neurochem Int, 57*(3), 198-205. doi: 10.1016/j.neuint.2010.05.008

Xi, G., Keep, R. F., & Hoff, J. T. (2006). Mechanisms of brain injury after intracerebral haemorrhage. *Lancet Neurol, 5*(1), 53-63. doi: 10.1016/S1474-4422(05)70283-0

Xie, Q., Gu, Y., Hua, Y., Liu, W., Keep, R. F., & Xi, G. (2014). Deferoxamine attenuates white matter injury in a piglet intracerebral hemorrhage model. *Stroke, 45*(1), 290-292. doi: 10.1161/STROKEAHA.113.003033

Xu, C., Zheng, H., Loh, H. H., & Law, P. Y. (2015). Morphine Promotes Astrocyte-Preferential Differentiation of Mouse Hippocampal Progenitor Cells via PKCepsilon-Dependent ERK Activation and TRBP Phosphorylation. [Morphine Promotes Astrocyte-Preferential Differentiation of Mouse Hippocampal Progenitor Cells via PKCe-Dependent ERK Activation and TRBP Phosphorylation.after morphine treatment, phospho-ERK remains in the cytosol and is capable of phosphorylating TAR RNA-binding protein (TRBP), a cofactor of Dicer. This augments Dicer activity and promotes the maturation of miR-181a.we confirmed the crucial role of TRBP phosphorylation in Dicer activity, miR-181a maturation, and finally the morphine-induced astrocyte-preferential differentiation of NPCs]. *Stem Cells, 33*(9), 2762-2772. doi: 10.1002/stem.2055

Xu, F., Shen, G., Su, Z., He, Z., & Yuan, L. (2019a). Glibenclamide ameliorates the disrupted blood-brain barrier in experimental intracerebral hemorrhage by inhibiting the activation of NLRP3 inflammasome. *Brain Behav, 9*(4), e01254. doi: 10.1002/brb3.1254

Xu, T., Ding, W., Ji, X., Ao, X., Liu, Y., Yu, W., & Wang, J. (2019b). Molecular mechanisms of ferroptosis and its role in cancer therapy. *J Cell Mol Med, 23*(8), 4900-4912. doi: 10.1111/jcmm.14511

Yang, Z., Zhou, C., Shi, H., Zhang, N., Tang, B., & Ji, N. (2020). Heme Induces BECN1/ATG5-Mediated Autophagic Cell Death via ER Stress in Neurons. *Neurotox Res, 38*(4), 1037-1048. doi: 10.1007/s12640-020-00275-0

Yu, S., Zutshi, I., Stoffel, R., Zhang, J., Ventura-Silva, A. P., Sousa, N., Costa, P. S., Holsboer, F., Patchev, A., & Almeida, O. F. (2017). Antidepressant responsiveness in adulthood is permanently impaired after neonatal destruction of the neurogenic pool. *Transl Psychiatry, 7*(1), e990. doi: 10.1038/tp.2016.255

Yuan, B., Shen, H., Lin, L., Su, T., Zhong, L., & Yang, Z. (2017). Autophagy Promotes Microglia Activation Through Beclin-1-Atg5 Pathway in Intracerebral Hemorrhage. *Mol Neurobiol, 54*(1), 115-124. doi: 10.1007/s12035-015-9642-z

Zahra, K., Turnbull, M. T., Zubair, A. C., Siegel, J. L., Venegas-Borsellino, C. P., Tawk, R. G., & Freeman, W. D. (2020). A Combined Approach to Intracerebral Hemorrhage: Intravenous Mesenchymal Stem Cell Therapy with Minimally Invasive Hematoma Evacuation. *J Stroke Cerebrovasc Dis, 29*(8), 104931. doi: 10.1016/j.jstrokecerebrovasdis.2020.104931

Zhang, N., Luo, Y., He, L., Zhou, L., & Wu, W. (2016). A self-assembly peptide nanofibrous scaffold reduces inflammatory response and promotes functional recovery in a mouse model of intracerebral hemorrhage. *Nanomedicine, 12*(5), 1205-1217. doi: 10.1016/j.nano.2015.12.387

Zhang, R., Wang, Y., Zhang, L., Zhang, Z., Tsang, W., Lu, M., & Chopp, M. (2002). Sildenafil (Viagra) induces neurogenesis and promotes functional recovery after stroke in rats. [Sildenafil (Viagra)a phosphodiesterase type 5 (PDE5) inhibitor, induces neurogenesis and promotes functional recovery after stroke in rats.The cortical levels of cGMP significantly increased after administration of sildenafil, and PDE5 mRNA was present in both nonischemic and ischemic brain.these data suggest that cGMP may regulate neurogenesis

]. *Stroke, 33*(11), 2675-2680.

Zhang, R. L., Chopp, M., Roberts, C., Wei, M., Wang, X., Liu, X., Lu, M., & Zhang, Z. G. (2012). Sildenafil enhances neurogenesis and oligodendrogenesis in ischemic brain of middle-aged mouse. [Sildenafil enhances neurogenesis and oligodendrogenesis in ischemic brain of middle-aged mouse. Treatment of the ischemic middle-aged mouse with Sildenafil increased nestin expressing neural stem cells, mature neurons, and oligodendrocytes by 33, 75, and 30%, respectively, in the ischemic brain]. *PLoS One, 7*(10), e48141. doi: 10.1371/journal.pone.0048141

PONE-D-12-20185 [pii]

Zhang, R. L., Zhang, Z., Zhang, L., Wang, Y., Zhang, C., & Chopp, M. (2006). Delayed treatment with sildenafil enhances neurogenesis and improves functional recovery in aged rats after focal cerebral ischemia. [more Ki67+ cells (a marker of proliferating cells) were doublecortin+ (a marker of migrating neuroblasts) in sildenafil-treated than in saline-treated aged animals.inhibition of PDE5 activity by sildenafil augments neurogenesis in the SVZ of aged ischemic rats, although these rats have reduced numbers of neural progenitor and stem cells in the SVZ.

]. *J Neurosci Res, 83*(7), 1213-1219. doi: 10.1002/jnr.20813

Zhang, Y., & Liu, C. (2020). Autophagy and Hemorrhagic Stroke. *Adv Exp Med Biol, 1207*, 135-147. doi: 10.1007/978-981-15-4272-5_8

Zhang, Z., Song, Y., Zhang, Z., Li, D., Zhu, H., Liang, R., Gu, Y., Pang, Y., Qi, J., Wu, H., & Wang, J. (2017). Distinct role of heme oxygenase-1 in early- and late-stage intracerebral hemorrhage in 12-month-old mice. *J Cereb Blood Flow Metab, 37*(1), 25-38. doi: 10.1177/0271678X16655814

Zhao, W., Wu, C., Stone, C., Ding, Y., & Ji, X. (2020). Treatment of intracerebral hemorrhage: Current approaches and future directions. *J Neurol Sci, 416*, 117020. doi: 10.1016/j.jns.2020.117020

Zhao, X., Song, S., Sun, G., Zhang, J., Strong, R., Zhang, L., Grotta, J. C., & Aronowski, J. (2011). Cytoprotective role of haptoglobin in brain after experimental intracerebral hemorrhage. *Acta Neurochir Suppl, 111*, 107-112. doi: 10.1007/978-3-7091-0693-8_17

Zhou, X. M., Zhang, X., Zhang, X. S., Zhuang, Z., Li, W., Sun, Q., Li, T., Wang, C. X., Zhu, L., Shi, J. X., & Zhou, M. L. (2014). SIRT1 inhibition by sirtinol aggravates brain edema after experimental subarachnoid hemorrhage. *J Neurosci Res, 92*(6), 714-722. doi: 10.1002/jnr.23359

Zhou, Y. F., Zhang, C., Yang, G., Qian, Z. M., Zhang, M. W., Ma, J., Zhang, F. L., & Ke, Y. (2017). Hepcidin Protects Neuron from Hemin-Mediated Injury by Reducing Iron. *Front Physiol, 8*, 332. doi: 10.3389/fphys.2017.00332

Zille, M., Farr, T. D., Przesdzing, I., Muller, J., Sommer, C., Dirnagl, U., & Wunder, A. (2012). Visualizing cell death in experimental focal cerebral ischemia: promises, problems, and perspectives. *J Cereb Blood Flow Metab, 32*(2), 213-231. doi: 10.1038/jcbfm.2011.150

Zille, M., Ikhsan, M., Jiang, Y., Lampe, J., Wenzel, J., & Schwaninger, M. (2019a). The impact of endothelial cell death in the brain and its role after stroke: A systematic review. *Cell Stress, 3*(11), 330-347. doi: 10.15698/cst2019.11.203

Zille, M., Karuppagounder, S. S., Chen, Y., Gough, P. J., Bertin, J., Finger, J., Milner, T. A., Jonas, E. A., & Ratan, R. R. (2017). Neuronal Death After Hemorrhagic Stroke In Vitro and In Vivo Shares Features of Ferroptosis and Necroptosis. *Stroke, 48*(4), 1033-1043. doi: 10.1161/STROKEAHA.116.015609

Zille, M., Kumar, A., Kundu, N., Bourassa, M. W., Wong, V. S. C., Willis, D., Karuppagounder, S. S., & Ratan, R. R. (2019b). Ferroptosis in Neurons and Cancer Cells Is Similar But Differentially Regulated by Histone Deacetylase Inhibitors. *eNeuro, 6*(1). doi: 10.1523/ENEURO.0263-18.2019

Zusso, M., Debetto, P., Guidolin, D., Barbierato, M., Manev, H., & Giusti, P. (2008). Fluoxetine-induced proliferation and differentiation of neural progenitor cells isolated from rat postnatal cerebellum. *Biochem Pharmacol, 76*(3), 391-403. doi: 10.1016/j.bcp.2008.05.014

Supplemental data

Search Strategy of the systematic review on the interaction of drugs used in the elderly and NSCs.

1. Neurogenesis [All Fields]
2. Neuronal cell therapy [All Fields]
3. Neuronal precursor cell [All Fields] OR Neuronal progenitor cell [All Fields]
4. Neuronal cell proliferation [All Fields]
5. Neuronal cell differentiation [All Fields]
6. #1 OR #2 OR #3 OR #4 OR #5
7. Statin [All Fields]
8. PCSK9 Inhibitor [All Fields]
9. Bile acid sequestrant [All Fields]
10. Alpha 2 adrenergic receptor agonist [All Fields]
11. Beta adrenergic receptor antagonist [All Fields]
12. Beta blocker [All Fields]
13. Angiotensin II Receptor Inhibitor [All Fields] OR ARB [All Fields]
14. Alpha glucosidase inhibitor [All Fields]
15. Amylin analogs [All Fields]
16. Dipeptyl peptidase 4 inhibitor [All Fields]
17. SGLT 2 Inhibitor [All Fields]
18. Incretin mimetics [All Fields]
19. Insulin [All Fields]
20. Meglitinides [All Fields]
21. Sulfonylurea [All Fields]
22. Non sulfonylurea [All Fields]
23. Loop diuretics [All Fields]
24. Calcium channel antagonist [All Fields]
25. Thiazolidinediones [All Fields]
26. Norephinephrine and dopamine receptor Inhibitor [All Fields] OR NDRI [All Fields]
27. Selective serotonin reuptake inhibitor [All Fields] OR SSRI [All Fields]
28. Serotonin and Norephinephrine Reuptake Inhibitor [All Fields] OR SNRI [All Fields]
29. Atypical Antidepressant [All Fields]
30. Potassium diuretics [All Fields]
31. Aldosterone receptor antagonist [All Fields]
32. Tricyclic antidepressant [All Fields]
33. Monoamine oxidase Inhibitor [All Fields] OR MAOI [All Fields]
34. Acetaminophen [All Fields] OR paracetamol [All Fields]
35. Nonsteroidal anti-inflammatory drug [All Fields] OR NSAID [All Fields]
36. Thiazide diuretics [All Fields]
37. Carbapenem [All Fields]
38. Penicillin [All Fields]
39. Tetracyclin [All Fields]
40. Cephalosporin [All Fields]
41. Quinolone [All Fields]
42. Lincomycin [All Fields]
43. Macrolide [All Fields]
44. Sulfonamide [All Fields]

45. Glycopeptide [All Fields]
46. Aminoglycoside [All Fields]
47. Opioid [All Fields]
48. COX-2 Inhibitor [All Fields]
49. #7 OR #8 OR #9 OR #10 OR#11 OR #12 OR#13 OR#14 OR #15 OR #16 OR #17 OR #18 OR #19 OR #20 OR #21 OR #22 OR #23 OR #24 OR #25 OR #26 OR #27 OR #28 OR#29 OR #30 OR #31 OR #32 OR #33 OR #34 OR #35 OR #36 OR #37 OR #38 OR #39 OR #40 OR #41 OR #42 OR #43 OR #44 OR #45 OR #46 OR #47 OR #48
50. #6 AND #49

Search Strategy of the systematic review on the interaction of drugs used in the elderly and EPCs.

1. Brain endothelial progenitor cells [All Fields]
2. Statin [All Fields]
3. PCSK9 Inhibitor [All Fields]
4. Bile acid sequestrant [All Fields]
5. Alpha 2 adrenergic receptor agonist [All Fields]
6. Beta adrenergic receptor antagonist [All Fields]
7. Beta blocker [All Fields]
8. Angiotensin II Receptor Inhibitor [All Fields] OR ARB [All Fields]
9. Alpha glucosidase inhibitor [All Fields]
10. Amylin analogs [All Fields]
11. Dipeptyl peptidase 4 inhibitor [All Fields]
12. SGLT 2 Inhibitor [All Fields]
13. Incretin mimetics [All Fields]
14. Insulin [All Fields]
15. Meglitinides [All Fields]
16. Sulfonylurea [All Fields]
17. Non sulfonylurea [All Fields]
18. Loop diuretics [All Fields]
19. Calcium channel antagonist [All Fields]
20. Thiazolidinediones [All Fields]
21. Norephinephrine and dopamine receptor Inhibitor [All Fields] OR NDRI [All Fields]
22. Selective serotonin reuptake inhibitor [All Fields] OR SSRI [All Fields]
23. Serotonin and Norephinephrine Reuptake Inhibitor [All Fields] OR SNRI [All Fields]
24. Atypical Antidepressant [All Fields]
25. Potassium diuretics [All Fields]
26. Aldosterone receptor antagonist [All Fields]
27. Tricyclic antidepressant [All Fields]
28. Monoamine oxidase Inhibitor [All Fields] OR MAOI [All Fields]
29. Acetaminophen [All Fields] OR paracetamol [All Fields]
30. Nonsteroidal anti-inflammatory drug [All Fields] OR NSAID [All Fields]
31. Thiazide diuretics [All Fields]
32. Carbapenem [All Fields]
33. Penicillin [All Fields]
34. Tetracyclin [All Fields]
35. Cephalosporin [All Fields]
36. Quinolone [All Fields]
37. Lincomycin [All Fields]
38. Macrolide [All Fields]
39. Sulfonamide [All Fields]
40. Glycopeptide [All Fields]
41. Aminoglycoside [All Fields]
42. Opioid [All Fields]
43. COX-2 Inhibitor [All Fields]
44. #1 AND #2 OR #3 OR #4 OR #5 OR #6 OR #7 OR #8 OR #9 OR #10 OR#11 OR #12 OR#13 OR#14 OR #15 OR #16 OR #17 OR #18 OR #19 OR #20 OR #21 OR #22 OR #23 OR #24 OR #25 OR #26 OR #27 OR #28 OR#29 OR #30 OR #31 OR #32 OR #33 OR #34 OR #35 OR #36 OR #37 OR #38 OR #39 OR #40 OR #41 OR #42 OR #43

Supplemental Table 1. Excluded studies of the systematic review on NSCs and drug interactions based on the full-text screening.

No	Author, Year	PMID	Review	Non-English publication	Use of other cell line	Non-mammalian animal	Non-available drug in the market	No adequate method	No interaction between drug and the stem cell	Non-proliferation or non-differentiation marker	Drug only used as procedure	Withdrawn article
1.	Abdelkader et al., 2017	28178754							*			
2.	Abdipranoto-Cowley et al., 2009	19489097					*					
3.	Aldkogius et al., 2009	9544468									*	
4.	Allani et al., 2018	29788733								*		
5.	Altinay et al., 2017	27593816					*					
6.	Aoki et al., 1993	16350568							*			
7.	Ashjian et al., 2003	14556988									*	
8.	Ayuob, 2017	27444866					*					
9.	Bae et al., 2017	29165354	*									
10.	Baka et al., 2004	15290185			*							
11.	Banks, 2012	22612379						*				
12.	Baravalle et al., 2017	27616271							*			
13.	Bassani et al., 2017	28801114					*					
14.	Bassani et al., 2018	28623617									*	
15.	Bateman & McNeill, 2006	16786222	*									
16.	Beech et al., 2004	15176089									*	
17.	Belovicova et al., 2017	28456144								*		
18.	Bernstein et al., 2014	24817634							*			
19.	Bianchi et al., 2017	29149058	*									
20.	Biggio et al., 2009	19309534					*					
21.	Boldrini et al., 2012	22652019								*		
22.	Borg et al., 2014	24898143							*			
23.	Bottcher et al., 2000	10837202			*							
24.	Bottcher et al., 2004	15584921						*				
25.	Boucher et al., 1998	9579401				*						

No	Author, Year	PMID	Review	Non-English publication	Use of other cell line	Non-mammalian animal	Non-available drug in the market	No adequate method	No interaction between drug and the stem cell	Non-proliferation or non-differentiation marker	Drug only used as procedure	Withdrawn article
26.	Brenza et al., 2017	27771430					*					
27.	Brooker et al., 2000	10679768					*					
28.	Brownjohn et al., 2017	28285880							*			
29.	Brustein et al., 2012	22888055				*						
30.	Burgdorf et al., 2017	28158790							*			
31.	Buzanska et al., 2009	19609937								*		
32.	Cabras et al., 2010	20356437								*		
33.	Calabria et al., 2008	18039545			*							
34.	Calderari et al., 2017	28911974					*					
35.	Campos et al., 2017	28588483	*									
36.	Cao et al., 2018	29736175	*									
37.	Carlson et al., 2018	29455576					*					
38.	Carson et al., 2012	3225598			*							
39.	Castilho et al., 2000	10877919								*		
40.	Cebolla et al., 2008	18579744							*			
41.	Cerri et al., 2015	26198165								*		
42.	Chalicem et al., 2017	28747063	*									
43.	Chao et al., 2013	23691054								*		
44.	Chen et al., 2005	15895831			*							
45.	Chen et al., 2012	23317920								*		
46.	Chesnokova & Pechnick, 2008	18682686	*									
47.	Chiba et al., 2010	19925560								*		
48.	Chilmonczyk et al., 2017	28324844	*									
49.	Choi et al., 2017	28045430					*					
50.	Cocchiarella, 2012	22256833						*				
51.	Cominski et al., 2012	22280973							*			
52.	Cominski et al., 2014	25086317							*			

No	Author, Year	PMID	Review	Non-English publication	Use of other cell line	Non-mammalian animal	Non-available drug in the market	No adequate method	No interaction between drug and the stem cell	Non-proliferation or non-differentiation marker	Drug only used as procedure	Withdrawn article
53.	Compagnucci et al., 2015	27160703								*		
54.	Conner et al., 2012	22595793					*					
55.	Coplan et al., 2014	25506432							*			
56.	Corso et al., 1998	9514310			*							
57.	Culberson et al., 2017	28253982	*									
58.	Czeh et al., 2001	11675510								*		
59.	De la Rosa et al., 1994	7535629				*						
60.	De Pablo et al., 1996	9087719	*									
61.	Diaz et al., 1999	10215915				*						
62.	Diaz et al., 2000	10725240				*						
63.	Dikmen, 2017	28338387					*					
64.	Dobarro et al., 2013	22824191						*				
65.	Doze et al., 2011	21791575			*							
66.	Einoch et al., 2017	28410959								*		
67.	Eisch & Mandyam, 2004	14992964	*									
68.	Ekström et al., 1993	8215035				*						
69.	Ericksson et al., 1992	1382177					*					
70.	Ericksson et al., 2008	18293414								*		
71.	Faijerson et al., 2009	19425175					*					
72.	Faivre et al., 2011	21273318							*			
73.	Faivre et al., 2012	22115896					*					
74.	Farrar et al., 2005	16304629					*					
75.	Ferrucci et al., 2017	28418837			*							
76.	Fesharaki et al., 2018	29633593			*							
77.	Fischer et al., 2002a	12435364				*						
78.	Fischer et al., 2002b	12417664				*						
79.	Fischer et al., 2002c	12176172				*						
80.	Fischer et al., 2003	12871698				*						

No	Author, Year	PMID	Review	Non-English publication	Use of other cell line	Non-mammalian animal	Non-available drug in the market	No adequate method	No interaction between drug and the stem cell	Non-proliferation or non-differentiation marker	Drug only used as procedure	Withdrawn article
81.	Fishwick et al., 2010	20004186				*						
82.	Foerster et al., 2017	27993979			*							
83.	Furuya et al., 2009	19651108								*		
84.	Garcia-de lacoba et al.,1999	9886830				*						
85.	Garcia-Perez et al., 2017	26742526			*							
86.	Geng et al., 2017	28782906			*							
87.	Goto et al., 2011	22025691						*				
88.	Goudarzi et al., 2018	29870058			*							
89.	Gu et al., 2017	28916193			*							
90.	Guo et al., 2010	20466036							*			
91.	Guo et al., 2017	28382978								*		
92.	Guo et al., 2017	28865290								*		
93.	Hafizi et al., 2012	23054438							*			
94.	Hahn et al., 2010	19895666							*			
95.	Hansel et al., 2001	11598996					*					
96.	Hao et al., 2017	27743319			*							
97.	Harburg et al., 2007	17055658							*			
98.	Hartman et al., 2013	24139800							*			
99.	Hauser et al., 1993	8244536								*		
100	Hayashi et al., 2012	22293695		*								
101	Hays et al., 2012	22061798			*							
102	Hay-Schmidt et al., 2017	28559473							*			
103	Heanue et al., 2011	21280162									*	
104	Heidenreich et al., 1996	8626622				*						
105	Hernandez-Sanchez et al., 1995	7568228				*						
106	Hicks et al., 2000	11090640					*					
107	Hidaka et al., 2013	23673084									*	
108	Hiramoto et al., 2008	18446092								*		

No	Author, Year	PMID	Review	Non-English publication	Use of other cell line	Non-mammalian animal	Non-available drug in the market	No adequate method	No interaction between drug and the stem cell	Non-proliferation or non-differentiation marker	Drug only used as procedure	Withdrawn article
109	Hitchcock et al., 2001	11481281				*						
110	Hori et al., 2005	15839736							*			
111	Hoshimaru et al., 1996	8643664									*	
112	Huang et al., 2017	28026149			*							
113	Huong et al., 2011	22130242						*				
114	Inta et al., 2016.	27352782	*									
115	Isaev et al., 2018	29684395								*		
116	Ishizuka et al., 2014	25058791					*					
117	Ito & Araki, 2010	20048438		*								
118	Jimenez-Gonzalez et al., 2017	29111275			*							
119	Jin et al., 2017	27324897								*		
120	Jukic et al., 2017	27895323							*			
121.	Katz et al., 2016	26772642			*							
122.	Kazma et al., 2010	19746435							*			
123.	Khurshid et al., 2010	20495180				*						
124.	King et al., 2017	28076682								*		
125.	Kisoh et al., 2017	27866373					*					
126.	Kitani et al., 1991	1917779									*	
127.	Klawitter et al., 2015	25912929	*									
128.	Koch et al., 2012	22510327							*			
129.	Kolarova et al., 2003	13129439					*					
130.	Kolodziej et al., 2008	18331339							*			
131.	Kompisch et al., 2010	20945072									*	
132.	Kozlova & Jansson, 2009	19421078							*			
133.	Kuhmonen et al., 1997	9286902						*				
134.	Kwon et al., 1998	23392671								*		
135.	Lafourcade et al., 2013	23392671			*							
136.	Lai et al., 2011	21933448			*							
137.	Landry et al., 2011	21762764			*							
138.	Lang et al., 2009	19596361							*			

No	Author, Year	PMID	Review	Non-English publication	Use of other cell line	Non-mammalian animal	Non-available drug in the market	No adequate method	No interaction between drug and the stem cell	Non-proliferation or non-differentiation marker	Drug only used as procedure	Withdrawn article
139.	Lecomte et al., 2017	28396216			*							
140.	Lee et al., 2007	17707770								*		
141.	Lehmann et al., 2013	23407954			*							
142.	Lennox et al., 2013	23138973					*					
143.	Leslie et al., 1998	9729266							*			
144.	Li et al., 2000	10956432									*	
145.	Li et al., 2012	22752192									*	
146.	Li et al., 2017	27590141					*					
147.	Liu et al., 2007	17663584					*					
148.	Liu et al., 2017	28339691					*					
149.	Lixing et al., 2017	29129800					*					
150.	Lu et al., 1996	8816274							*			
151.	Lucassen et al., 2004	15050859								*		
152.	Ma et al., 2017	28430602								*		
153.	Ma EY et al., 2008	18305259			*							
154.	Malaterre et al., 2003	12918022				*						
155.	Manev et al., 2001	11462800					*					
156.	Mao et al., 2005	16221970							*			
157.	Martone et al., 2014	24689961			*							
158.	Marxreiter et al., 2009	19291219									*	
159.	Masuda et al., 2012	21914456								*		
160.	Matrisciano et al., 2008	18082849					*					
161.	Mazur-Kolecka et al., 2006	17112488					*					
162.	Mazur-Kolecka et al., 2012	16105709					*					
163.	McCreedy et al., 2014	25346848									*	
164.	McEwen & Chattarji, 2004	15550348	*									
165.	McGovern et al., 2012	22867941					*					
166.	McNeill et al., 2008	18505882							*			

No	Author, Year	PMID	Review	Non-English publication	Use of other cell line	Non-mammalian animal	Non-available drug in the market	No adequate method	No interaction between drug and the stem cell	Non-proliferation or non-differentiation marker	Drug only used as procedure	Withdrawn article
167.	Mehta et al., 2017	28939429					*					
168.	Mendez-David et al., 2015	25916883					*					
169.	Menendez & Vazquez-Martin, 2012	22935702	*									
170.	Mertens et al., 2013	24371804								*		
171.	Min et al., 2011	21471976			*							
172.	Min et al., 2017	28601633					*					
173.	Mir et al., 2017	28607354					*					
174.	Miyamoto et al., 2011	21626864		*								
175.	Mogi et al., 2012	22868412								*		
176.	Moon et al., 2013	23224631							*			
177.	Morel et al., 2017	28405590					*					
178.	Mostany et al., 2008	18511088							*			
179.	Motaghinejad et al., 2017	28082019								*		
180.	Mrkusich et al., 2004	14766199							*			
181.	Na et al., 2017	28966575			*							
182.	Naoi et al., 2018	28293733	*									
183.	Narita et al., 2006	16696856					*					
184.	Nataf & Monier, 1992	1358479									*	
185.	Nava et al., 2017	26523035								*		
186.	Newton & Duman, 2007	17696572	*									
187.	Nieto et al., 2017	28794445					*					
188.	Niu et al., 2017	28179206					*					
189.	Noor et al., 2017	29147492							*			
190.	Norambuena et al., 2017	27693185							*			
191.	Novozhilova et al., 2015	25514049					*					
192.	Ohmasa & Saito, 2004	15140564									*	
193.	Olianas et al., 2017	28815598							*			
194.	Olivius et al., 2003	12850564									*	
195.	Omar et al., 2017	28801265							*			

No	Author, Year	PMID	Review	Non-English publication	Use of other cell line	Non-mammalian animal	Non-available drug in the market	No adequate method	No interaction between drug and the stem cell	Non-proliferation or non-differentiation marker	Drug only used as procedure	Withdrawn article
196.	Ostapcuk et al., 2018	29795351							*			
197.	Otsuki et al., 2018	29622651							*			
198.	Palazuelos et al., 2012	22102284					*					
199.	Pan et al., 2016	26873855							*			
200.	Park et al., 2017	29299155			*							
201.	Park et al., 2002	12213294									*	
202.	Parmar et al., 2017	28164768			*							
203.	Parng et al., 2007	16769228							*			
204.	Parween et al., 2017	29311838							*			
205.	Patnaik et al., 2016	7807796								*		
206.	Pfisterer et al., 2016	27917895								*		
207.	Pixley et al., 1998	9929614						*				
208.	Popova et al., 2018	28887184						*				
209.	Powell et al., 2017	28394502			*							
210.	Pradillo et al., 2017	27856349					*					
211.	Procaccini et al., 2011	21073553					*					
212.	Qiu et al., 2018	29165691							*			
213.	Quartier et al 2018	29428674						*				
214.	Quinta et al., 2010	20796173						*				
215.	Quinte et al., 2012	22091865								*		
216.	Rachmani et al., 2013	24024202								*		
217.	Ramalingayya et al., 2017	28408800			*							
218.	Ramkumar et al., 2017	28420370			*							
219.	Ramos-Rodriguez et al., 2014	24586614							*			
220.	Ray et al., 1999	10473288							*			
221.	Raymon et al., 1999	10377351									*	
222.	Revsin et al., 2005	15748869						*				
223.	Ridet et al., 1999	10022551									*	
224.	Riederer et al., 2017	27998194	*									

No	Author, Year	PMID	Review	Non-English publication	Use of other cell line	Non-mammalian animal	Non-available drug in the market	No adequate method	No interaction between drug and the stem cell	Non-proliferation or non-differentiation marker	Drug only used as procedure	Withdrawn article
225.	Robinson et al., 1994	7988444				*						
226.	Rossi et al., 2018	29531474				*						
227.	Safford et al., 2002	12051722									*	
228.	Sagir et al., 2017	28461249			*							
229.	Sairanen et al., 2007	17049169			*							
230.	Sajan et al., 2017	29032894					*					
231.	Saliba et al., 2017	28143498								*		
232.	Salzberg et al., 2017	28114319							*			
233.	Sanchez Simon et al., 2012	22062135				*						
234.	Santa-Olalla et al., 1995	8568917					*					
235.	Santos et al., 2017	27871898			*							
236.	Sargeant et al., 2007	17888889							*			
237.	Sarkar & Das, 2003	14511111			*							
238.	Sarlak et al., 2013	23985544					*					
239.	Scheller et al., 2017	28274821					*					
240.	Schmidt et al., 1999	10631639						*				
241.	Schmidt et al., 2015	25470346					*					
242.	Schmitz et al., 2018	29324300							*			
243.	Selden et al., 2013	23581634									*	
244.	Sevc et al., 2013	23748136								*		
245.	Sheng et al., 2007	17538007							*			
246.	Shin et al., 2004	14999075							*			
247.	Singer et al., 2009	19363795							*			
248.	Singh et al., 1997	9163577								*		
249.	Smith-Arica et al., 2000	11124058							*			
250.	Solbrig et al., 2006	16399805									*	
251.	Stranahan et al., 2008	18278039									*	
252.	Suh et al., 2005	15677508							*			
253.	Tai et al., 2018	29050859					*					

No	Author, Year	PMID	Review	Non-English publication	Use of other cell line	Non-mammalian animal	Non-available drug in the market	No adequate method	No interaction between drug and the stem cell	Non-proliferation or non-differentiation marker	Drug only used as procedure	Withdrawn article
254.	Tan et al., 2018	29635048							*			
255.	Tian et al., 2017	28663724					*					
256.	Tondreau et al., 2008	18405367							*			
257.	Tong et al., 1997	9192297								*		
258.	Tramutola et al., 2017	27715341	*									
259.	Tripathi et al., 2008	18455254							*			
260.	Trivedi et al., 2016	27611101								*		
261.	Tzeng et al., 2018	29463001					*					
262.	Umschweif et al., 2014	24957202					*					
263.	Uyanigkgil et al., 2004	14963685							*			
264.	Val-Laillet et al., 2017	29242276					*					
265.	Van Gorp et al., 2013	23710605									*	
266.	Varghese, eta l., 2017	29147115			*							
267.	Vicario-Abejon et al., 2003	12574418					*					
268.	Vilchez et al., 2013	23551888							*			
269.	Waetzig, et al., 2017	28479141			*							
270.	Wang et al., 2016	25567530					*					
271.	Wang et al., 2003	12801891							*			
272.	Wang et al., 2017	28780644					*					
273.	Wang G et al., 2017	28780644							*			
274.	Wong chitrat et al., 2016	27620814							*			
275.	Wu et al., 2013	23357262		*								
276.	Xiong et al., 2009	18726712								*		
277.	Yamashita et al., 1995	7724532			*							
278.	Yanagisawa et al., 2009	19598243								*		
279.	Yanai et al., 2016	27229654							*			
280.	Yang et al., 2006	16955841		*								
281.	Yilmaz et al., 2014	24831366			*							

No	Author, Year	PMID	Review	Non-English publication	Use of other cell line	Non-mammalian animal	Non-available drug in the market	No adequate method	No interaction between drug and the stem cell	Non-proliferation or non-differentiation marker	Drug only used as procedure	Withdrawn article
282.	Ying et al., 2002	11932748							*			
283.	Ying et al., 2012	22569742									*	
284.	Yoles et al., 1999	9888428			*							
285.	Yoon et al., 2013	24095011					*					
286.	Yu et al., 2005	15789426									*	
287.	Zackenfels et al., 1995	7718236				*						
288.	Zang et al., 2017	28456716							*			
289.	Zhang et al., 2004	15026250									*	
290.	Zhang et al., 2008	17854417							*			
291.	Zhang et al., 2017	28842345					*					
292.	Zhao et al., 2007	17980966								*		
293.	Zheng & Chen, 2007	17687392										*

Supplemental Table 2. Distribution of included records in the systematic review on NSCs and drug interactions according to the source of the sample.

No	Condition	Author, Year	PMID	Type of experiment				Source of cells				Location of the cells		
				In vitro	*In vivo*	*In utero*	*Ex vivo*	Rat	Mouse	Human	Other mammals (e.g., Guinea pigs or Mongolian Gerbils)	Hippocampus/ Subgranular zone/Dentate gyrus	Subventricular/ periventricular zone	Other regions (e.g., striato-pallidum complex, mesenchepalon, spinal cord, hypothalamus)
1	Physiologic	Alvarez et al., 2009	19041902		*				*					
2		Alves et al.,2017	28291258		*			*				*		
3		Amellem et al., 2017	28925998		*				*			*		
4		Arguello et al., 2008	19356684		*				*			*		
5		Arguello et al., 2009	18832014		*				*			*		
6		Arsenijevic et al., 1998	9482798	*					*					*
7		Asokan et al., 2014	24896246		*			*				*		
8		Bath et al., 2017	28884281		*			*				*		
9		Beauquis et al., 2006	16553617		*				*			*		
10		Brooker et al., 2017	27698430		*				*			*		
11		Chang et al., 2008,	18760539		*				*			*		
12		Chen et al., 2013	29548728		*				*			*		
13		Chen et al., 2018	23836293		*						*	*		
14		Chen et al., 2018	18063826		*				*			*		
15		Christie et al., 2012,	22338017		*			*				*		
16		Cowen et al., 2008	18616933		*			*				*		
17		Deng et al., 2015	25445352	*				*					*	
18		Desai et al., 2011	21652728		*			*						*
19		Desai et al., 2011	21215735	*				*						*
20		Dholakiya et al., 2016	26877219	*					*					*
21		Eisch et al., 2000	10840056	*				*				*		
22		Fex Svenningsen et al., 1996	8891693	*				*						*
23		Fischer et al., 2008	18248906		*				*			*		
24		Gatt et al., 2017	29393203	*						*		*		
25		Gemmel et al., 2017	29203333		*			*				*		
26		Gemmel et al., 2018	28735226		*			*				*		
27		Ghoochani et al., 2011	22099177	*					*					*
28		Gomez-pinedo et al., 2010	19958812		*			*				*		
29		Gupta et al., 2009	19487244	*					*				*	
30		Han et al., 2008	18620060	*				*						*
31		Han et al., 2011	21463148		*				*			*		
32		Hanson et al., 2011	21220416		*			*				*		

No	Condition	Author, Year	PMID	Type of experiment				Source of cells				Location of the cells		
				In vitro	*In vivo*	*In utero*	*Ex vivo*	Rat	Mouse	Human	Other mammals (e.g., Guinea pigs or Mongolian Gerbils)	Hippocampus/ Subgranular zone/Dentate gyrus	Subventricular/ periventricular zone	Other regions (e.g., striato-pallidum complex, mesenchepalon, spinal cord, hypothalamus)
33		Hauser et al., 2000	10762357	*					*					*
34		Holick et al., 2008	17429410		*				*			*		
35		Huang et al., 2007	17510525	*				*				*		
36		Hui et al., 2014	25522429	*				*				*		
37		Hunter et al., 2012	22443187		*				*			*		
38		Jackson-guilford et al., 2000	11027841		*			*				*		
39		Jenrow et al., 2010	20122169		*			*				*		
40		Jhaveri et al., 2010	20164362	*					*			*		
41		Kahn et al., 2005	15673448		*			*				*		
42		Kanakasabai et al., 2012	23185633	*					*					*
43		Kang et al., 2017	28614773	*						*				*
44		Kawahara et al., 2012	22194416				*				*			*
45		Keilhoff et al., 2006	16205774		*			*				*	*	
46		Kelland et al., 2014	25125045	*						*				*
47		Kim et al., 2006	16697980	*				*						*
48		Kitamura et al., 2015	21212521		*			*				*		
49		Kitamura et al., 2017	26057360		*			*				*		
50		Kodama et al., 2004	15476686		*			*				*		*
51		Kohl et al., 2012	22211740		*				*			*		
52		Kota et al., 2015	26586775	*				*		*		*		
53		Kudo et al., 2003	12826271	*					*					*
54		Kumihashi et al., 2001	11303759		*						*	*		
55		Kusakawa et al., 2010	20857517	*					*					*
56		Lee et al., 2009	20298677		*				*			*		
57		Lee et al., 2010	27388240		*				*			*		
58		Lee et al., 2016	26143260	*						*				*
59		Li et al., 2014	18711744	*				*						*
60		Li et al., 2017	24890505	*						*				*
61		Liu et al., 2017	29054390		*			*				*		
62		Marlatt et al., 2010	20381469		*				*			*		
63		Meneghini et al., 2014	24516101		*				*			*		
64		Meyer et al., 2017	27569185		*				*			*	*	
65		Mishra et al., 2017	29174383		*			*				*		
66		Misumi et al., 2008	18783370	*				*						*
67		Monje et al., 2003	14615545		*			*				*		
68		Nackenoff et al., 2017	28272863		*				*			*		

No	Condition	Author, Year	PMID	Type of experiment				Source of cells				Location of the cells		
				In vitro	*In vivo*	*In utero*	*Ex vivo*	Rat	Mouse	Human	Other mammals (e.g., Guinea pigs or Mongolian Gerbils)	Hippocampus/ Subgranular zone/Dentate gyrus	Subventricular/ periventricular zone	Other regions (e.g., striato-pallidum complex, mesenchepalon, spinal cord, hypothalamus)
69		Nam et al., 2015	25549214		*				*			*		
70		Nasrallah et al., 2010	20682307		*			*				*		
71		Ohira et al., 2011	21385396		*				*			*		
72		Olesen et al., 2017	28461249		*				*			*		
73		Opanashuk et al., 1998	9729296	*					*					*
74		Paliouras et al., 2012	23100423	*					*				*	*
75		Park et al., 2013	23773068		*				*			*		
76		Patnaik et al., 2016	27807796	*						*				*
77		Pechnick et al., 2008	22076148		*				*			*		
78		Pechnick et al., 2011	18172194		*				*			*		
79		Peng et al., 2008	17566715		*			*				*		
80		Pereira et al.,2013	24312632	*					*					*
81		Persson et al., 2003	12670304	*				*				*		
82		Petit et al., 2013	22079577		*				*					*
83		Pettit et al., 2012	23573275		*				*			*		
84		Piacentini et al., 2008	17941084	*					*					*
85		Ping et al., 2013	24844704		*				*			*		
86		Rayen et al., 2011	21912658			*		*				*		
87		Sah et al., 1997	25583694	*						*				*
88		Sankararaman et al., 2012	22487733		*			*				*		
89		Santarelli et al., 2003	12907793		*				*			*		
90		Schiavon et al., 2016	26187374		*				*				*	
91		Skardelly et al., 2013	24001738	*						*				*
92		Sugimoto et al., 2008	18996208	*					*					*
93		Sultan et al., 2013	23898238		*				*			*		
94		Sun et al., 2010	20123967	*					*					*
95		Sun et al., 2013	26159196	*					*					*
96		Sun et al., 2015	29867451		*			*				*		
97		Sun et al., 2018	24040509		*			*				*		
98		Teh et al., 2014	25283796	*				*				*		
99		Toran-allerand et al., 1991	1782546	*					*					*
100		Traudt et al., 2012	21971612		*			*				*		
101		Tsai et al., 2010	19953654	*				*						*
102		Uchida et al., 2002	12499663		*			*				*		
103		Wang et al., 2011	15815584		*				*			*		
104		Wang et al., 2014	28754619	*				*				*		
105		Wang et al., 2017	23876404		*				*					*

No	Condition	Author, Year	PMID	Type of experiment				Source of cells				Location of the cells		
				In vitro	*In vivo*	*In utero*	*Ex vivo*	Rat	Mouse	Human	Other mammals (e.g., Guinea pigs or Mongolian Gerbils)	Hippocampus/ Subgranular zone/Dentate gyrus	Subventricular/ periventricular zone	Other regions (e.g., striato-pallidum complex, mesenchepalon, spinal cord, hypothalamus)
106		Willner et al., 2014	25072277	*					*					*
107		Wu et al., 2014	24321744			*		*						*
108		Xu et al., 2006	24964978		*			*				*		
109		Xu et al., 2014	26012717		*				*			*		
110		Xu et al., 2015	16652337		*				*			*		
111		Xu et al., 2017	26960329		*			*					*	
112		Yoneyama et al., 2014	24389877		*				*			*		
113		Yu et al., 2017	28045461		*			*				*		
114		Zheng et al., 2013	23303051		*				*			*		
115		Zusso et al., 2008	18573488	*				*						*
116	Injury (incl. mental disorders)	Alboni et al., 2017	26645631		*				*			*		
117		Bastos et al., 2008	18616986		*				*			*		
118		Biscaro et al., 2012	22584394		*				*			*		
119		Boldrini et al., 2009	19606083	*						*		*		
120		Chadwick et al., 2011	21738757		*				*			*		
121		Chang et al., 2006	16887358		*			*				*		
122		Chen et al., 2003	12783420		*			*				*		
123		Chen et al., 2008	29846284		*			*					*	
124		Chiu et al., 2014	24291466		*				*					*
125		Christensen et al., 2012	22406239		*			*				*		
126		Ding et al., 2010	19913617		*				*			*		
127		Duan et al., 2008	18403212		*				*			*	*	
128		Engels et al., 2016	28343223		*				*					*
129		Espinera et al., 2013	23590907		*				*			*		
130		Gault e tal., 2015	25580570		*				*			*		
131		Gobinath et al., 2017	29579632		*			*				*		
132		Gobinath et al., 2018	28580124		*			*				*		
133		Goldshmit et al., 2015	25936601		*				*					*
134		Goncalves et al., 2010	20136845		*				*				*	
135		Guan et al., 2015	25702528	*				*				*		
136		Hays et al., 2013	23026365		*			*				*		
137		He et al., 2008	18606181		*				*				*	
138		Hoehn et al., 2005,	16282546		*			*						*
139		Hsieh et al., 2017	28576659		*			*				*		
140		Hu, et al., 2017	28161194		*			*				*		
141		Hwang et al., 2010	20219444		*			*				*		
142		Jaako et al., 2009	19596274		*				*			*		

No	Condition	Author, Year	PMID	Type of experiment				Source of cells				Location of the cells		
				In vitro	*In vivo*	*In utero*	*Ex vivo*	Rat	Mouse	Human	Other mammals (e.g., Guinea pigs or Mongolian Gerbils)	Hippocampus/ Subgranular zone/Dentate gyrus	Subventricular/ periventricular zone	Other regions (e.g., striato-pallidum complex, mesenchepalon, spinal cord, hypothalamus)
143		Jaako-movits et al., 2006	16783525		*			*						*
144		Jayakumar et al., 2017	28764145		*			*				*		
145		Jenrow et al., 2011	20617366		*			*				*		
146		Jung et al., 2006	16806953	*	*			*		*		*		*
147		Khodanovich et al., 2017	29304004		*			*				*		
148		Kim et al., 2015	28208711		*				*			*		
149		Kim et al., 2017	25845738	*					*					*
150		Kuipers et al., 2013	23994757		*			*				*		
151		Li et al., 2009	28244646		*				*			*		
152		Lu et al., 2007	17610353		*			*				*		
153		Lu et al., 2014	24621884		*				*			*		
154		Ma et al., 2015	26910812		*			*				*		
155		Malberg et al., 2003	12838272		*			*				*		
156		Marissal-Arvy et al., 2018	29702445		*			*				*		
157		Matsuda et al., 2017	27911310		*				*			*		
158		McClean et al., 2013	23973293		*				*			*		
159		Meng et al., 2011	21889575		*			*						*
160		Morais et al., 2014	28585931		*			*				*		
161		Morais et al., 2017	25315831		*			*				*		
162		Ortega et al., 2013	23149556		*			*						*
163		Ou-Yang et al., 2016	26700432		*			*				*		
164		Petersen et al., 2009	19135130		*			*				*		
165		Ramos-Rodriguez et al., 2017	28768549		*				*				*	
166		Sasaki et al., 2003	12704808		*				*			*		
167		Seyfried et al., 2008	18573239		*					*				*
168		Stevenson et al., 2009	18563059		*				*			*		
169		Su et al., 2005	16254493		*			*						*
170		Suri et al., 2013	23237316		*			*				*		
171		Thau-Zuchman et al., 2012	21561314		*				*					*
172		Van bokhoven et al., 2011	21488984		*			*				*		
173		Vitale et al., 2017	28417659		*			*				*		
174		Wang et al., 2005	21175261		*			*					*	
175		Wang et al., 2013	24679950		*			*				*		
176		Wu et al., 2008	18260796		*			*				*		
177		Xie et al., 2015	25445996		*			*						*
178		Xu et al., 2017	29787769		*			*					*	

No	Condition	Author, Year	PMID	Type of experiment				Source of cells				Location of the cells		
				In vitro	*In vivo*	*In utero*	*Ex vivo*	Rat	Mouse	Human	Other mammals (e.g., Guinea pigs or Mongolian Gerbils)	Hippocampus/ Subgranular zone/Dentate gyrus	Subventricular/ periventricular zone	Other regions (e.g., striato-pallidum complex, mesencephalon, spinal cord, hypothalamus)
179		Xu et al., 2018	29787769		*				*			*		
180		Zhang et al., 2006	25519973		*			*					*	
181		Zhang et al., 2012	12411660		*				*			*		
182		Zhang et al., 2002	23118941		*			*				*		
183		Zheng et al., 2009	23303051		*			*				*		
184		Zhu et al. 2017	28481152		*				*			*		
185	Modified	Anacker et al., 2013	23303060	*						*		*		
186		Borsini et al., 2017	28529072	*						*		*		
187		Cheng et al., 2015	25330741		*				*			*		
188		Clark et al., 2006	16624293		*				*			*		
189		Conti et al., 2017	28916331		*				*			*		
190		Ding, et al. 2009	19447168	*					*			*		
191		Diniz et al., 2013	23098799		*			*				*		
192		Encinas et al., 2006	16702546		*				*			*		
193		Esmaili et al., 2016	26562432	*					*					*
194		Fenton et al., 2015	25681757		*			*				*		
195		Hicks et al., 2012	23213573		*			*				*		
196		Ishizuka et al., 2012	22828480	*					*					*
197		Kanemura et al., 2005	16405078	*						*				*
198		Kitamura et al., 2011	28064347		*			*				*		
199		Lee et al., 2016	24890505	*						*				*
200		Liu et al., 2018	29054390		*				*			*		
201		Nautiyal et al., 2012	22632453		*				*			*		
202		Rainer et al., 2012	21473810		*				*			*		
203		Raman et al., 2013	23395832		*				*			*		
204		Sargeant et al., 2008	18783375			*			*					*
205		Sawada et al., 2018	29530528		*				*				*	
206		Siopi et al., 2016	26758842		*				*			*		
207		Surget et al., 2016	27395785		*				*			*		
208		Tikhinova et al., 2017	28487222		*			*				*		
209		Wong et al., 2005	16115202		*			*				*		
210		Yanpallewar et al., 2010	20089918	*				*				*		
211		Yoo et al., 2014	24136217		*				*			*		
212		Zhang et al., 2014	16511865	*				*						*
213		Zhang et al., 2016	27078155		*				*			*		
214		Zhao et al., 2015	26236713		*				*			*		
215		Zhou et al., 2016	27598965		*				*			*		

Supplemental Table 3. Characteristics of the publications included in the meta-analysis assessing the proliferation of NSCs in the context of drug interactions.

Author	Year	PMID	Type of experiment	Source of the sample	Result	Sub-class of drugs	Drug	Statistical analysis	*P* value	Mecha-nism	Con-trol group	Blind expe-riment	Outlier	Technical (TR)/ biological replicate (BR)
Alves et al.	2017	28291258	*In vivo*	Dorsal dentate gyrus of male Wistar Han rats	Positive (BrdU): Fluoxetine Neutral (BrdU): Imipramine	SSRI and tricyclic antidepressant	Fluoxetine and Imipramine	Student t test	$P < 0.05$	Proposed	Yes	No	NA	BR
Brooker et al.	2017	27698430	*In vivo*	Dentate gyrus of C57BL/6 male and female mice	Positive (BrdU)	SSRI	Fluoxetine	Unpaired t test	$P < 0.05$	Tested	Yes	Yes	NA	BR
Cowen et al.	2008	18616933	*In vivo*	Dentate gyrus of male Sprague Dawley rats	Neutral (Ki67 and BrdU)	SSRI	Fluoxetine	Two way ANOVA	$P < 0.05$	NA	Yes	Yes	NA	BR
Hanson et al.	2011	21220416	*In vivo*	Dentate gyrus of adult male	Neutral (BrdU)	SSRI	Fluoxetine	Two way ANOVA	$P < 0.0001$	Proposed	Yes	Yes	NA	BR

Author	Year	PMID	Type of experiment	Source of the sample	Result	Sub-class of drugs	Drug	Statistical analysis	*P* value	Mecha-nism	Con-trol group	Blind expe-riment	Outlier	Technical (TR)/ biological replicate (BR)
				Sprague Dawley rats										
Holick et al.	2008	17429410	*In vivo*	Dentate gyrus of BALB7cJ male mice	Neutral (BrdU)	SSRI	Fluoxetine	ANOVA with Newman-Keuls	$P < 0.05$	Proposed	Yes	No	NA	BR
Hui et al.	2014	25522429	*In vitro*	Hippocampal neural progenitor cells of fetal Sprague Dawley rats	Positive (BrdU)	SSRI	Fluoxetine	ANOVA	$P < 0.01$	Tested	Yes	No	NA	TR
Kodama et al.	2004	15476686	*In vivo*	Hippocampal, prelimbic. striatum of male Sprague Dawley rats	Positive (BrdU)	SSRI	Fluoxetine	ANOVA	$P < 0.05$	Proposed	Yes	Yes	NA	BR
Kohl et al.	2012	22211740	*In vivo*	Hippocampus of male and female	Positive (BrdU)	SSRI	Fluoxetine	Two way ANOVA with	$P < 0.05$	Tested	Yes	Yes	NA	BR

Author	Year	PMID	Type of experiment	Source of the sample	Result	Sub-class of drugs	Drug	Statistical analysis	*P* value	Mecha-nism	Con-trol group	Blind expe-riment	Outlier	Technical (TR)/ biological replicate (BR)
				C57/BL6 mice				Bonferroni posthoc						
Lee et al.	2009	19819298	*In vivo*	Hippocampus of male ICR mice	Positive (BrdU)	Tricyclic antidepressant	Imipramine	ANOVA with Student-Newman - Keuls posthoc	$P < 0.05$	Proposed	Yes	No	NA	BR
Marlatt et al.	2010	20381469	*In vivo*	Dentate gyrus of female C57BL6 mice	Positive (BrdU/NeuN)	SSRI	Fluoxetine	One way ANOVA	$P < 0.003$	Proposed	Yes	No	NA	BR
Meyer et al.	2017	27569185	*In vivo*	Subgranular zone and subventricular zone of male Babl/C mice	Positive (BrdU)	Tricyclic antidepressant	Imipramine	One way ANOVA	$P < 0.001$	Proposed	Yes	Yes	NA	BR

Author	Year	PMID	Type of experiment	Source of the sample	Result	Sub-class of drugs	Drug	Statistical analysis	*P* value	Mecha-nism	Con-trol group	Blind expe-riment	Outlier	Technical (TR)/ biological replicate (BR)
Nackenoff et al.	2017	28272863	*In vivo*	Hippocampus of male C57BL/6 mice	Positive (BrdU)	SSRI	Vortioxetine & Paroxetine	ANOVA and horn sidak post hoc	$P < 0.05$	Proposed	Yes	Yes	NA	BR
Nasrallah et al.	2010	20682307	*In vivo*	Dentate gyrus and subventricular zone of male Sprague Dawley rats	Positive (BrdU): Paliperidone	SSRI	Paliperidone Fluoxetine	One way ANOVA	$P < 0.05$	NA	Yes	Yes	NA	BR
					Neutral (BrdU): Fluoxetine and Risperidone		Risperidone							
Ohira et al.	2011	21385396	*In vivo*	Dentate gyrus of male C57BL6 mice	Positive (BrdU and Ki67)	SSRI	Fluoxetine	One way ANOVA with Scheffe posthoc	$P < 0.01$	Proposed	Yes	No	NA	BR
Pechnick et al.	2011	22076148	*In vivo*	Subgranular zone of male C57BL6 mice	Positive (BrdU)	Tricyclic antidepressant	Imipramine	Two way ANOVA with Newman-	$P < 0.05$	Tested	Yes	Yes	NA	BR

Author	Year	PMID	Type of experiment	Source of the sample	Result	Sub-class of drugs	Drug	Statistical analysis	*P* value	Mecha-nism	Con-trol group	Blind expe-riment	Outlier	Technical (TR)/ biological replicate (BR)
								Keuls posthoc						
Petit et al.	2013	23573275	*In vivo*	Granule cells of the olfactory bulb of male and female C56/BL7 mice	Neutral (BrdU)	MAO inhibitor	Rasagiline	One way ANOVA	NA	NA	Yes	Yes	NA	BR
Rayen et al.	2011	21912658	*In utero*	Dentate gyrus of Sprague Dawley rat pups	Negative (Ki67)	SSRI	Fluoxetine	ANOVA	$P < 0.05$	Proposed	Yes	No	NA	BR
Santarelli et al.	2003	12907793	*In vivo*	Hippocampus of female and male 129/sv mice	Positive (BrdU)	SSRI	Fluoxetine	ANOVA with Fischer posthoc	$P < 0.01$	Tested	Yes	No	NA	BR
Schiavon et al.	2016	26187374	*In vivo*	Subventricular zone and subgranular zone of male	Positive (BrdU)	Tricyclic antidepressant	Imipramine	One way ANOVA	$P < 0.0001$	Proposed	Yes	No	NA	BR

Author	Year	PMID	Type of experiment	Source of the sample	Result	Sub-class of drugs	Drug	Statistical analysis	*P* value	Mecha-nism	Con-trol group	Blind expe-riment	Outlier	Technical (TR)/ biological replicate (BR)
				Swiss Albino mice										
Sun et al.	2010	20123967	*In vitro*	Neural stem cells from (unspecified strain and sex) mouse brain	Negative (BrdU)	MAO inhibitor	Pargyline *	Student-t-test	$P < 0.001$	Tested	Yes	No	NA	TR
							Tranylcypromine**		$P < 0.01$					
Yu et al.	2017	28045461	*In vivo*	Subgranular zone of male Wistar dams rats	Neutral (Ki67)	SSRI	Fluoxetine	Two way ANOVA	$P < 0.05$	Proposed	Yes	Yes	NA	BR

Supplemental Table 4. Characteristics of the publications included in the meta-analysis assessing the differentiation of NSCs in the context of drug interactions.

Author	Year	PMID	Type of experi-ment	Source of the sample	Result	Sub-class of drugs	Drug	Statistical analysis	P value	Mechanism	Control group	Blind experiment	Outlier	Technnical (TR)/ biological replicate (BR)
Asokan et al.	2014	24896246	*In vivo*	Dentate gyrus of male Long Evans rats	Negative (DCX)	SNRI	Desvenlafaxine	One way ANOVA with Duncan post hoc	$P < 0.05$	Proposed	Yes	No	NA	BR
Gemmel et al.	2017	28735226	*In vivo*	Granule cells of female Spraque Dawleys rats	Neutral (DCX)	SSRI	Fluoxetine	ANOVA	$P < 0.05$	Proposed	Yes	Yes	NA	BR
Gemmel et al.	2018	29203333	*In vivo*	Dorsal hippocampus of female Spraque Dawleys rats	Positive (DCX)	SSRI	Fluoxetine	ANOVA	$P < 0.05$	Proposed	Yes	No	NA	BR
Holick et al.	2008	17429410	*In vivo*	Dentate gyrus of male Balb/cJ mice	Neutral (DCX)	SSRI	Fluoxetine	ANOVA with Neuman-Keuls Post hoc	$P < 0.05$	Proposed	Yes	No	NA	BR
Meyer et al.	2017	27569185	*In vivo*	Subgranular zone and subventricular zone of male Babl/C mice	Positive (DCX)	Tricyclic antidepressant	Imipramine	One way ANOVA	$P < 0.001$	Proposed	Yes	Yes	NA	BR
Olesen et al.	2017	28461249	*In vivo*	Granule cells of male B6C3 hybrid rats	Neutral (DCX)	SSRI	Paroxetine	ANOVA with Tukey post hoc	$P < 0.05$	Proposed	Yes	No	NA	BR
Pechnick et al.	2011	22076148	*In vivo*	Subgranular zone of male C57BL6 mice	Positive (DCX)	Tricyclic antidepressant	Imipramine	Two way ANOVA with Neuman-Keuls Post hoc	$P < 0.05$	Tested	Yes	Yes	NA	BR
Rayen et al.	2011	21912658	*In utero*	Dentate gyrus of Sprague Dawley rat pups	Nutral (DCX))	SSRI	Fluoxetine	ANOVA	$P < 0.05$	Proposed	Yes	No	NA	BR

Supplemental Table 5. Characteristics of the publications included in the meta-analysis assessing the proliferation of NSCs in the context of models of depression.

Author	Year	PMID	Source of the sample	Result	Sub-class of drugs	Drug	Statistical analysis	P value	Mechanism	Control group	Blind experiment	Outlier	Technnical (TR)/ biological replicate (BR)
Alboni et al.	2017	26645631	Hippocampus of C57BL/6 mice	Negative (Ki67)	SSRI	Fluoxetine	One way ANOVA	$P < 0.05$	Investigated	Yes	No	NA	BR
Christensen et al.	2012	22406239	Dentate gyrus of rats	Neutral (BrdU)	SSRI	Gaboxadol	Student t test	$P < 0.05$	Proposed	Yes	No	NA	BR
Jayakumar et al.	2017	28764145	Hippocampus of male Wistar albino rats	Positive (BrdU)	SSRI	Fluoxetine	ANOVA with Tukey post hoc	$P < 0.05$	Proposed	Yes	No	NA	BR
Kuipers et al.	2013	23994757	Hippocampus of male and female Wistar rats	Positive (BrdU)	Tricyclic antidepressant	Tianeptine	ANOVA	$P < 0.05$	Proposed	Yes	Yes	NA	BR
Petersen et al.	2009	19135130	Hippocampus of female Flinders sensistive Line rats	Neutral (BrdU)	Tricyclic antidepressant	Nortryptiline	Student t test	$P < 0.05$	Proposed	Yes	No	NA	BR
Vitale et al.	2017	28417659	Hippocampus of male Wistar rats	Positive (BrdU)	SSRI	Fluoxetine	ANOVA with student-Newman-Keuls post hoc	$P < 0.05$	Proposed	Yes	Yes	NA	BR

Supplemental Table 6. Excluded studies of the systematic review on EPCs and drug interactions based on the full-text screening.

No.	Author, Year	PMID	Review	Use of other cell line	Not observed drug effect on brain disease	No interaction between drugs and EPCs	Non-proliferation or non-differentiation marker
1	Aberg, 2010	19955757	*				
2	Aberg et al., 2006	16432628	*				
3	Argente-Arizon et al., 2015	25859240	*				
4	Cimino et al., 2007	17519364	*				
5	Conti, et al., 2008	18855638	*				
6	Forostyak et al., 2013	23994163	*				
7	Guardia Clausi et al., 2016	26804249	*				
8	Isgaard, J. et al., 2007	17557036	*				
9	Liu et al., 2013	23211013	*				
10	Maffei et al., 2019	31396153	*				
11	Marzo, et al., 2008	18338108	*				
12	Seidah et al., 2007	17351764	*				
13	Werner et al., 2008	18454336	*				
14	Zieden et al., 2005	16105479	*				
15	Berezin, et al., 2014	25082501			*		
16	Boldrini, et al., 2012	22652019		*			
17	He et al., 2011	20735164				*	
18	Arguello et al., 2009	19356684		*			
19	Chen, et al., 2005	15678129		*			
20	Mannari, et al., 2014	24962546					*
21	Ueno et al., 2011	21701082			*		
22	Yang et al., 2015	25813059				*	

Supplemental Table 7. Characteristics of the publications included in the systematic review assessing the effect of drugs used in the elderly on EPCs.

Author	Year	PMID	Type of experiment	Source of the sample	Result	Sub-class of drugs	Drug	Statistical analysis	P value	Mechanism of work	Technical (TR) or biological replicate (BR)
Dong et al.	2017	28928014	*In vivo*	Bone marrow-derived EPC	Subchronic treatment of antibiotic affecting the potentiation of EPC	Tetracycline	Tetracycline	Student's unpaired t test	$P < 0.01$	NA	BR
Golab-Janowska et al.	2018	29886830	Human	Circulating EPC	Statins increased the number of EPC	Statins	Statins	Student's unpaired t test	$P < 0.05$	NA	BR
Marti-fabregas et al.	2013	24363968	Human	Circulating EPC	Statins increased the number of EPC	Statins	Statins	ANOVA with mann whitney test	$P = 0.079$	NA	BR
Meamar et al.	2016	27904593	Human	Circulating EPC	Statins increased the number of EPC	Statins	Statins	ANOVA with tukey test	$P < 0.001$	NA	BR
Riddel et al.	2015	25747743	Human	Circulating EPC	Beta adrenergic drug had no effect on the number of EPC	Beta adrenergic	Beta-adrenergic	Student's Paired t test	$P = 0.333$	NA	BR
Wang et al.	2012	22658532	*In vivo*	Circulating EPC	Statins increased the level of EPC	Statins	Statins	ANOVA with LSD posthoc	$P < 0.05$	NA	BR